Final Technical Report

Reporting Period:

October 1, 2008 to September 30, 2011

DOE Cooperative Agreement Number: DE-NT0004113
Validation of Novel Planar Cell Design for MW-Scale SOFC Power Systems

to:

U.S. Department of Energy

Submitted by:

NexTech Materials, Ltd.
404 Enterprise Drive
Lewis Center, OH 43035

Authors: Dr. Scott L. Swartz, Ph.D.; Dr. Lora B. Thrun, Ph.D.; Mr. Gene B. Arkenberg; Ms. Kellie M. Chenault

December 31, 2011

Abstract

This report describes the work completed by NexTech Materials, Ltd. during a three-year project to validate an electrolyte-supported planar solid oxide fuel cell design, termed the *FlexCell*, for coal-based, megawatt-scale power generation systems. This project was focused on the fabrication and testing of electrolyte-supported *FlexCells* with yttria-stabilized zirconia (YSZ) as the electrolyte material. YSZ based *FlexCells* were made with sizes ranging from 100 to 500 cm^2. Single-cell testing was performed to confirm high electrochemical performance, both with diluted hydrogen and simulated coal gas as fuels. Finite element analysis modeling was performed at The Ohio State University was performed to establish *FlexCell* architectures with optimum mechanical robustness. A manufacturing cost analysis was completed, which confirmed that manufacturing costs of less than $50/kW are achievable at high volumes (500 MW/year).

Table of Contents

Introduction

This SECA Core Technology project was aimed at advancing planar solid oxide fuel cell technology for coal-based, megawatt-scale power generation systems. Such systems will be comprised of a multitude of SOFC stack modules to achieve targeted power outputs. Planar SOFC cells with large active areas will be required in order to increase the power output per stack (and reduce the number of stacks in the system). NexTech Materials has established a novel electrolyte-supported planar cell design, termed the *FlexCell* (see Figure 1), which offers intrinsic scalability to large areas, as well as other important performance attributes. NexTech originally proved its *FlexCell* membrane concept with scandium stabilized zirconia (ScSZ-6) as the electrolyte material. The SCSZ-6 material offers an excellent combination of high ionic conductivity and high mechanical strength, but its cost will be prohibitive for large-scale power generation systems. This project was conducted to validate the manufacturability and electrochemical performance of *FlexCell* membranes made with lower-cost yttrium stabilized zirconia (YSZ) as the electrolyte material. Specific tasks included manufacture of large-area YSZ-based *FlexCells*, electrochemical performance evaluations, finite element analysis of mechanical robustness of *FlexCell*s, and manufacturing cost analyses. This report describes the results obtained during the three-year duration of the project (October 2008 through September 2011).

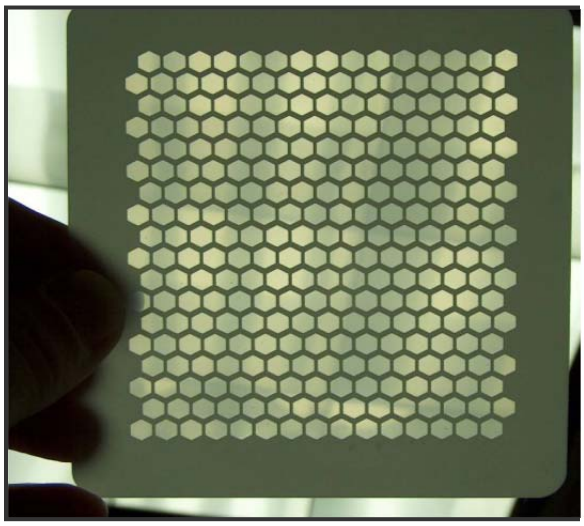

Figure 1. Example of a *FlexCell* membrane.

Fabrication and Testing of YSZ-Based FlexCells

YSZ-3 Based FlexCells

As was shown in Figure 1, the *FlexCell* is an electrolyte-supported planar element based on a two-layer structure comprising a thin electrolyte layer that is mechanically supported by a "honeycomb" mesh layer of electrolyte material. With the *FlexCell*, approximately 60 to 70 percent of the electrolyte membrane within the active area is thin (30 microns), and the periphery of the cell is dense. Anode and cathode layers are subsequently deposited onto the major faces within the active cell regions to complete the fabrication of an SOFC based on the *FlexCell* design. Initial work on the project focused on the fabrication of YSZ-based *FlexCells* with nominally 100-cm^2 total areas and single-cell SOFC testing of these components. NexTech's single-cell testing methodology utilizes a planar membrane with a total area of 110-cm^2 and an "active" area of 37 cm^2 (note that the extra wide periphery provides a sealing area for single-cell testing). A CAD drawing of the targeted *FlexCell* membrane design for the YSZ-based *FlexCells* is shown in Figure 2. *FlexCell* membranes were successfully fabricated with YSZ-3 as the electrolyte material, as shown in Figure 3. NexTech's proprietary anode and cathode layers were applied in separate deposition/sintering steps, with the anode applied to the support (corrugated) face of the *FlexCell* membrane and the cathode applied to the non-corrugated face.

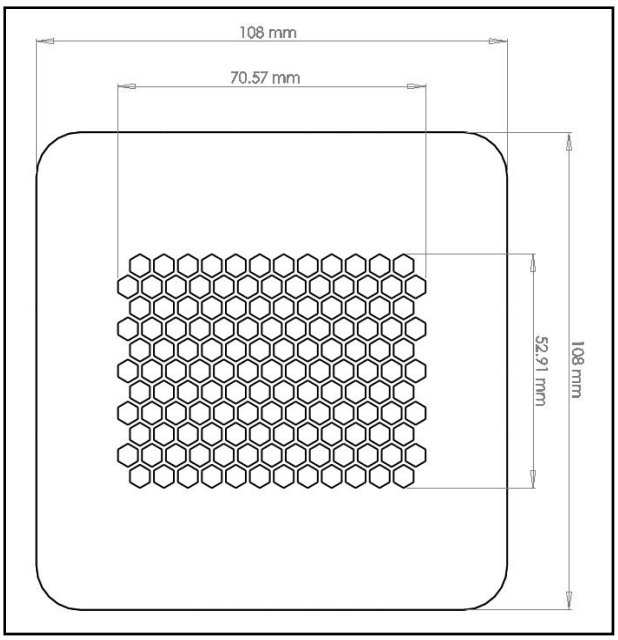

Figure 2: CAD drawing of 110-cm² area *FlexCell* membrane

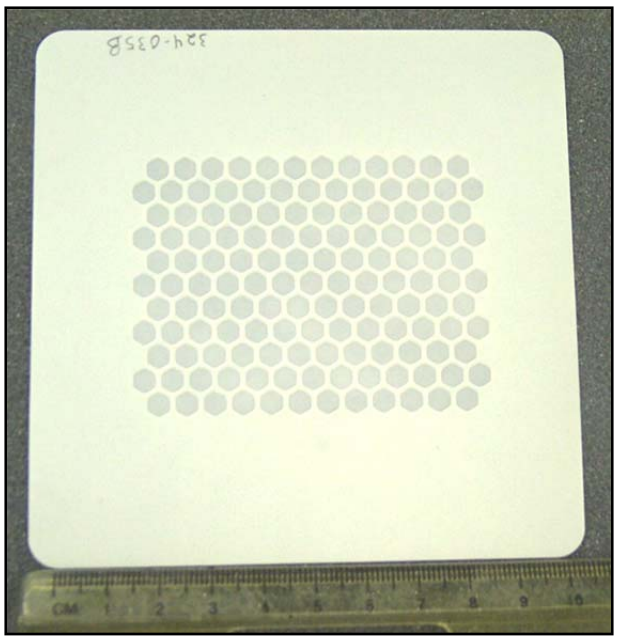

Figure 3: *FlexCell* membrane made with YSZ-3 electrolyte (shown without electrodes).

Initial work on the project involved the manufacture of *FlexCells* with YSZ-3 as the electrolyte material, with varying membrane architectures (i.e., thickness of the support and membrane layers and percentage of thin regions within the active cell area). The goal of cell fabrication work at this stage of the project was to reduce membrane thicknesses as much as possible, to mitigate the lower ionic conductivity of the YSZ-3 electrolyte material (compared to ScSZ-8). *FlexCells* were successfully made with support and membrane layer thicknesses of 80 and 24 microns, respectively. This compares to thicknesses of 160 and 32 microns for the support and membrane layers in NexTech's ScSZ-based *FlexCells* (which served as a baseline for comparison). Figure 4 demonstrates the translucency of the one of the ultra-thin YSZ-based *FlexCell* membranes.

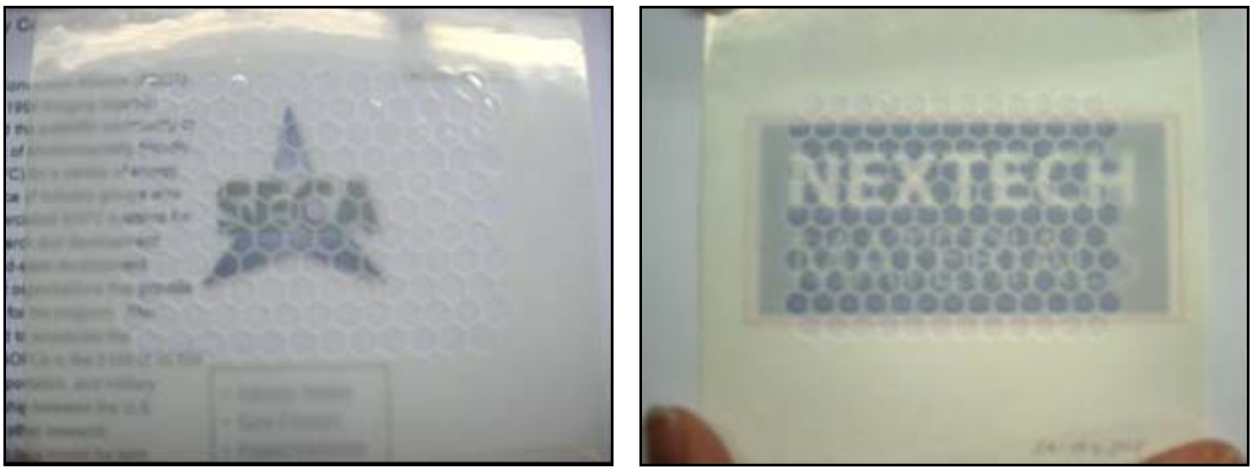

Figure 4. Photographs of varied architecture *FlexCells*, indicating high translucency.

Two types of SOFC performance tests were performed on *FlexCells* (with 28-cm^2 active area as defined by geometry of current collector meshes). In the first set of tests, I-V data were collected at different temperatures (700 to 850°C) with constant fuel and air flow rates of 450 sccm H_2 and 1500 sccm air. These low fuel utilization conditions enable intrinsic performance characteristics to be assessed and area specific resistance (ASR) values to be calculated. ASR and power density data for the YSZ-3 *FlexCells* are provided in Table 1. The results indicated that ASR values decreased and area-specific power density increased as constituent membrane layer thicknesses were reduced (as expected). The YSZ-3 *FlexCell* made with ultra-thin support and membrane layers exhibited performance equivalent to that of one of NexTech's standard ScSZ based *FlexCells* (see Figure 5).

Table 1. SOFC performance for ScSZ-6 and YSZ-3 Based *FlexCells*.

Sample Number	Electrolyte Material	Membrane Geometry	T (°C)	Power Density (mW/cm²)	ASR (Ω-cm^2)
324-041D	ScSZ	Support thickness: 160 µm Membrane thickness: 32 µm 62% thin membrane	700	241	0.949
			750	372	0.579
			800	572	0.357
			850	786	0.254
324-075A	YSZ-3	Support thickness: 160 µm Membrane thickness: 32 µm 62% thin membrane	700	201	1.29
			750	307	0.794
			800	438	0.524
			850	598	0.366
324-059A	YSZ-3	Support thickness: 160 µm Membrane thickness: 24 µm 62% thin membrane	700	184	1.28
			750	304	0.749
			800	490	0.491
			850	680	0.310
324-060C	YSZ-3	Support thickness: 112 µm Membrane thickness: 32 µm 62% thin membrane	700	180	1.30
			750	316	0.744
			800	470	0.475
			850	679	0.318
324-080C	YSZ-3	Support thickness: 80 µm Membrane thickness: 24 µm 62% thin membrane	700	n/a	n/a
			750	428	0.550
			800	599	0.373
			850	778	0.281

Notes:
Power density values obtained at 0.7 volts (H_2 fuel, low fuel utilization)
ASR values calculated from 0.6 to 0.8 volts (H_2 fuel, low fuel utilization)

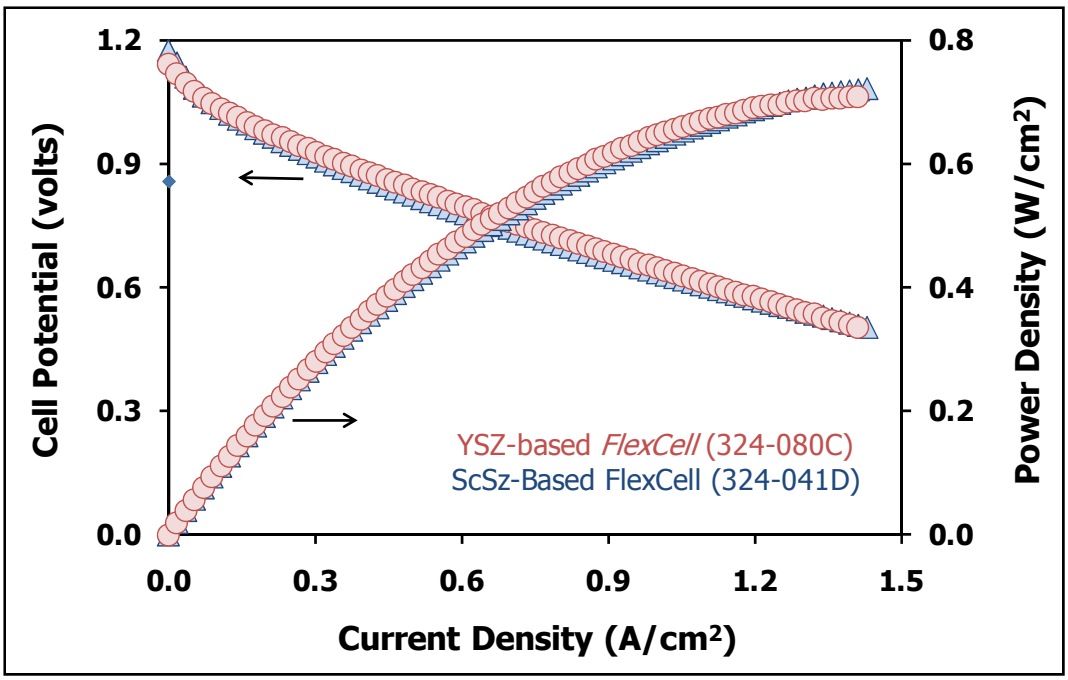

Figure 5. Comparison of SOFC performance between one of NexTech's standard ScSZ-based *FlexCells* and an YSZ-based *FlexCell* fabricated with thin support and membrane layers (tested at 800°C).

In the second set of tests, I-V data (pole curves) were recorded under conditions of constant fuel utilization (50 to 80 percent) at different temperatures (700 to 850°C), with diluted hydrogen (50% H_2, 50% N_2) as fuel. Data obtained at 0.7 volts and 70% fuel utilization are presented in Table 2. Constant stoichiometry pole curve data for the best performing YSZ-based *FlexCell* (Sample No. 324-080C, with the thinnest support and membrane layers) are presented in Figures 6 and 7. When tested at 800°C with 70% fuel utilization, this *FlexCell* achieved power densities of 287 mW/cm^2 at 0.8 volts and 475 mW/cm^2 at 0.7 volts (see Figure 8).

Table 2. Constant stoichiometry pole curve data for ScSZ-based and YSZ-based *FlexCells*.

Sample Number	Electrolyte Material	Support / Membrane Thicknesses (µm)	PD at 0.7 volts and 70% U_F (mW/cm²)			
			700°C	750°C	800°C	850°C
324-041D	ScSZ	160 / 32	182	285	432	593
324-075A	YSZ-3	160 /32	n/a	234	333	453
324-059A	YSZ-3	160 / 24	n/a	221	339	456
324-060C	YSZ-3	112 / 32	128	238	359	488
324-080C	YSZ-3	80 / 24	n/a	306	475	620

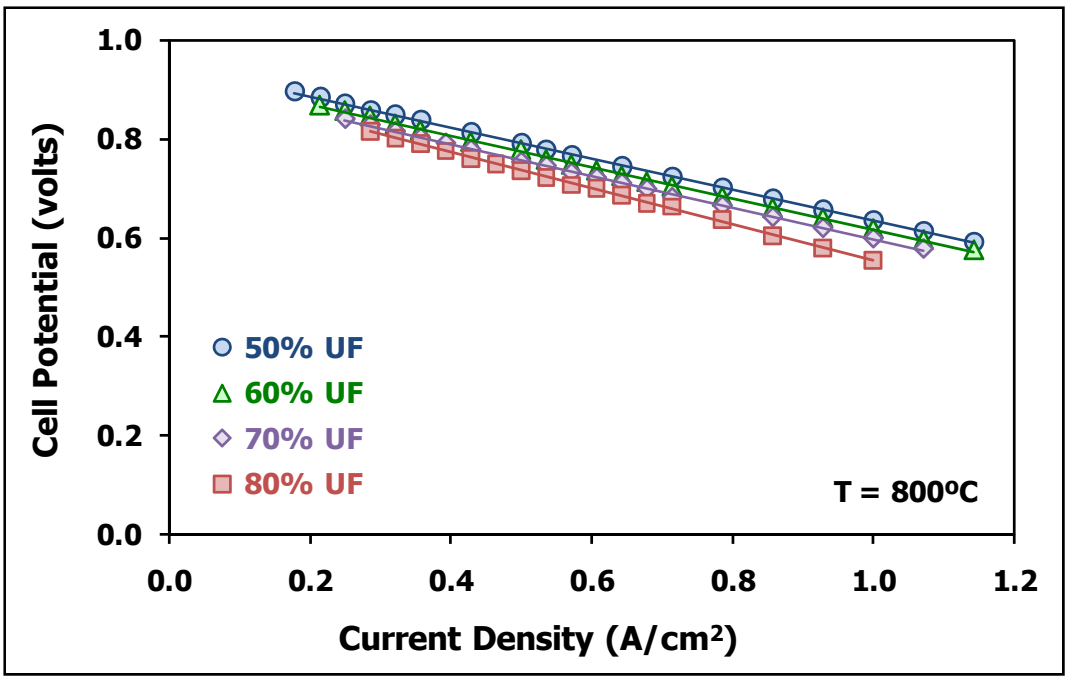

Figure 6. Pole curves obtained at 800ºC with different fuel utilizations for the YSZ-based *FlexCell* with thin support and membrane layers (Sample No. 324-080C).

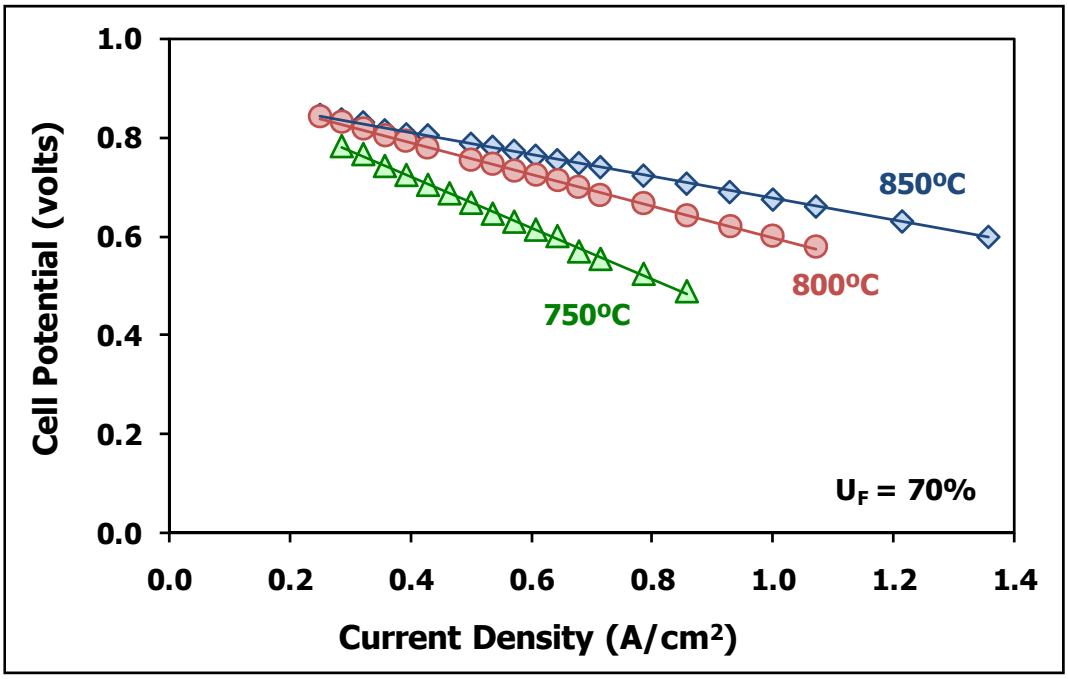

Figure 7. Pole curves obtained at different temperatures with 70% fuel utilization for the YSZ-based *FlexCell* with thin support and membrane layers (Sample No. 324-080C).

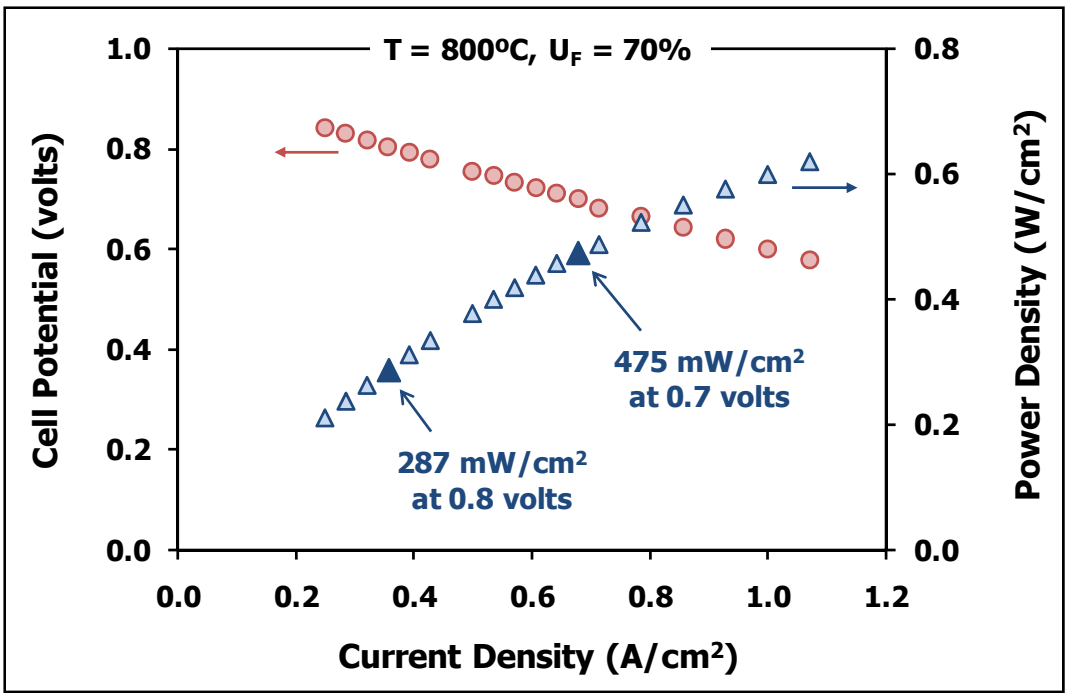

Figure 8. Constant stoichiometry pole curve data obtained at 800°C with 70% fuel utilization for the YSZ-based *FlexCell* with ultra-thin support and membrane layers (Sample No. 324-080C).

In addition to support and membrane layer thickness, another important *FlexCell* architectural variable is the percentage of unsupported (thin) membrane within the active cell area. *FlexCells* also were made and tested to evaluate this variable. The thicknesses of the support and membrane layers were held constant (160 and 24 microns, respectively) and the percentage of unsupported thin membrane was varied from 58 to 74 percent. Approximate geometries of the three *FlexCell* membranes fabricated in this study are provided in Table 3, along with performance data obtained in low-fuel utilization testing. As would be expected, performance improvements were observed as the percentage of thin unsupported membrane in the active cell regions increased.

Table 3. SOFC performance data for YSZ-3 *FlexCells* with different percentages of thin membrane within the active cell area.

Sample Number	Support Thickness	Membrane Thickness	Percent Thin Membrane in Active Cell Area	Power Density (mW/cm^2)	ASR (Ω-cm^2)
324-118A	160 µm	24 µm	74%	526	0.40
324-121B	160 µm	24 µm	62%	462	0.56
324-120A	160 µm	24 µm	58%	447	0.53

Notes:
Power density values obtained at 0.7 volts (H_2 fuel, low fuel utilization).
ASR values calculated from 0.6 to 0.8 volts (H_2 fuel, low fuel utilization).

FlexCells made with Composite YSZ Electrolyte Formulations

Within the YSZ electrolyte family, YSZ-3 has high mechanical strength and low ionic conductivity, and YSZ-8 has higher ionic conductivity and lower strength. To evaluate this trade-off, two *FlexCells* were made from mixtures of YSZ-3 and YSZ-8 powders; these initial YSZ-3/8 FlexCells were made with very thin support and membrane layers. Cell geometries and performance data are summarized in Table 4. The combination of thin support/membrane layers with the higher ionic conductivity of the membrane led to superior performance compared to previously tested *FlexCells* made with YSZ-3 as the electrolyte material. These two cells also were subjected to constant utilization I-V testing with diluted hydrogen (50% H_2) as fuel. Data obtained at 0.7 volts and 70% fuel utilization are summarized in Table 5. Pole curve data for the best performing YSZ-based *FlexCell* are presented in Figures 9 and 10. When tested at 800°C with 70% fuel utilization, this *FlexCell* achieved power densities of 457 mW/cm^2 at 0.8 volts and 606 mW/cm^2 at 0.7 volts (see Figure 11).

Table 4. SOFC performance data for *FlexCells* made from mixtures of YSZ-3 and YSZ-8 powders.

Sample Number	Electrolyte Material	Support Thickness (µm)	Membrane Thickness (µm)	T (°C)	Power Density (mW/cm²)	ASR (Ω-cm^2)
324-140B	60%YSZ-3 40%YSZ-8	67	24	700	313	0.747
				750	487	0.467
				800	701	0.320
				850	892	0.256
324-145D	70%YSZ-3 30%YSZ-8	91	24	700	316	0.747
				750	484	0.487
				800	698	0.329
				850	898	0.263

Notes:
Power density values obtained at 0.7 volts (H_2 fuel, low fuel utilization).
ASR values calculated from 0.6 to 0.8 volts (H_2 fuel, low fuel utilization).

Table 5. Summary of constant-utilization pole curve data obtained on *FlexCells* made from mixtures of YSZ-3 and YSZ-8 powders.

Sample Number	Electrolyte Material	Support / Membrane Thicknesses (µm)	PD at 0.7 volts and 70% U_F (mW/cm²)			
			700°C	750°C	800°C	850°C
324-140B	60%YSZ-3 40%YSZ-8	67 / 24	248	396	594	796
324-145D	70%YSZ-3 30%YSZ-8	91 / 24	275	440	606	794

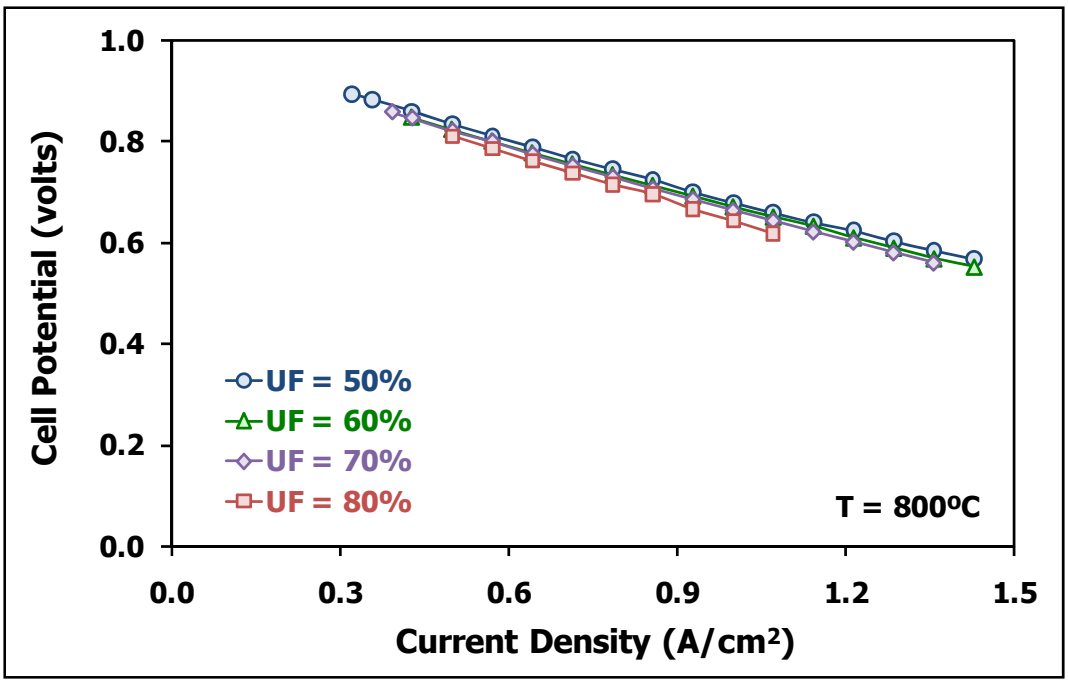

Figure 9. Pole curves obtained at 800ºC with different fuel utilizations for the YSZ-based *FlexCell* with ultra-thin support and membrane layers (Sample No. 324-145D).

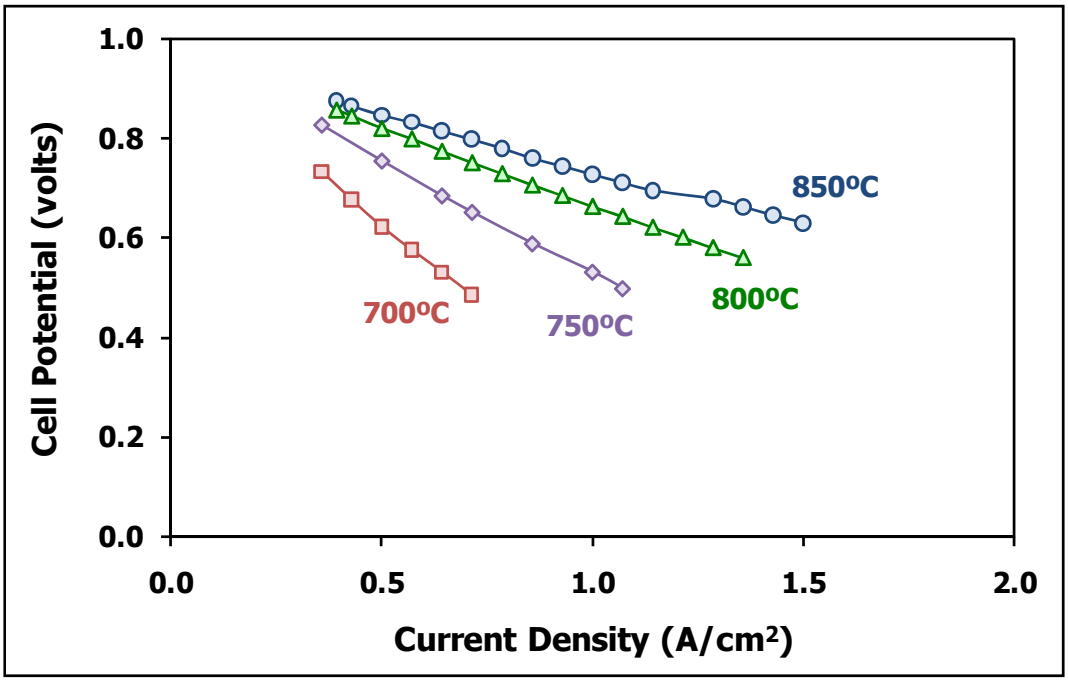

Figure 10. Pole curves obtained at different temperatures with 70% fuel utilization for the YSZ-based *FlexCell* with ultra-thin support and membrane layers (Sample No. 324-145D).

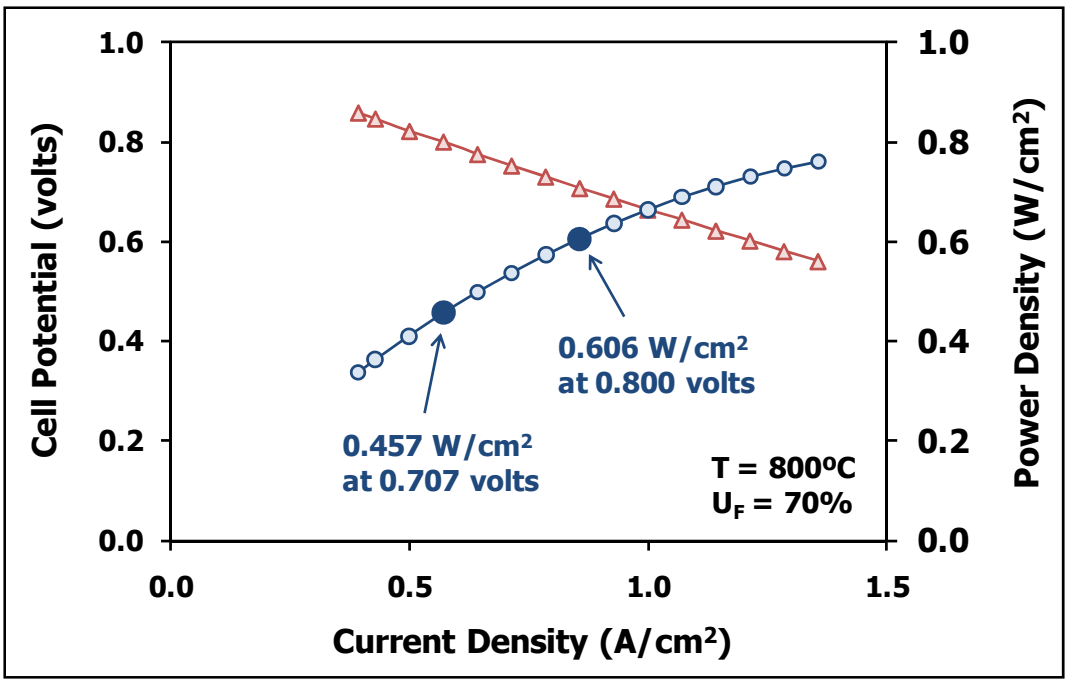

Figure 11. Constant stoichiometry pole curve data obtained at 800°C with 70% fuel utilization for the YSZ-based *FlexCell* with ultra-thin support and membrane layers (Sample No. 324-145D).

FlexCells with ultra-thin support and membrane layers (80 and 24 microns, respectively) were routinely made at the 100 cm^2 scale. However, the fabrication of *FlexCells* of this geometry became progressively more challenging as cell area was increased, due to green-state failures during the fabrication process. Support and membrane layer thickness were increased to successfully fabricate large-area *FlexCells*, with minimum support and membrane layer thicknesses of approximately 120 and 36 microns, respectively, required for high yield manufacture of large-area *FlexCells*. Also, as cell area increased, imperfections within the sintered electrolyte substrates became more evident and were traced to quality of green electrolyte tape used to make the *FlexCells*. Tests were performed to optimize the ingredients within the electrolyte tape slurries to reduce the amount of cracks, pin-holes and imperfections in sintered *FlexCells*. SEM images were taken of the green tapes to evaluate porosity. SEM micrographs are presented in Figure 12, which show improvements in green density achieved through formulation optimization work.

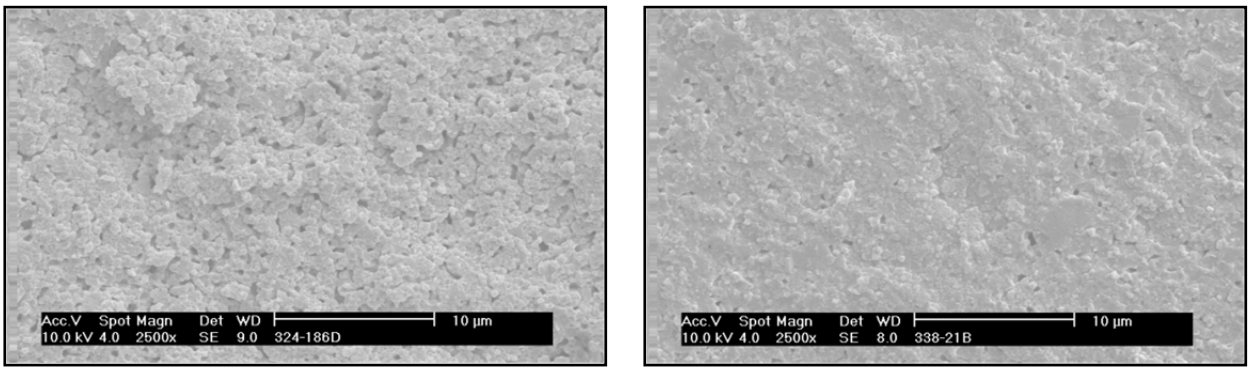

Figure 12. SEM micrographs of green electrolyte tapes made with: original tape formulation (left); and optimized tape formulation (right).

The impact of YSZ composition and improved tape formulations on sintered densities of YSZ substrates was evaluated. With the original tape casting formulation and with the YSZ-3 electrolyte composition, sintered membrane densities were relatively low (94-95 percent of theoretical). Sintered densities of YSZ membranes were increased to the 97 percent theoretical level by making the *FlexCells* from a mixture of YSZ-3 and YSZ-8 powders (30 mole percent YSZ-8). This improvement was attributed to the higher surface area of YSZ-8 powder (13 m^2/gram), compared to YSZ-3 powder (7 m^2/gram). By optimizing the tape casting slurry formulations, sintered densities of composite YSZ-3/8 membranes were increased to the 99-100 percent level.

Single-cell SOFC tests were performed on 28-cm^2 active area *FlexCells* of the high-density composite YSZ-3/8 formulation. These *FlexCells* were made with a support and membrane thicknesses of 160 and 40 microns, respectively (with 62 percent of the active cell area comprised of thin membrane). Results of a single-cell SOFC test performed with hydrogen as fuel at low utilization is shown in Figure 13. This represents the highest performance obtained to date for an YSZ-based *FlexCell*, with ASR values of 0.41, 0.27 and 0.19 Ω-cm^2 at temperatures of 750, 800 and 850°C, respectively (calculated between 0.85 to 0.75 volts). The performance of this cell was better than at first thought possible, so the test was repeated on an identical *FlexCell* (see Figure 14). The second cell exhibited slightly lower performance than the first cell (0.46, 0.30 and 0.23 Ω-cm^2 at temperatures of 750, 800 and 850°C, respectively), but still was better than any previously tested YSZ-based *FlexCell*. These tests confirmed that increasing membrane density resulted in a significant and beneficial impact on SOFC performance. As shown in Figure 15, the performance of YSZ-based *FlexCells* equaled ScSZ-based *FlexCells* at 850°C and nearly replicated ScSZ performance at 750°C (despite the improved density and performance of ScSZ-based *FlexCells* enabled by the optimized tape formulations).

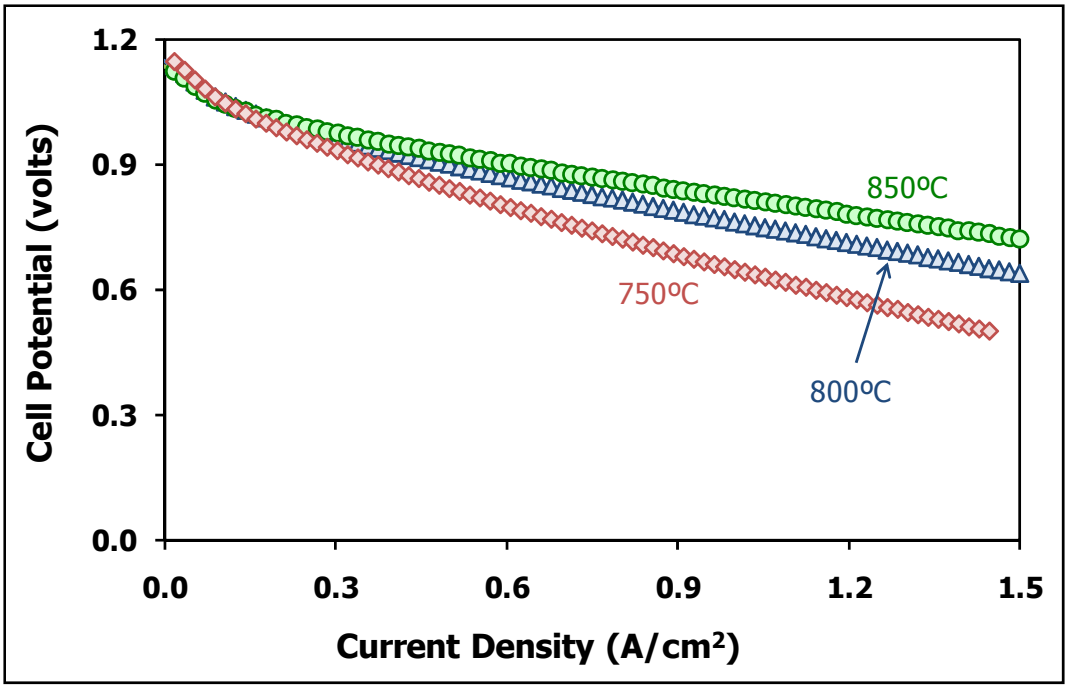

Figure 13. SOFC performance of a YSZ-3/8 *FlexCell* made from the high-density tape formulation (Sample No. 338-027C).

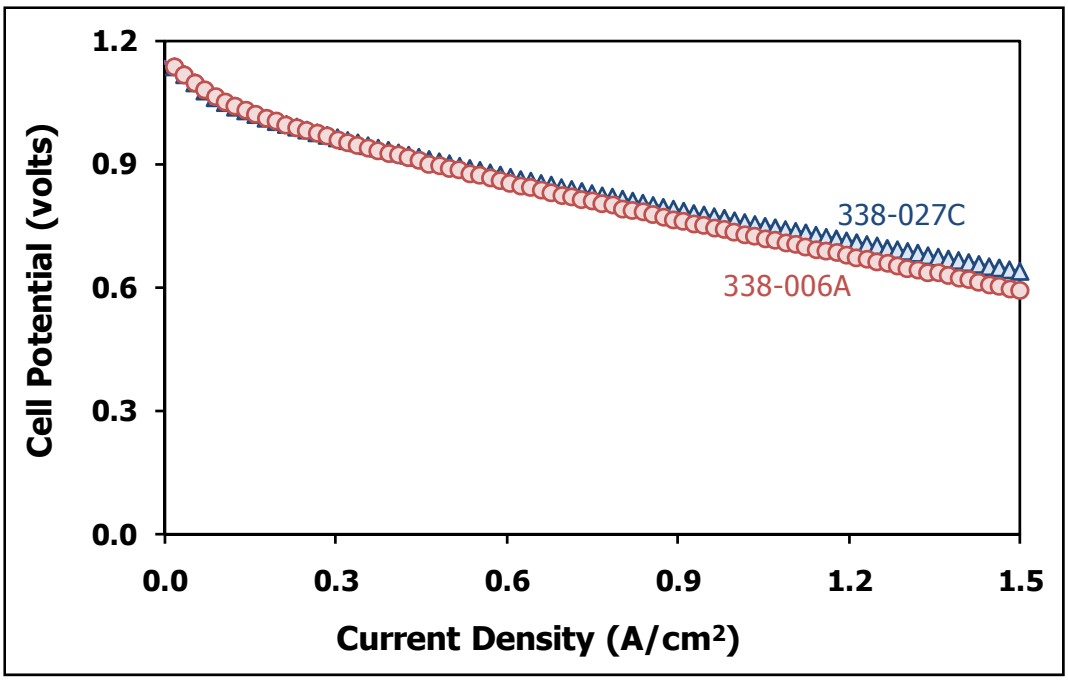

Figure 14. SOFC performance at 800°C for two identical YSZ-3/8 *FlexCells*.

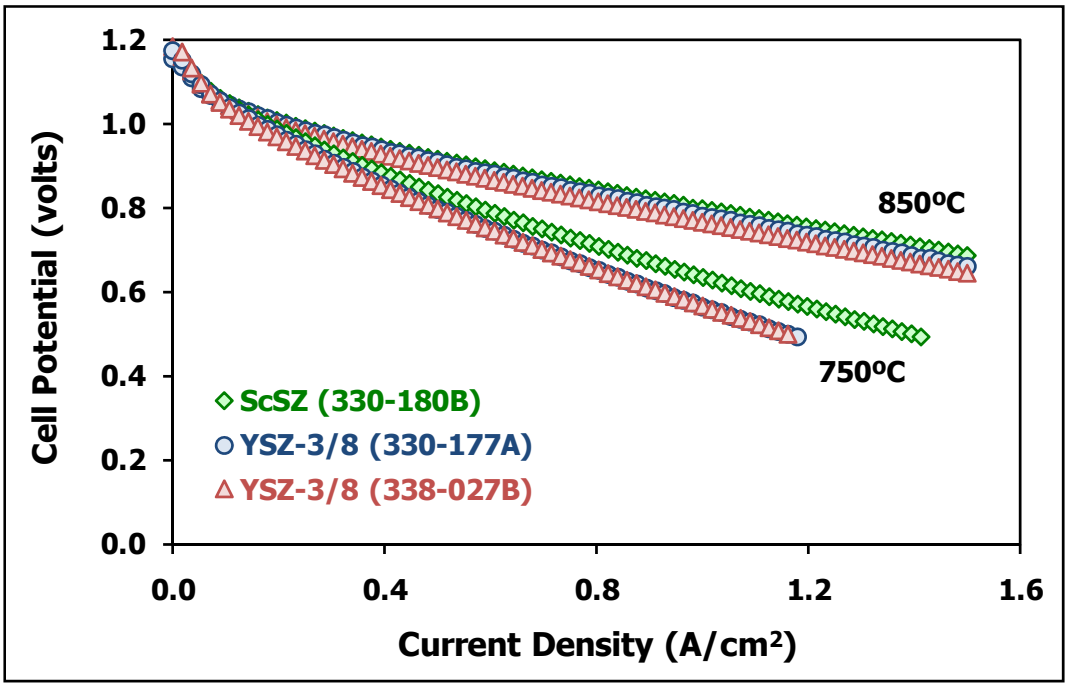

Figure 15. Single-cell SOFC performance of two YSZ-3/8 *FlexCells* and a SCSZ-based *FlexCell* at 750 and 850°C (hydrogen fuel, low utilization).

Several YSZ-3/8 *FlexCells* were made with the optimized tape formulations, process, and the improved performance was observed repeatedly (see Table 6). The performance improvement achieved compared to the original YSZ-3 *FlexCell* with thin support/membrane layers is shown in Figure 16. The YSZ-3/8 cell achieved 0.80 volts at 0.86 A/cm^2 compared to 0.70 volts at 0.86 A/cm^2 for the YSZ-3 cell, despite the YSZ-3 cell having approximately half the thickness of the YSZ-3/8 cell. The improved performance is substantially larger than can be explained on the basis of the higher ionic conductivity of the YSZ-3/8 composition compared to YSZ-3.

Table 6. Summary of SOFC performance data obtained on YSZ-3/8 based *FlexCells*.

Sample Number	Electrolyte Material	Support Thickness	Membrane Thickness	Percent Thin Membrane	PD (mW/cm²)	ASR (Ω-cm^2)
330-180B	ScSZ	160 µm	40 µm	62%	812	0.295
338-006A	YSZ-3/8 (70/30)	160 µm	40 µm	62%	787	0.287
338-052B	YSZ-3/8 (70/30)	160 µm	40 µm	62%	850	0.280
338-053C	YSZ-3/8 (70/30)	160 µm	40 µm	62%	712	0.329
330-177A	YSZ-3/8 (70/30)	160 µm	40 µm	62%	725	0.311

Notes
Power density data obtained at 800°C (H_2 fuel, 0.7 volts, low fuel utilization).
ASR calculated from 800°C data (0.6 to 0.8 volts, low fuel utilization).

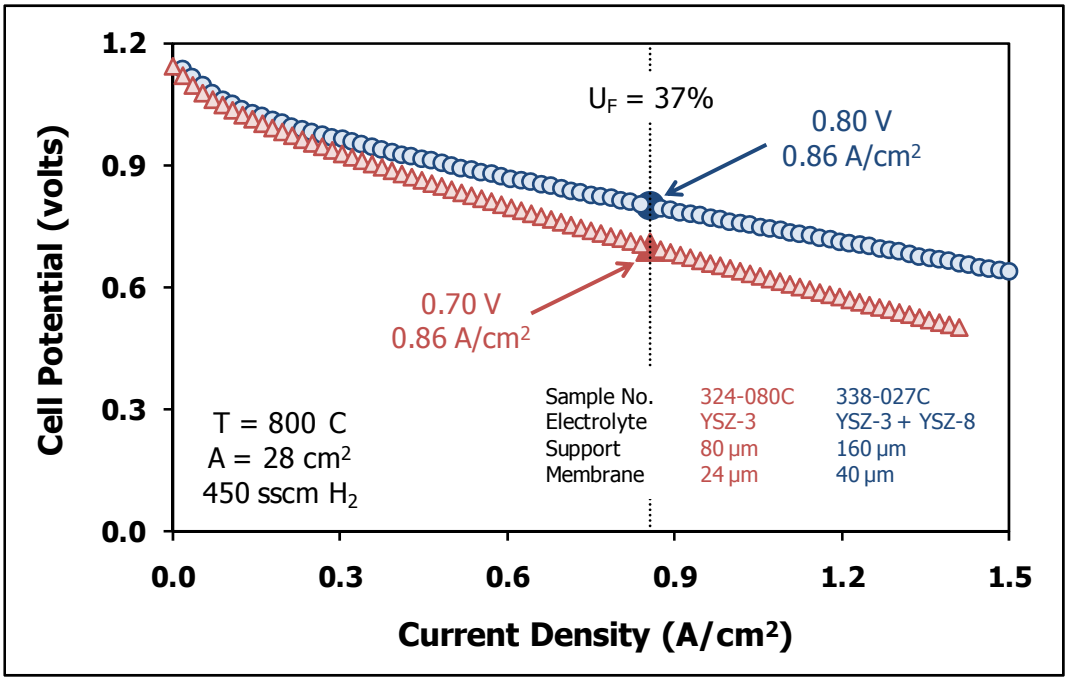

Figure 16. Comparison of single-cell SOFC performance of a thin YSZ-3 *FlexCell* and a thick YSZ-3/8 *FlexCell* (hydrogen fuel, low utilization).

In order to better understand the observed performance improvements, ionic conductivity measurements were performed on a sintered ceramic of the YSZ 3/8 formulation and compared to previous data obtained on YSZ-3 and YSZ-8 ceramics. A ball-milled mixture of YSZ-3 and YSZ-8 powders (30% YSZ-8) was isostatically pressed into discs and sintered at 1450°C; bar-shaped specimens were cut from the discs and subjected to four-point conductivity measurements over the range of 700 to 850°C. From these data, conductivity values were calculated. Arrhenius plots are compared for YSZ-3, YSZ-8 and YSZ-3/8 ceramics in Figure 17. Arrhenius slopes (i.e., activation energies) are similar for YSZ-3, YSZ-8 and YSZ-3/8 ceramics, and the ionic conductivity of YSZ-3/8 ceramic is intermediate to that of YSZ-3 and YSZ-8. Electrochemical impedance spectroscopy (EIS) data also were obtained during single-cell SOFC testing of two YSZ-3/8 based *FlexCells* during operation at 0.7 volts with diluted hydrogen as fuel. An example of the type of data collected is shown in Figure 18. From these data, ohmic and non-ohmic contributions to area-specific resistance (ASR) were determined (see Table 7).

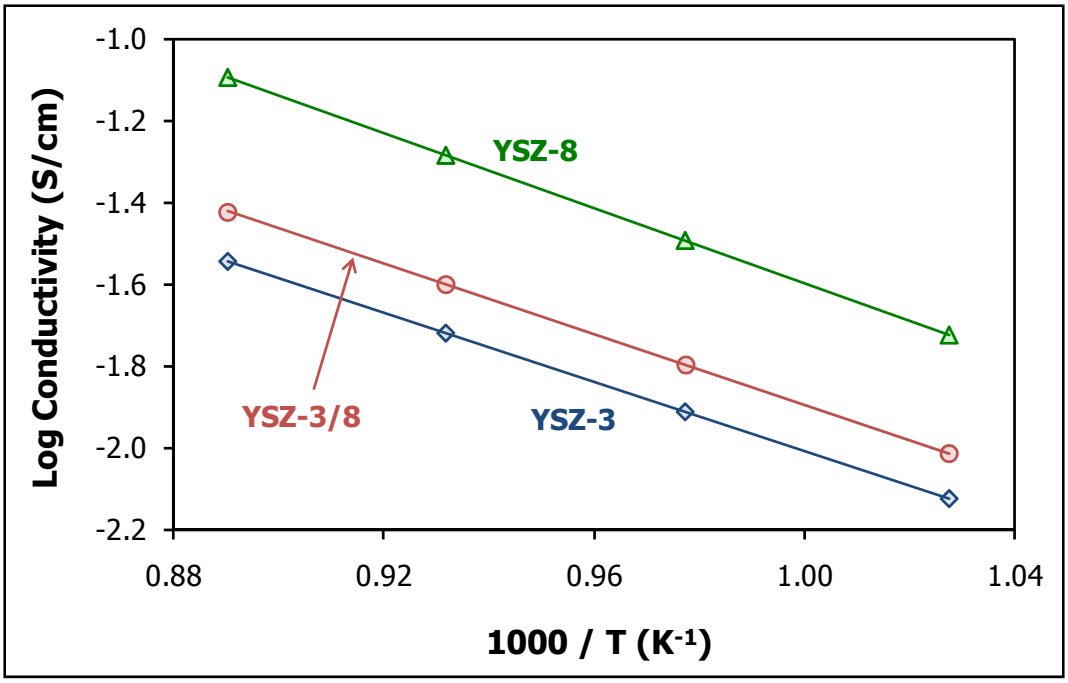

Figure 17. Arrhenius plots of ionic conductivity data for YSZ-3, YSZ-8 and YSZ-3/8 ceramics.

Table 7. Ohmic and non-ohmic contributions to area-specific resistance for YSZ-3/8 *FlexCells* during SOFC operation at 0.7 volts with hydrogen as fuel (measured by electrochemical impedance spectroscopy).

T (°C)	Sample No. 338-53C (Ω-cm^2)			Sample No. 338-58A (Ω-cm^2)		
	Ohmic	Non-Ohmic	Total	Ohmic	Non-Ohmic	Total
700	0.57	0.36	0.93	0.51	0.88	1.39
750	0.33	0.29	0.62	0.39	0.53	0.92
800	0.23	0.13	0.36	0.27	0.34	0.61
850	0.18	0.07	0.25	0.19	0.22	0.41

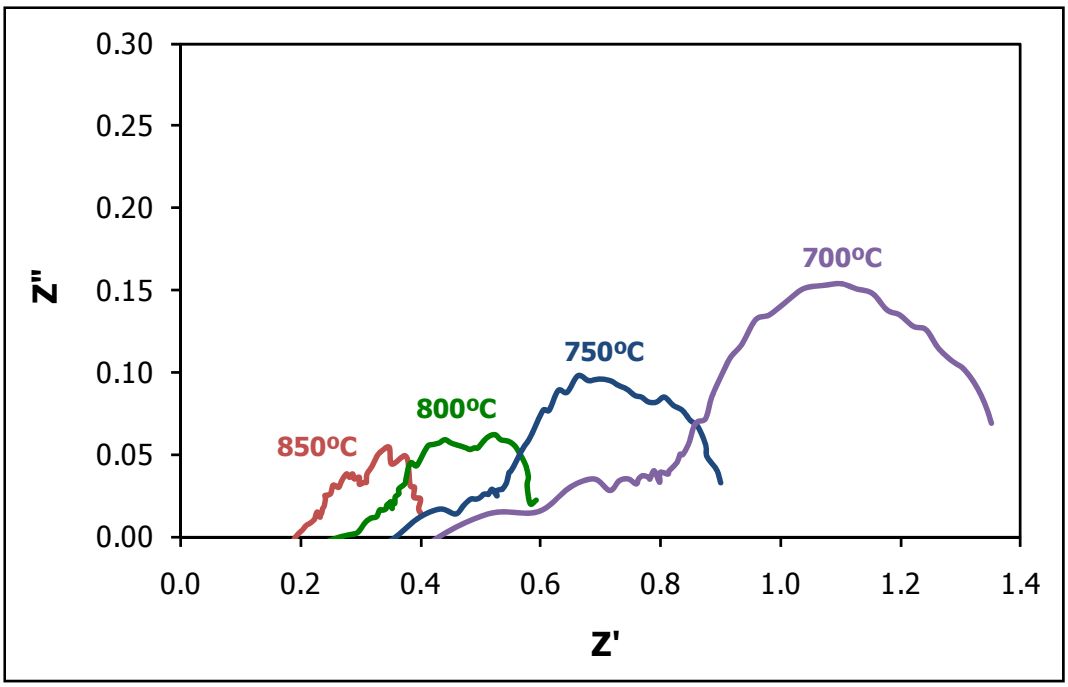

Figure 18. Impedance results of YSZ-3/8 cell (Sample Number 338-053C).

The above ohmic ASR values (corresponding to electrolyte resistance) are compared to electrolyte ASR values calculated from four-point conductivity data in the Arrhenius plot shown in Figure 19. The calculated ASR values were based on an assumption of the parallel resistance model.

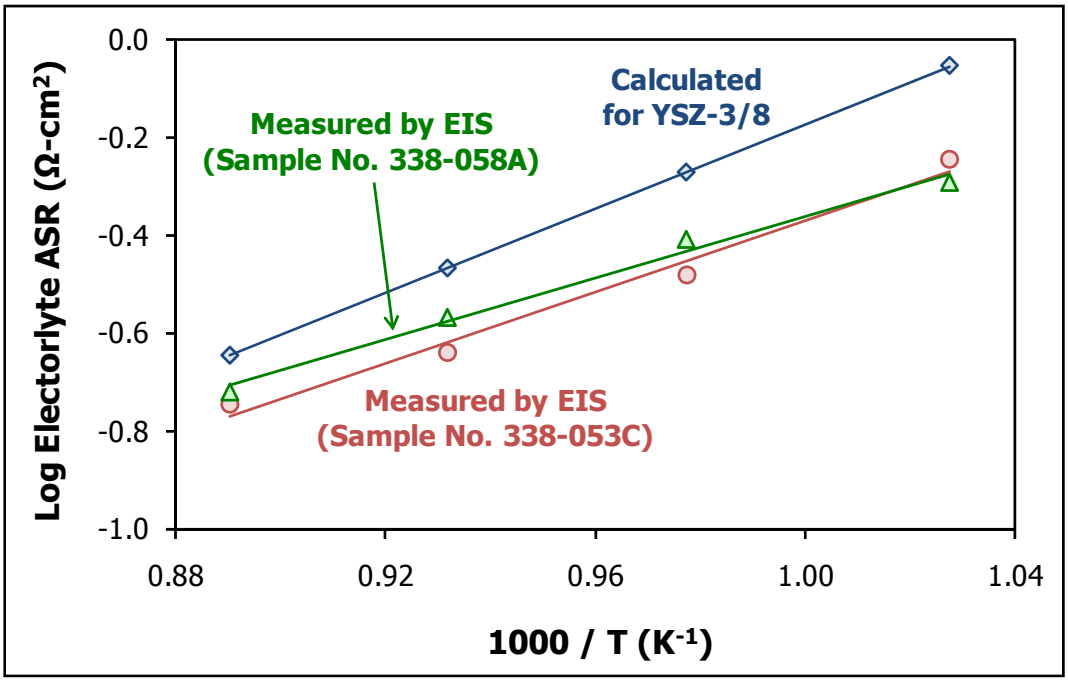

Figure 19. Arrhenius plots of electrolyte ASR for YSZ-3/8 *FlexCells*.

The electrolyte ASR values measured by EIS during SOFC testing are significantly lower than those predicted based on bulk ionic conductivity measurements. This is consistent with higher than expected SOFC performance of YSZ-3/8 *FlexCells*. We hypothesize that thickness is an important consideration, given thicknesses differences between the bi-layer *FlexCell* membranes (~40 μm) and the bar-shaped specimens used for measuring four-point conductivity (~5 mm). Specifically, NexTech applies sintered ceria barrier layers on both faces of the *FlexCell* membranes. One could hypothesize that ceria diffusion into the partially stabilized YSZ electrolyte layer could positively impact ionic conductivity, either by increasing ionic conductivity due to a compositional change or by creating a synergistic stress state in the YSZ membrane.

Long-Term Single-Cell Testing

Several long-term single-cell tests were conducted during the project on 28-cm^2 active area cells, initially on YSZ-3 *FlexCells* and subsequently with YSZ-3/8 *FlexCells*. A long-term test was conducted on the YSZ-3 *FlexCell* with 80-micron thick support and 24-micron thick membrane layers. This cell was tested under constant current conditions for more than 1300 hours at 750°C with diluted hydrogen (50% H_2, 50% N_2 as fuel) at a current density of 0.36 A/cm^2 and 70% fuel utilization. These data are presented in Figure 20, which indicate that some degradation occurred during the test, but that this degradation slowed with time.

Single-cell SOFC tests were conducted on a similar cell with simulated coal gas (20% H_2, 18% CH_4, 22% CO_2, and 40% H_2O) as fuel. These tests were conducted with a fuel utilization of 70 percent, at temperatures of 750, 800 and 850°C (see Figure 21). The initial degradation rate observed in this test was lower compared to the above described test with diluted hydrogen as fuel. However, the degradation rate was higher at lower temperatures (60 μv/hour at 800°C and 113 μv/hr at 750°C). These coal gas data were obtained with a mass spectrometer being used to analyze the anode exhaust gas composition. Data obtained at 800°C and 70% fuel utilization are presented in Figure 22. It should be noted that with electrolyte supported *FlexCells*, the nickel-based anode layer is too thin to provide internal reforming capability – the nickel foam anode current collector provides this function. In these initial tests, complete methane conversion was achieved, but the H_2 content was lower and CO content higher than expected based on water-gas-shift equilibrium. Subsequent work was performed to incorporate reforming catalysts into nickel foam anode current collectors used during single-cell and short-stack testing. Data presented in Figure 23 demonstrates that infiltration of catalyst material greatly improves the methane reforming activity of nickel foams.

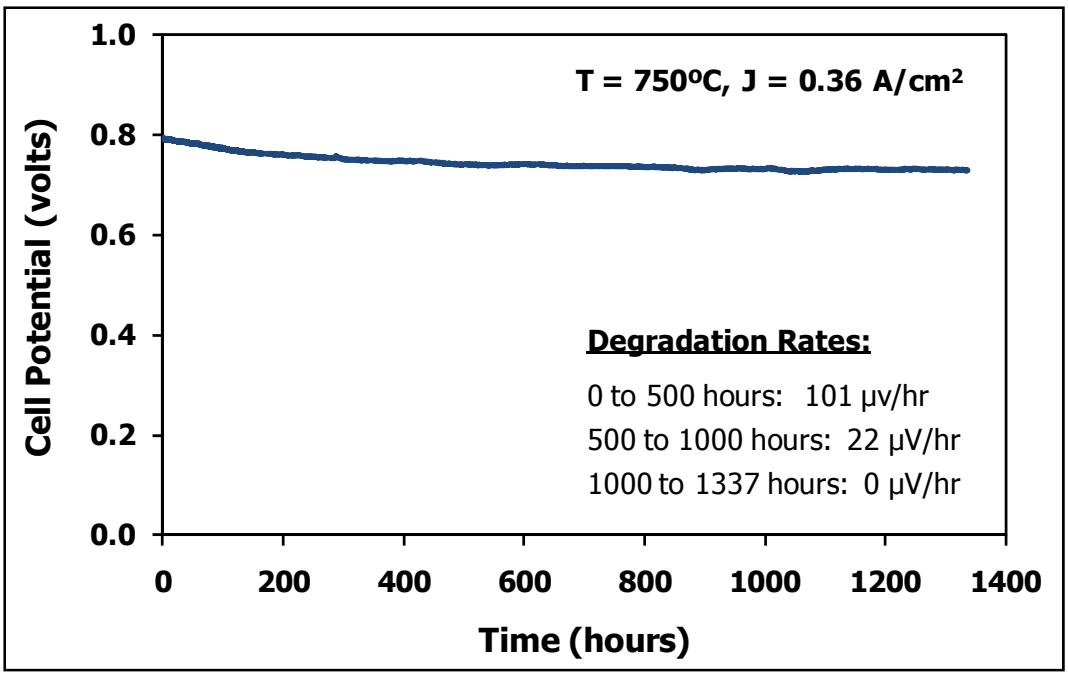

Figure 20. Long-term, constant-current test results for the YSZ-3 *FlexCell* with ultra-thin support and membrane layers (Sample No. 324-080C).

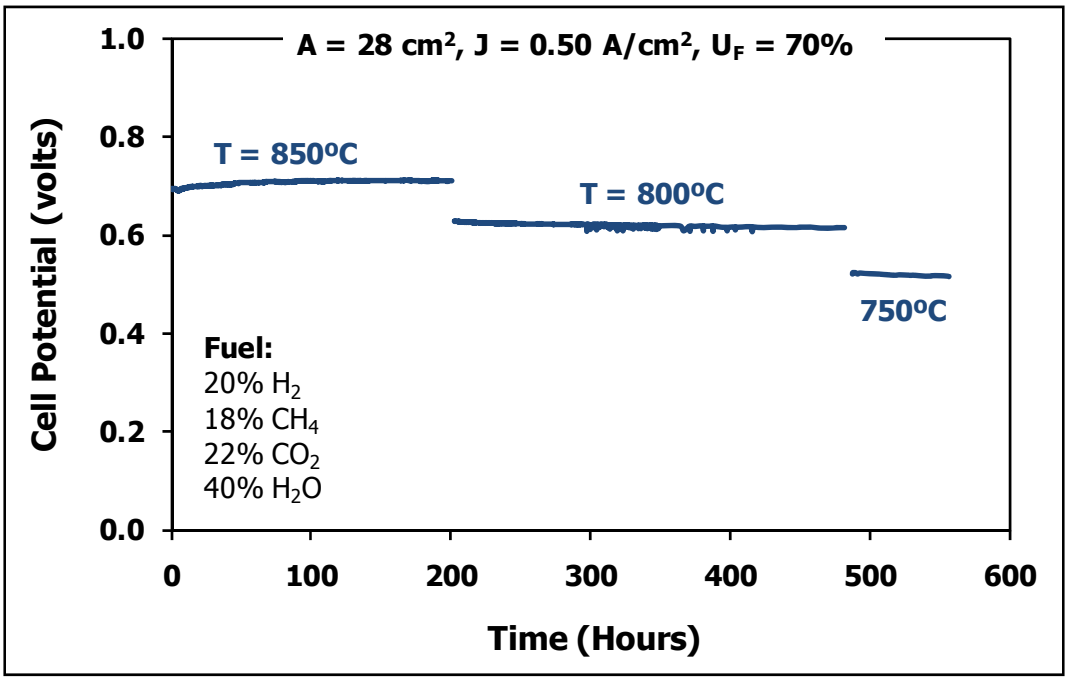

Figure 21. Long-term coal gas test results for YSZ-3 *FlexCell* with thin support and membrane layers (Sample No. 324-103B).

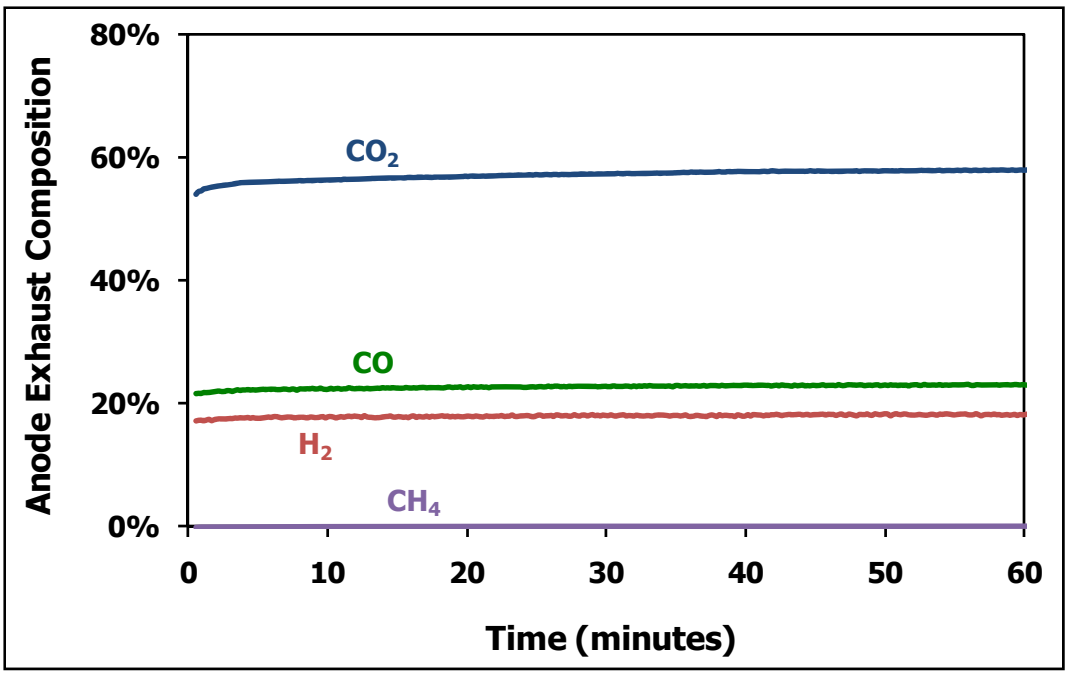

Figure 22. Mass spectrometer analysis of anode exhaust composition during simulated coal gas testing at 800°C and 70 percent fuel utilization (Sample No. 324-103B).

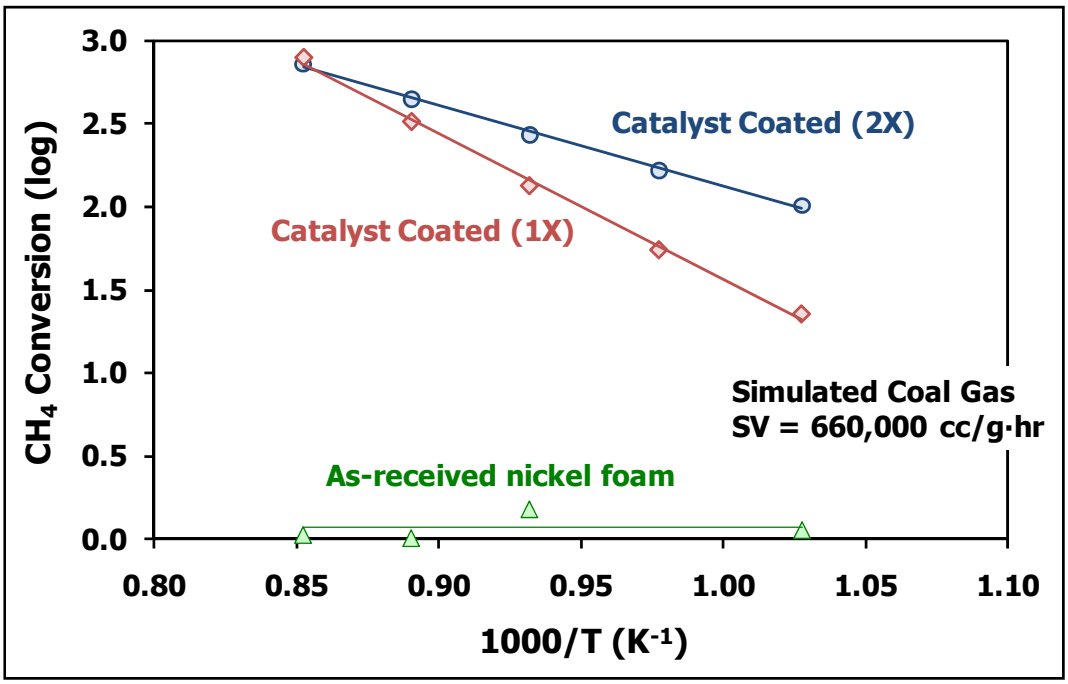

Figure 23. Methane steam reforming activity of nickel foams, with and without infiltrated catalyst.

Long-term coal gas tests were performed on YSZ-3/8 *FlexCells* using the catalyst-infiltrated nickel foam anode current collectors and a fuel composition (dry basis) consisting of 30.0% CH_4, 33.3% H_2, and 36.7% CO_2. The impact of steam content on cell performance and long-term stability was evaluated to determine the optimum steam content in fuel feed. A minimum amount of steam is required for efficient and coke-free internal methane reforming, whereas excessive steam potentially will cause degradation via anode oxidation. Initial tests were conducted with coal gas feed having a steam to methane ratio of 2.2. Mass spectrometry was used during SOFC testing to measure anode exhaust composition, from which steam contents were calculated (see Figure 24). As is shown in the figure, under these conditions, steam content in the anode exhaust was reduced from 64 to 51 percent, as fuel utilization was reduced from 70 to 50 percent.

A long-term test was conducted at 800°C with an input H_2O/CH_4 ratio of 2.2, current density of 0.46 A/cm^2 and fuel utilization of 60 percent (see Figure 25). Under these conditions, the initial area-specific cell power density was 330 mW/cm^2 and the steam content in the anode exhaust was approximately 64 percent. A steady-state degradation rate of 68 μV/hour was observed over 600 hours of testing. Two additional tests were conducted at 800°C with an H_2O/CH_4 ratio of 1.5, current density of 0.54 A/cm^2, and fuel utilization of 50 percent (see Figure 26). Under these conditions, initial power density for both cells was 390 mW/cm^2, and the exit steam content was approximately 50 percent. Steady-state degradation rates of 40 and 57 μV/hour were observed in these tests. It was apparent that the lower steam content in the anode exhaust led to an improvement in degradation rate.

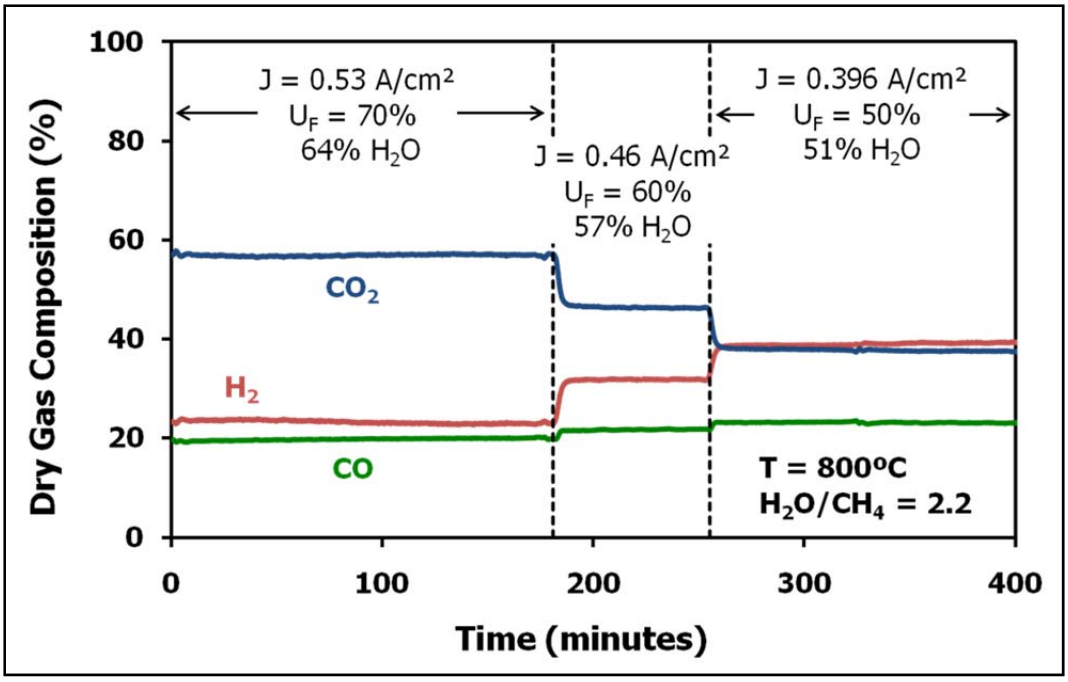

Figure 24. Mass spectrometry data used to determine steam content in anode exhaust at varying current densities and fuel utilizations during SOFC testing with simulated coal gas (T=800°C, H_2O/CH_4 = 2.2).

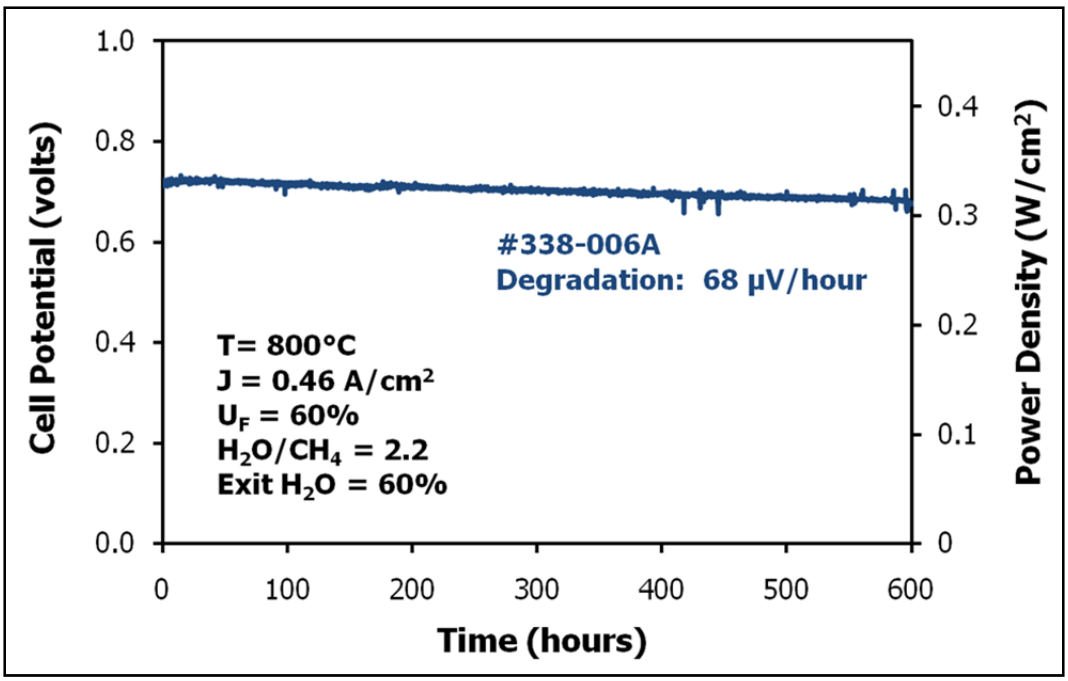

Figure 25. Long-term, test results for a YSZ-3/8 based *FlexCell* at 800°C with simulated coal gas as fuel (H_2O/CH_4 = 2.2, J = 0.46 A/cm^2, U_F = 60 percent).

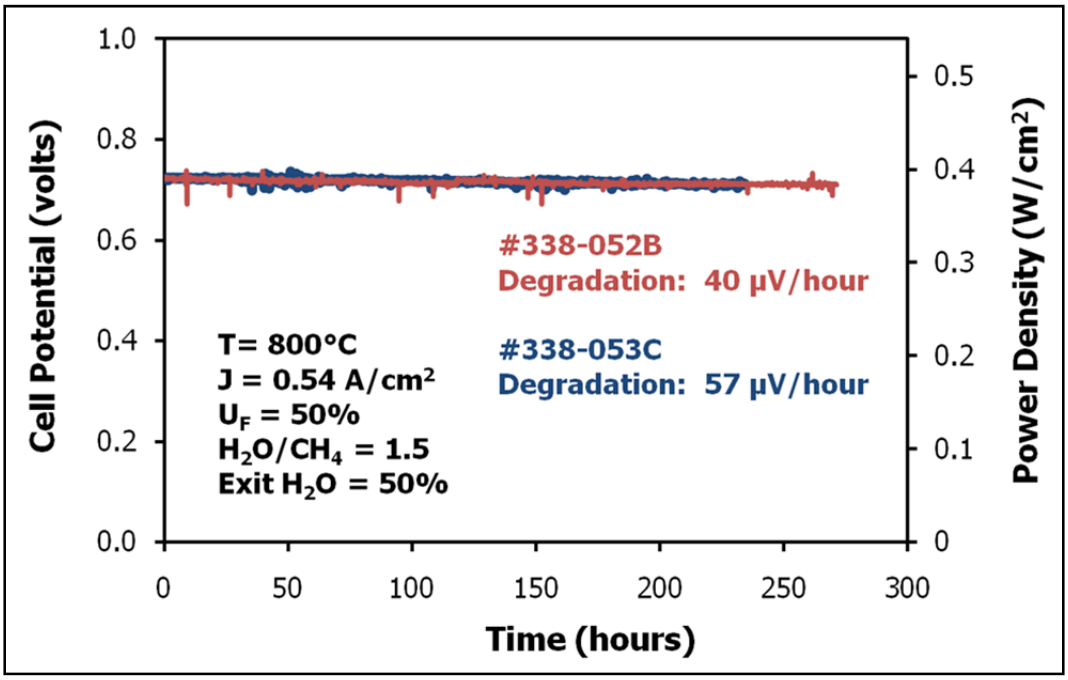

Figure 26. Long-term, test results for two YSZ-3/8 based *FlexCells* at 800°C with simulated coal gas as fuel (H_2O/CH_4 = 1.5, J = 0.54 A/cm^2, U_F = 50 percent).

Degradation rates in the above described coal-gas tests were significantly higher than originally targeted, and one potential cause was attributed to non-uniform steam delivery to the cell. Lower degradation rates were observed with improved steam delivery methods and with optimized catalyst loading in the anode current collector foam (see Figure 27). The observed degradation rate was significantly lower (30 µV/hr), but still higher than targeted. Cathode current collection was suspected to be responsible for some of this degradation, based on comparison of degradation rates observed in long-term testing of ScSZ-based *FlexCells* with diluted hydrogen as fuel (also shown in Figure 27). The degradation rates were essentially the same. It was believed that this degradation was related to the use of silver for cathode current collection. As shown in Figure 28, the replacement of silver mesh with manganese cobalt oxide coated alloy current collector meshes significantly improved long-term durability in tests on ScSZ-based *FlexCells* with diluted hydrogen fuel. There still was some degradation with the alloy mesh current collector, but this could be due to the presence of silver in the cathode contact paste or to chromium poisoning of the cathodes.

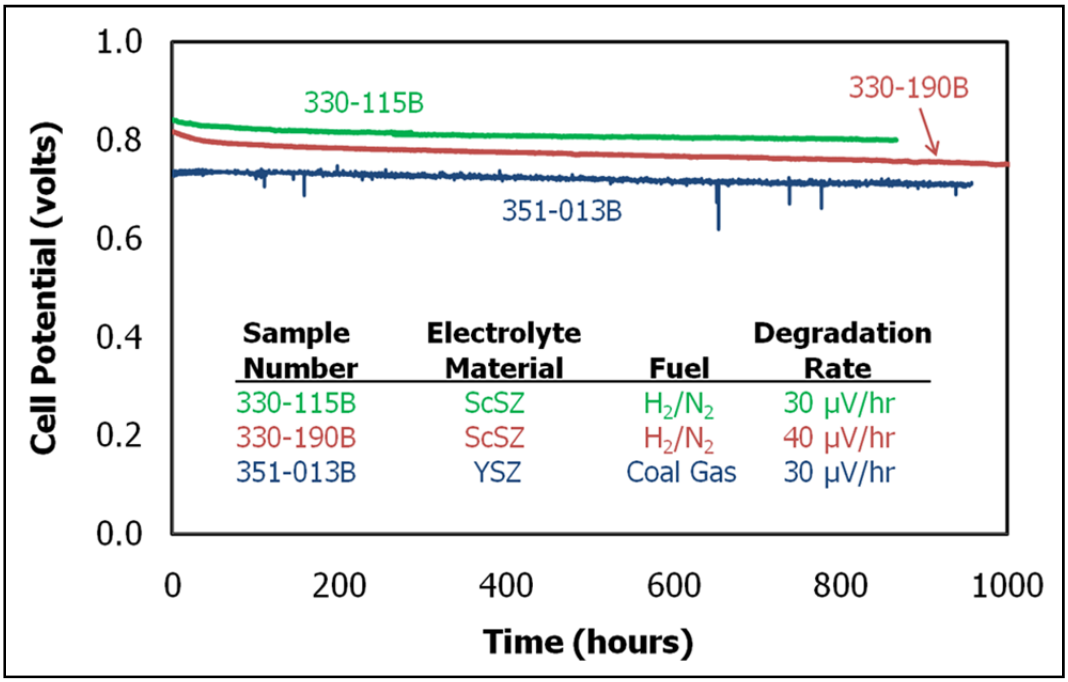

Figure 27. Comparison of long-term single-cell tests: YSZ-based *FlexCell* with simulated coal gas as fuel and ScSZ-based *FlexCells* with diluted hydrogen as fuel.

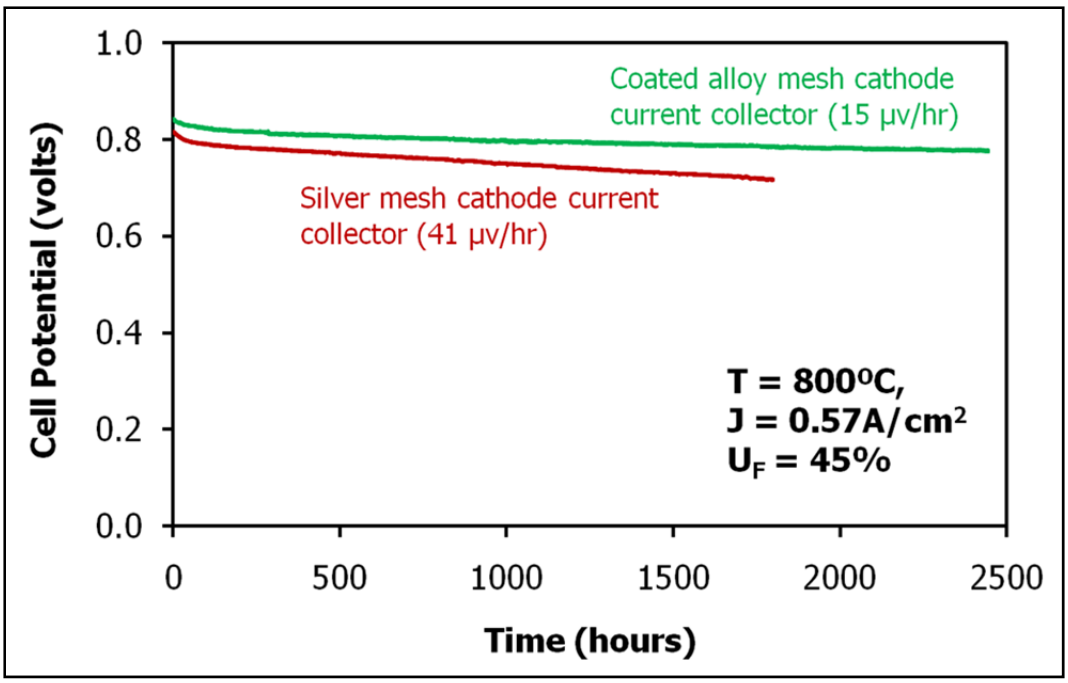

Figure 28. Long-term single-cell tests on ScSZ-based *FlexCells* with diluted hydrogen fuel, showing lower degradation rate with an MCO-coated alloy mesh cathode current collectors.

Process Enhancements and Quality Control

A key accomplishment of the project was the successful transition of all stack fabrication and testing work at NexTech to YSZ-based *FlexCells*. This transition was enabled by the high performance obtained in YSZ-3/8 *FlexCells* (as described previously) and by the successful fabrication of stack-intent *FlexCells* (see Figure 29). This greatly increased the number of YSZ-based *FlexCells* that were manufactured during the project (more than 700 *FlexCells* were made for stack builds at NexTech). Fabricating cells at such volumes enabled NexTech to identify and implement process improvements, collect process control data, establish quality control protocols. Process improvements and quality controls implemented for *FlexCell* manufacturing at NexTech during the project are listed in Table 7.

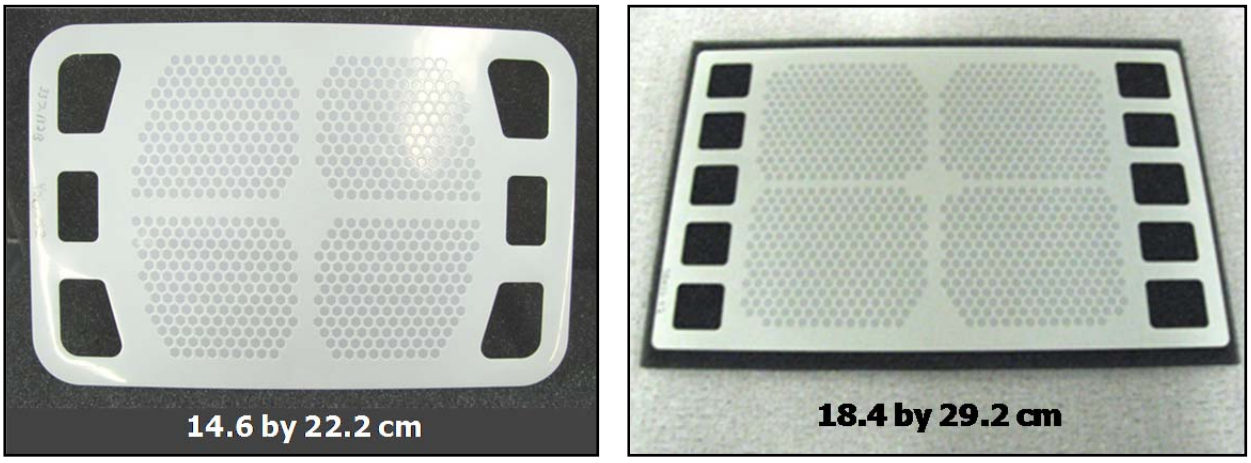

Figure 29. *FlexCell* membranes for NexTech's G-13 (left) and G-15 (right) stack designs.

Table 7. Improved quality and process controls implemented for *FlexCell* manufacturing.

Year/Process	Electrolyte Tape	Laminate and Cut Substrates	Sintering of Substrates	Electrode Deposition	Annealing of Electrodes
2008	▪ Tape thickness ▪ Visual inspection ▪ Tape lot records	▪ Machine controls ▪ Tape shrinkage check ▪ Visual inspection	▪ Thermocouple readings ▪ Visual inspection ▪ Thickness measurement	▪ Raw material qualifications ▪ Visual inspection ▪ Print weights	▪ Visual inspection ▪ Tape adhesion testing
2009	▪ Improved raw material acceptance system and batch documentation	▪ Document control over cutting designs ▪ Laminate thickness ▪ Laminate orientation	▪ Process temperature control rings ▪ Furnace position traceability ▪ Ethanol leak check ▪ Visual flatness check	▪ Improved batch records ▪ Process control to target print weight	▪ Process temperature control rings ▪ Furnace position traceability ▪ Ethanol leak check ▪ Flatness check (visual)
2010	▪ Improved green tape qualification process	▪ Protocols for removing debris after laser cutting ▪ Additional SPC data	▪ Red dye check ▪ High potential test ▪ Laser flatness test ▪ He leak test	▪ Improved masking of active area ▪ Uniform electrode deposition	▪ Helium leak test ▪ SPC data ▪ High potential test ▪ Laser flatness test
2011	▪ Improved materials qualification testing	▪ Integrated SPC charting with electronic batch templates	▪ Improved high potential test protocols	▪ Retargeting of anode and cathode thicknesses	▪ Improved high potential test protocols and final inspection standards

Through Pareto analysis of manufacturing loss, initiatives were launched to improve electrolyte tape quality, improve cell flatness, increase density of sintered electrolyte substrates, and reduce part-to-part variation in deposited electrode coating thickness. Optimization of unit operations (including lamination, laser cutting, sintering, and electrode deposition) was instrumental in achieving these quality improvements. The process optimization work enabled NexTech to increase manufacturing yields to more than 80 percent and reduce manufacturing cost by approximately 70 percent. Examples of SPC charts are shown in Figures 30 and 31, which provide quantitative evidence of the quality improvements made with respect to deposited electrode weights and overall cell flatness. Other examples of SPC charts are shown in Figures 32 and 33. The importance of the process enhancements described above (as pertaining to stack fabrication) is exemplified by the improvements in overall cell flatness (see Figure 34) and surface quality (see Figure 35). Success of the process optimization and quality control work at NexTech during the project is evidenced by the high manufacturing yields (see Figure 36).

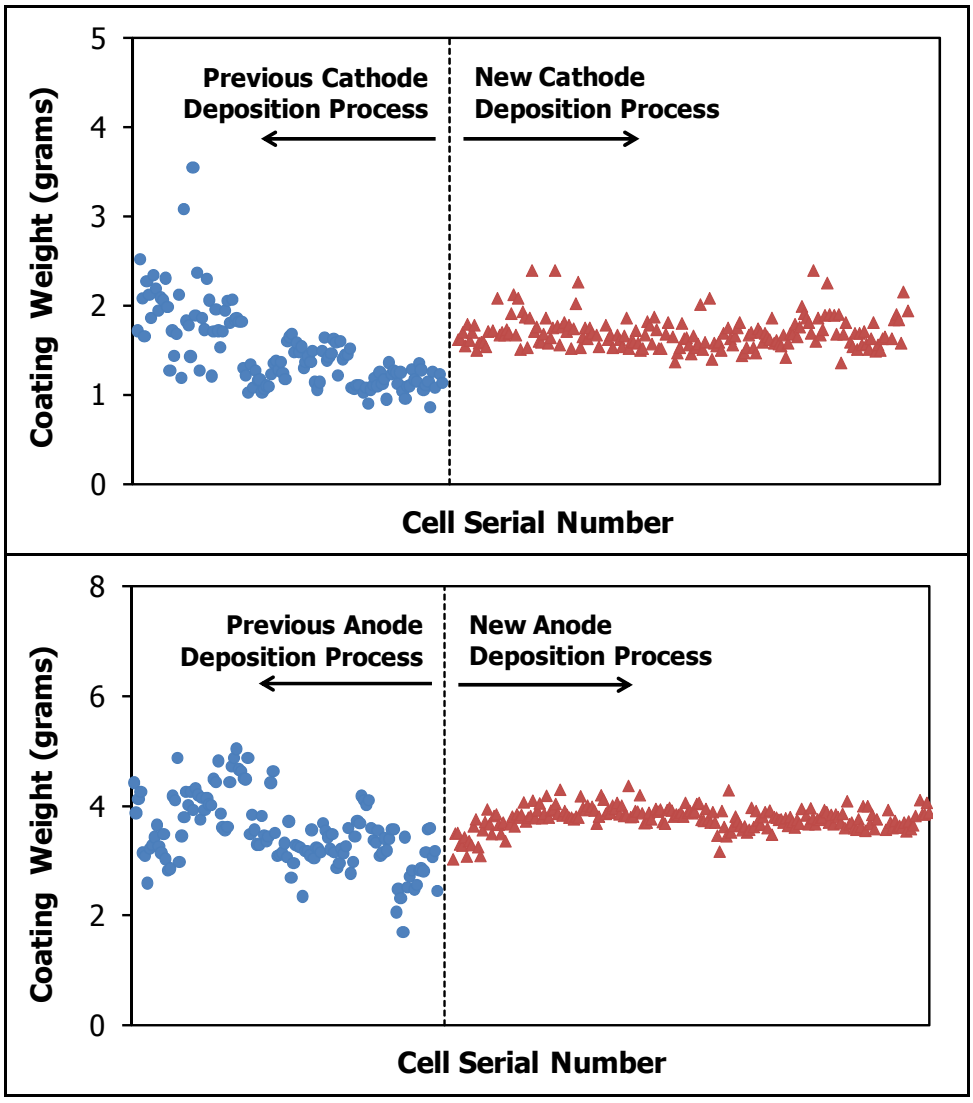

Figure 30. Improvements made to the electrode deposition processes at NexTech led to tighter tolerances on deposited electrode weights.

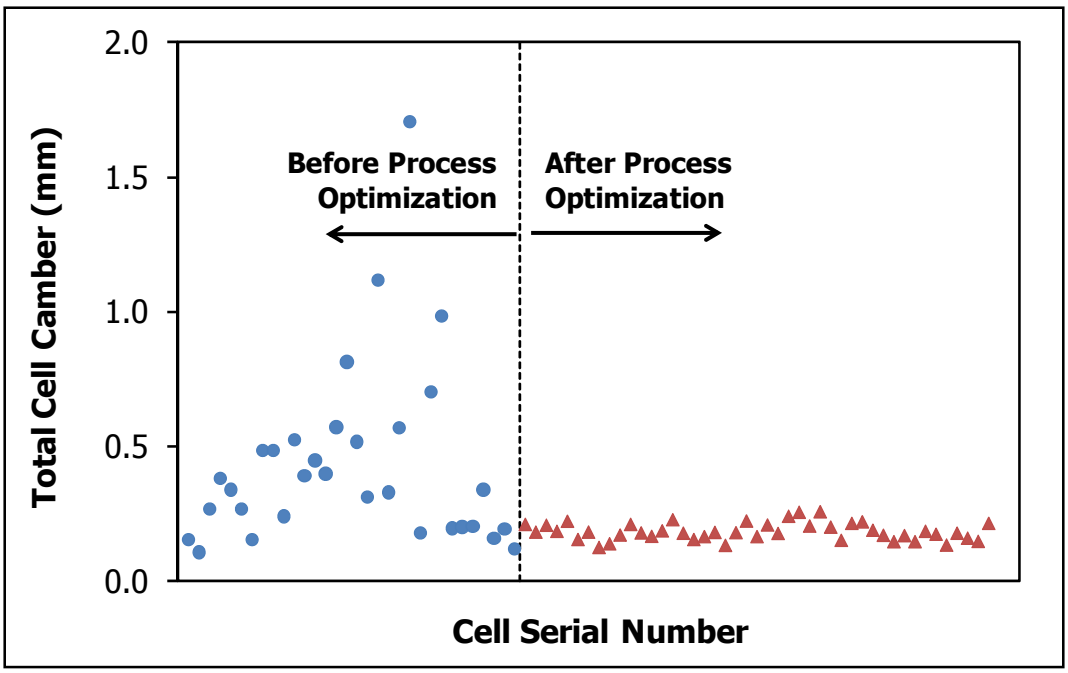

Figure 31. Substantial improvements in cell flatness obtained were made by implementing improved tape casting formulations and by optimizing sintering cycles and kiln furniture arrangements.

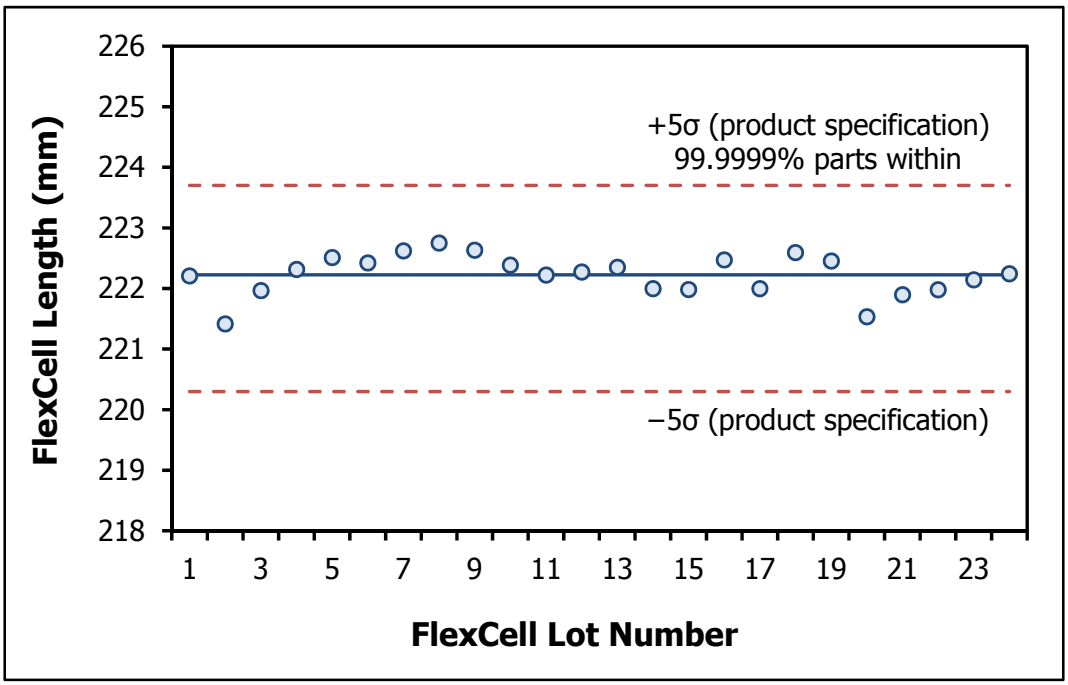

Figure 32. Example of SPC chart, showing conformity of *FlexCell* geometry specifications.

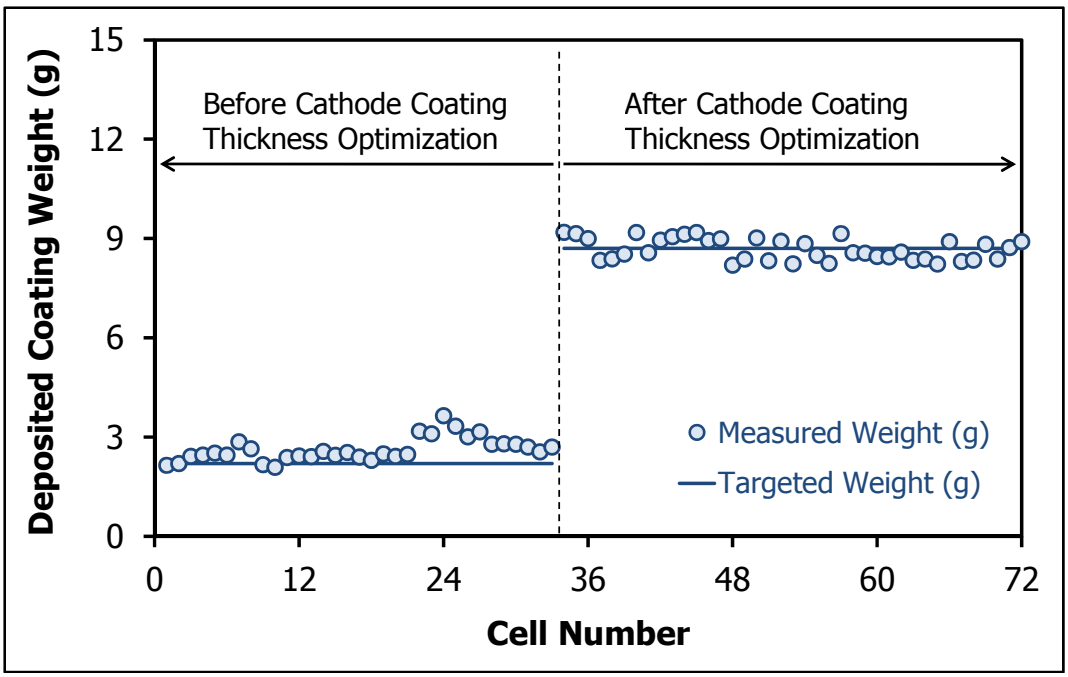

Figure 33. Example of SPC chart, showing conformity of cathode coating weight specifications before and after optimization efforts.

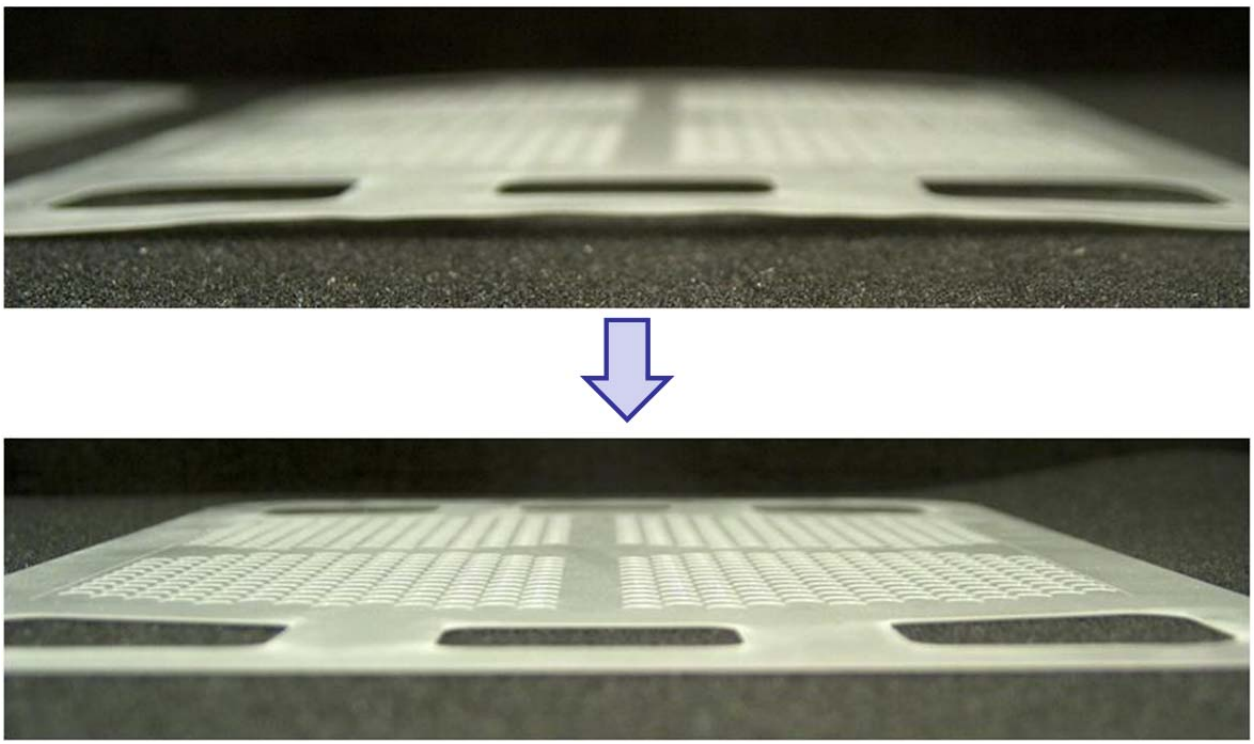

Figure 34. Improved flatness in *FlexCells* obtained with process improvements and quality control.

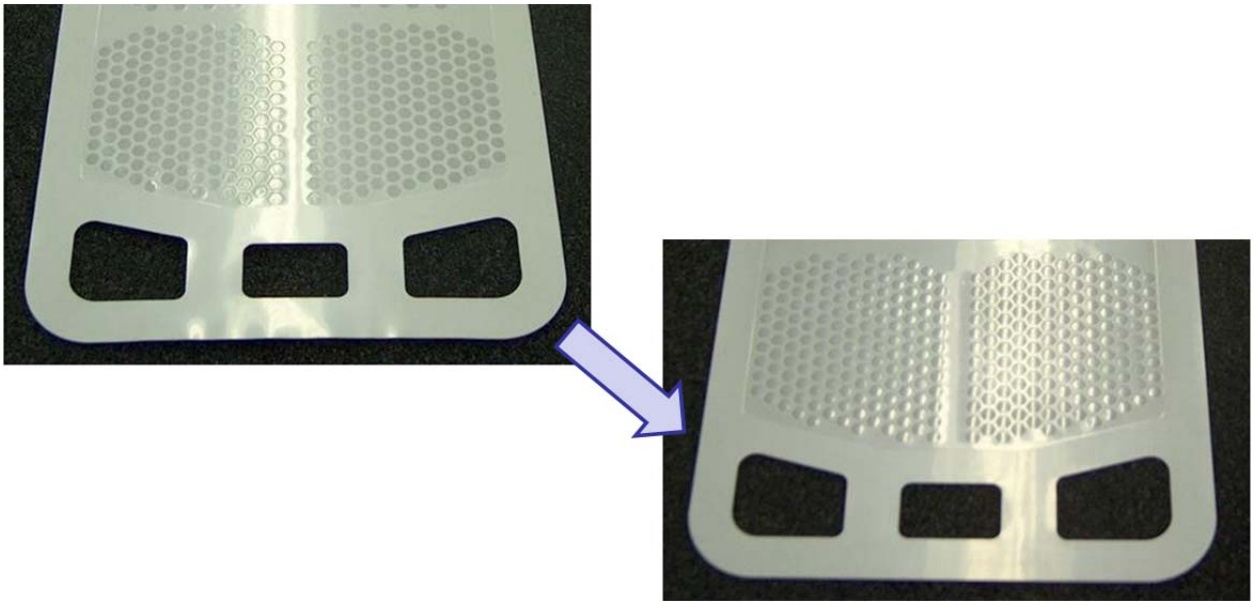

Figure 35. Improved *FlexCell* surface quality obtained with process improvements and quality control.

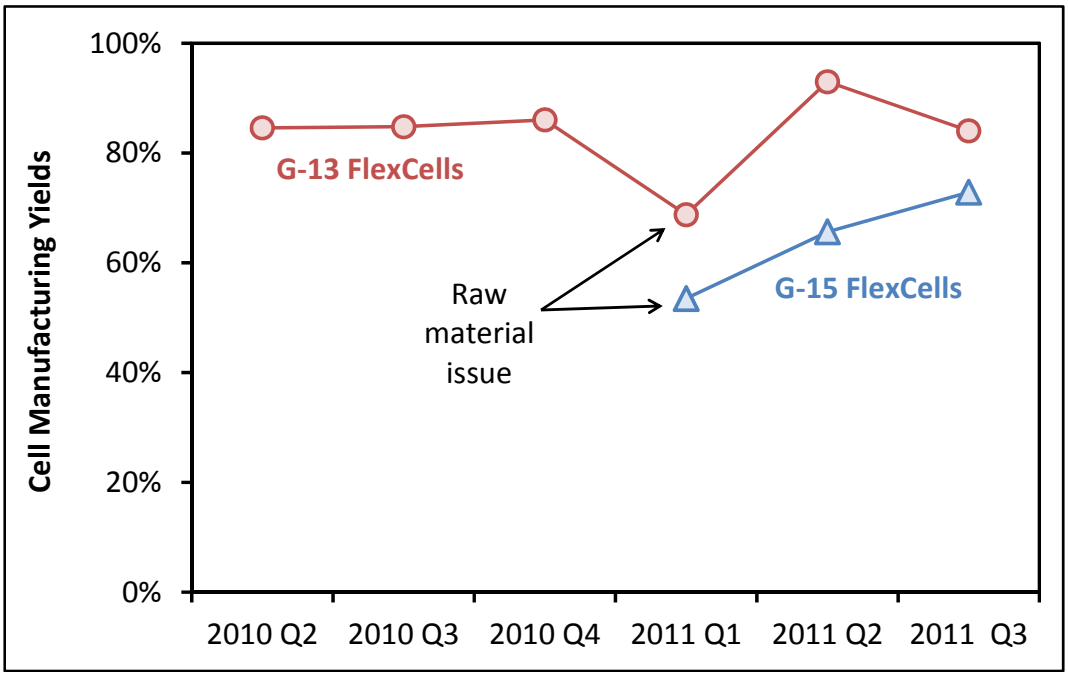

Figure 36. Manufacturing yields of stack intent *FlexCells* during the project.

Fabrication and Testing of Large-Area *FlexCells*

Results of finite element analysis modeling work performed by Ohio State University (to be described separately) were used to aid the design of the large-area *FlexCells* with improved mechanical robustness. In some of the early large-area *FlexCells* made at NexTech, the membrane width was higher at the cell perimeters (see Figure 37). This "frame" was intended to provide additional mechanical support to the membrane structure. One of the first design changes suggested by Ohio State's modeling work was to

eliminate this frame, a design change that led to an immediate (and significant) improvement in cell manufacturing yield. Additional modeling work at Ohio State led to the large-area *FlexCell* membrane design shown in Figure 38. The total cell area is 475 cm² and the active cell area (exclusive of internal ribs) was 330 cm². A production run was completed on a batch of large-area YSZ-based *FlexCells* of the design shown in Figure 38 (the batch size was 27 cells). In this production run, all 27 cells passed quality checks through the substrate sintering operation, and 23 completed cells passed quality checks after the electrode deposition operations. This corresponds to a manufacturing yield of 85 percent. Examples of completed YSZ-based *FlexCells* are shown in Figure 39.

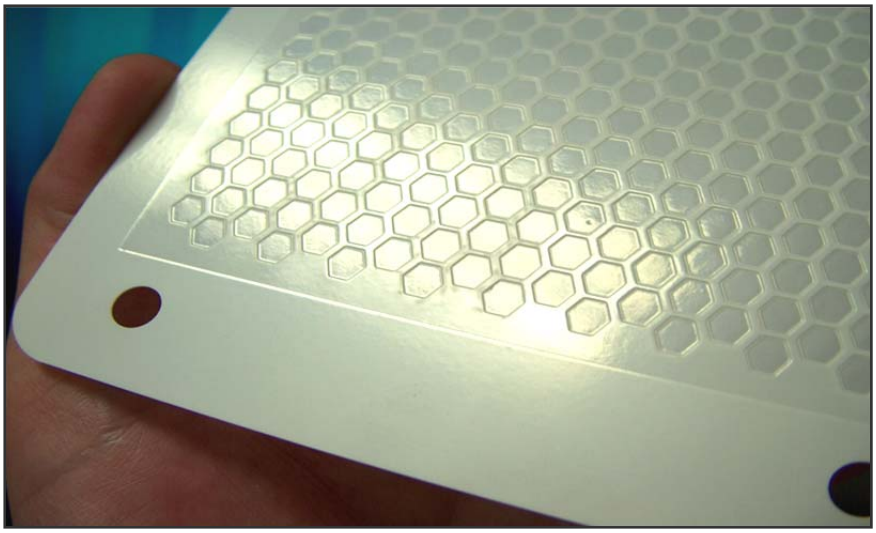

Figure 37. *FlexCell* membrane made with additional width at cell perimeter.

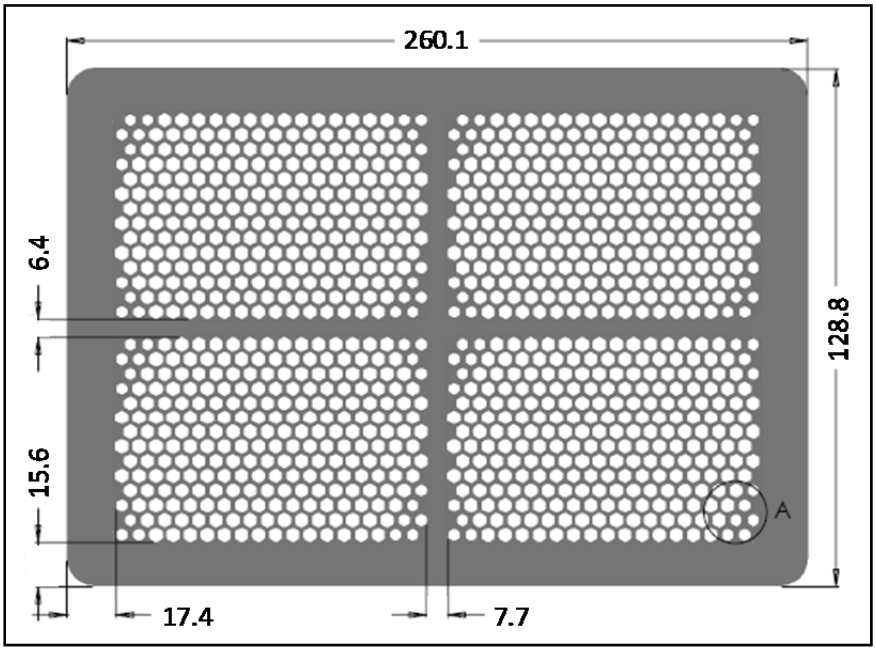

Figure 38. Large-area *FlexCell* membrane design incorporating modeling results (dimensions in mm).

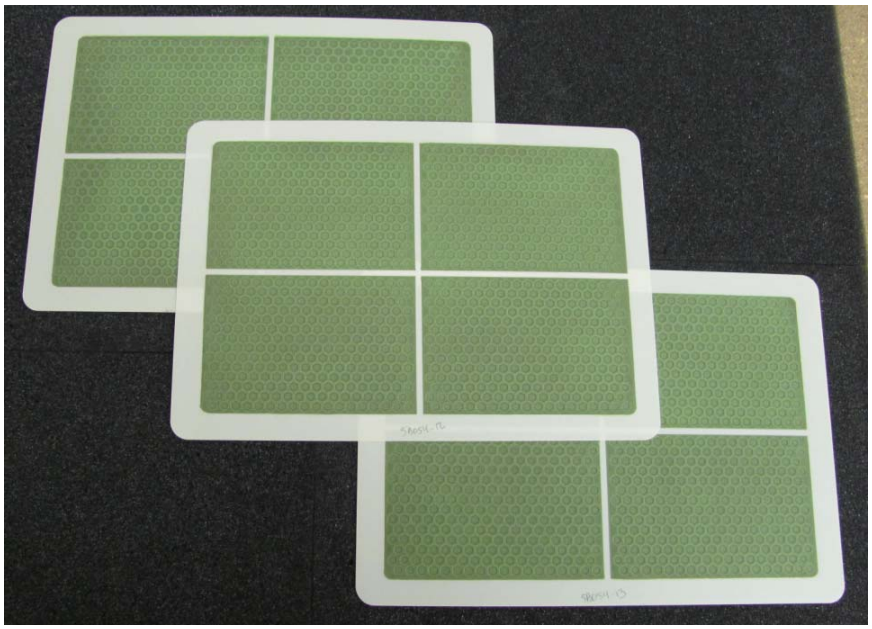

Figure 39. Large-area YSZ-based *FlexCells* (475 cm^2 total area, 330 cm^2 active area).

A number of large-area single-cell tests were completed for the large-area *FlexCells* shown in Figure 40. Manifolds for these tests are made from Crofer 22 APU alloy, and are shown in Figure 40. Nickel foam anode current collectors are pressed into hexagonal patterns and placed on the corrugated face of the anode manifold, along with a vermiculite seal, as shown in Figure 41. For testing with coal gas, the nickel foams are infiltrated with NexTech's proprietary catalyst material. The *FlexCell* then is placed anode-face down on the anode current collectors, as shown in Figure 42. Silver mesh cathode current collectors then are placed on the cathode face of the *FlexCell*, as shown in Figure 43. A cathode-face seal (also vermiculite) is placed on the periphery of the *FlexCell*, and cathode manifold then is placed on top to complete the assembly. Nickel metal inks are applied to the anode faces of the *FlexCell* and to the mating face of the anode manifold to facilitate anode-side electrical contacts. Similarly, LSM based inks are applied to the cathode faces of the *FlexCell* and to the mating face of the cathode manifold to facilitate cathode-side electrical contacts. Platinum wire leads are used for voltage pickups, which are located between the *FlexCell* and the corresponding current collector foam/mesh components.

Computational fluid dynamics (CFD) modeling was used to support the deign of the large-area single-cell testing manifolds. CFD modeling data presented in Figures 44 and 45 show that the as-designed manifolds provided uniform fuel flow distribution and low pressure drop.

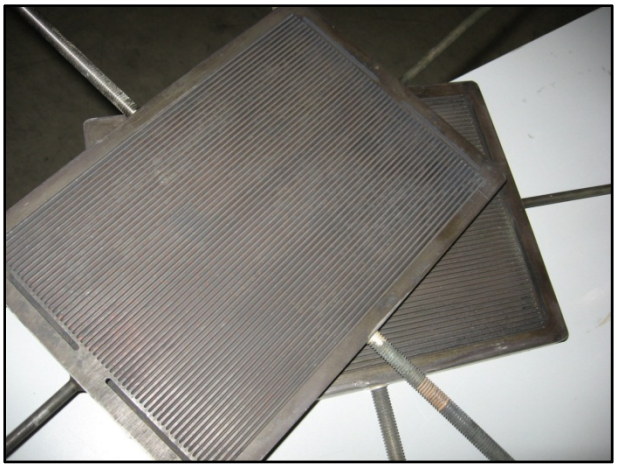

Figure 40. Manifolds for large-area cell tests.

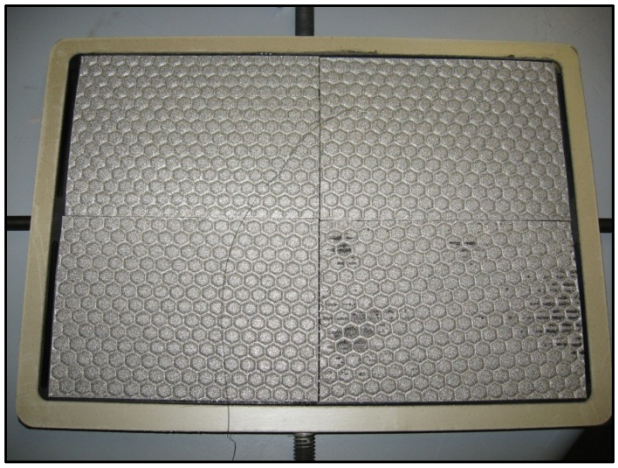

Figure 41. Ni-foam anode current collectors and vermiculite seal are placed on the anode manifold.

Figure 42. *FlexCell* (anode-face down) placed on the Ni-foam current collectors.

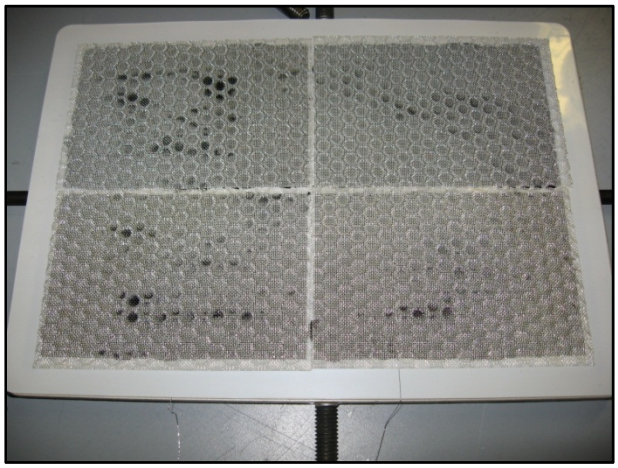

Figure 43. Silver-mesh cathode current collectors placed on cathode face of *FlexCell*.

The above-described assembly then is placed in the testing furnace and a relatively small load is applied. The assembly is heated to the operating temperature with nitrogen flowing through the anode channels and air flowing through cathode channels. Once at temperature, the anodes are reduced according to NexTech's proprietary protocols, and the cell then is subjected to testing. Tests were conducted with the furnace temperature set at 800ºC, with diluted hydrogen as fuel (50% H_2, 50% N_2). In the first test, the fuel flow rate was set at 4.6 lpm (2.3 lpm H_2) and the air flow rate was set at 16 lpm. Under these conditions, the open circuit voltage was 1.255 volts. Current then was stepped up at a rate of 2.5 amps per minute to generate a pole curve. As shown in Figure 46, 148 watts was obtained at 0.725 volts. This corresponded to a current density of 0.621 A/cm^2 and fuel utilization of approximately 60 percent. The fuel flow rate was lowered to 4.0 lpm (2.0 lpm H_2) without changing the air flow rate (16 lpm). Under these conditions, the open circuit voltage was 1.246 volts. A second pole curve was generated as described above (see Figure 47), and 135 watts was obtained at a potential of 0.680 volts. This corresponded to a current density of 0.602 A/cm^2, and fuel utilization of approximately 70 percent.

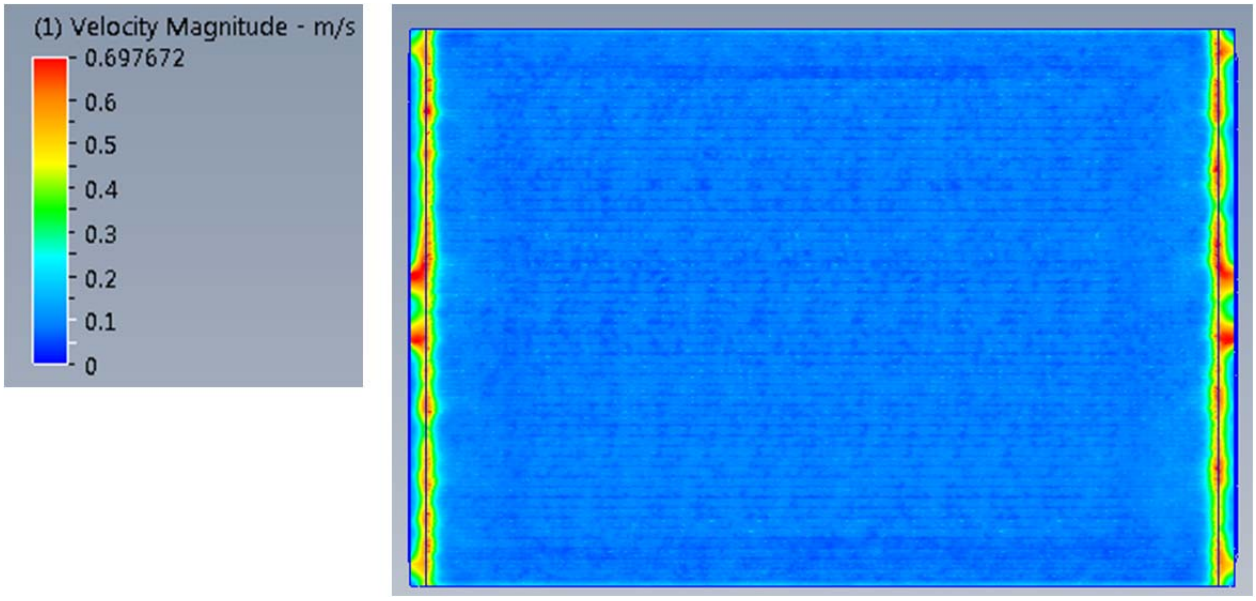

Figure 44. CFD modeling confirmed relatively narrow fuel velocity distribution over the active cell area (0.06 to 0.09 m/S)

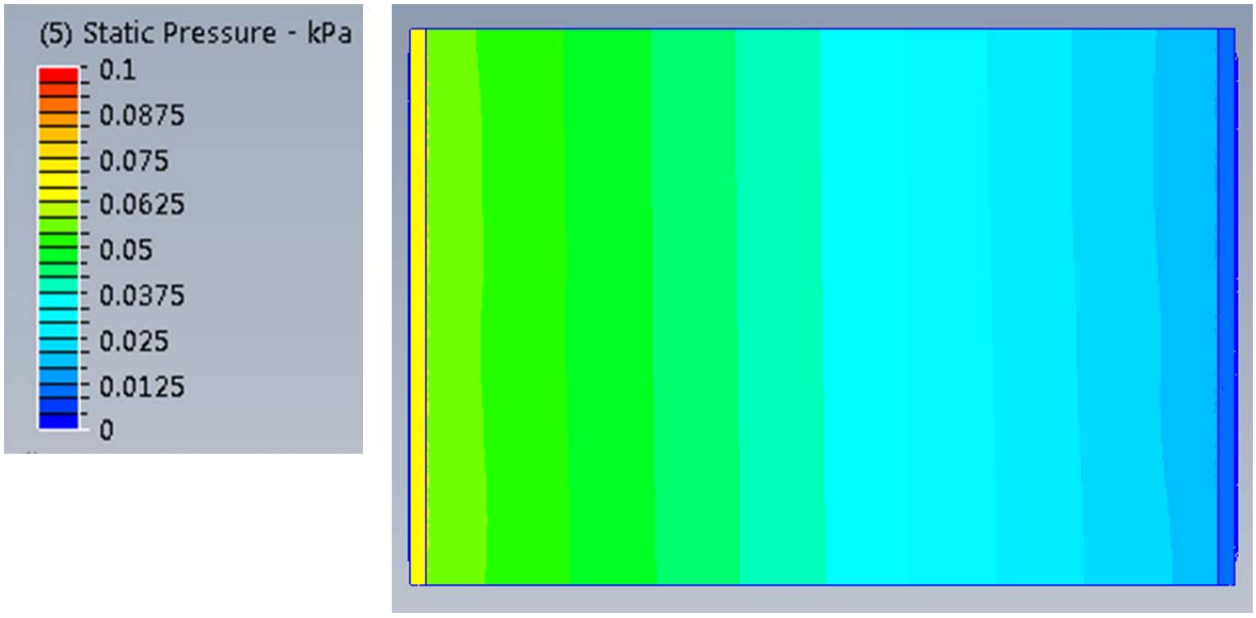

Figure 45. CFD modeling confirmed relatively low pressure drop across the active cell area (0.04 kPa).

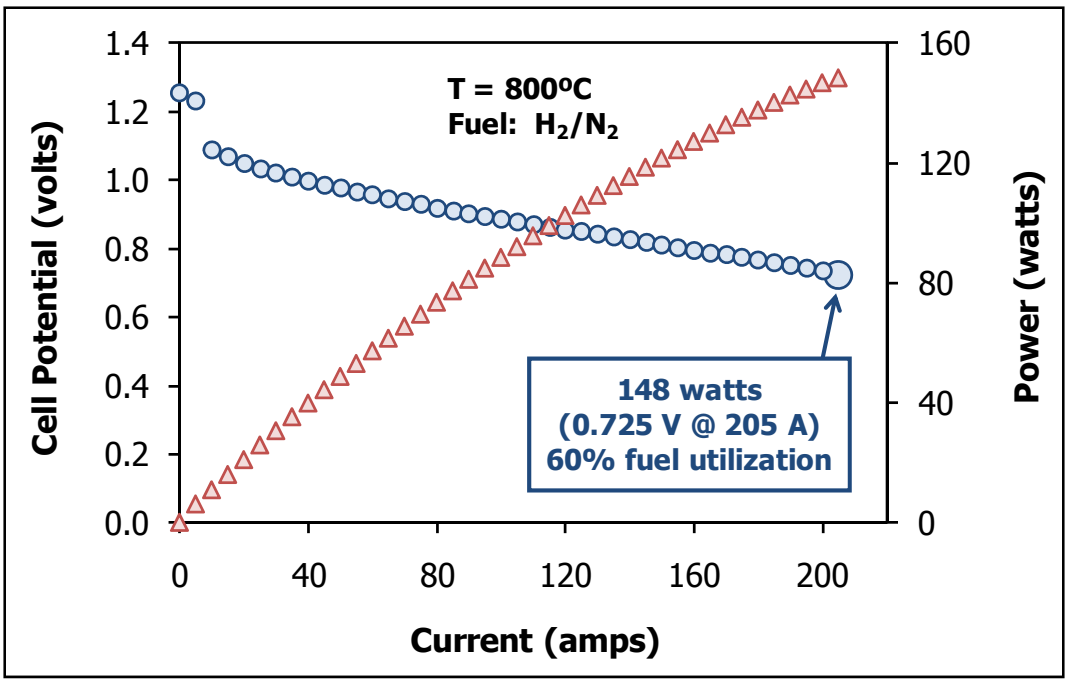

Figure 46. I-V-P curve obtained on large-area YSZ-based *FlexCell* at 800ºC (fuel flow was 2.3 lpm H_2 and 2,3 lpm N_2, air flow was 16 lpm).

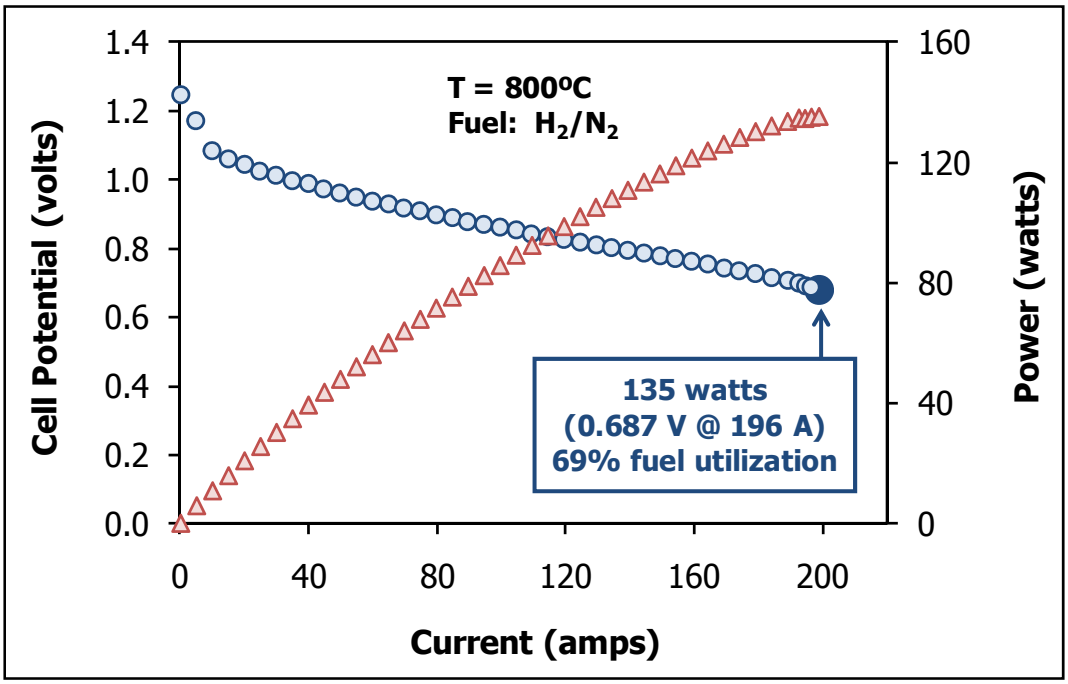

Figure 47. I-V-P curve obtained on large-area YSZ-based *FlexCell* at 800ºC (fuel flow was 2.0 lpm H_2 and 2,0 lpm N_2, air flow was 16 lpm).

Multiple long-term tests on a large-area *FlexCell* also were completed. For one such cell test, the initial performance at 800°C, with hydrogen as fuel, is shown in Figure 48. With a hydrogen fuel flow rate of 2.13 lpm, and a cathode air flow if 15 lpm, the cell achieved 119 watts (187 amps at 0.64 volts), corresponding to a power density of 0.36 W/cm^2 at 0.57 A.cm^2. There was some evidence of either leaking or imperfect fuel flow distribution, because fuel utilization was limited to approximately 60 percent. The fuel then was switched to simulated coal gas, with a dry basis composition of 30.0% CH_4, 33.3% H_2, and 36.7% CO_2, with a steam-to-carbon (S/C) ratio of 1.5. The fuel flow rate and applied current were adjusted such that the cell was operating at a current density of 0.43 A/cm^2 and fuel utilization of 55 percent. Under these conditions, the area specific cell power density was approximately 0.30 W/cm^2 at 0.70 volts. The cell was operated under these steady-state conditions for 1000 hours, with data presented in Figure 49. Over 1000 hours of testing, the cell degraded at a rate of 54 µV/hr. After about 750 hours of testing, an adjustment was made to the compression force on the cell, and a fan was directed at the condensing section of the anode exhaust. As shown in Figure 50, this led to a significant reduction in degradation rate over the final 230 hours of the test (12 µV/hour). Thus, we currently believe that the much of the degradation over the first 750 hours was test-related and not intrinsic cell degradation. Specifically, ineffective condensation of water from the anode exhaust may have been causing a backpressure in the fuel flow rate that adversely affected the test.

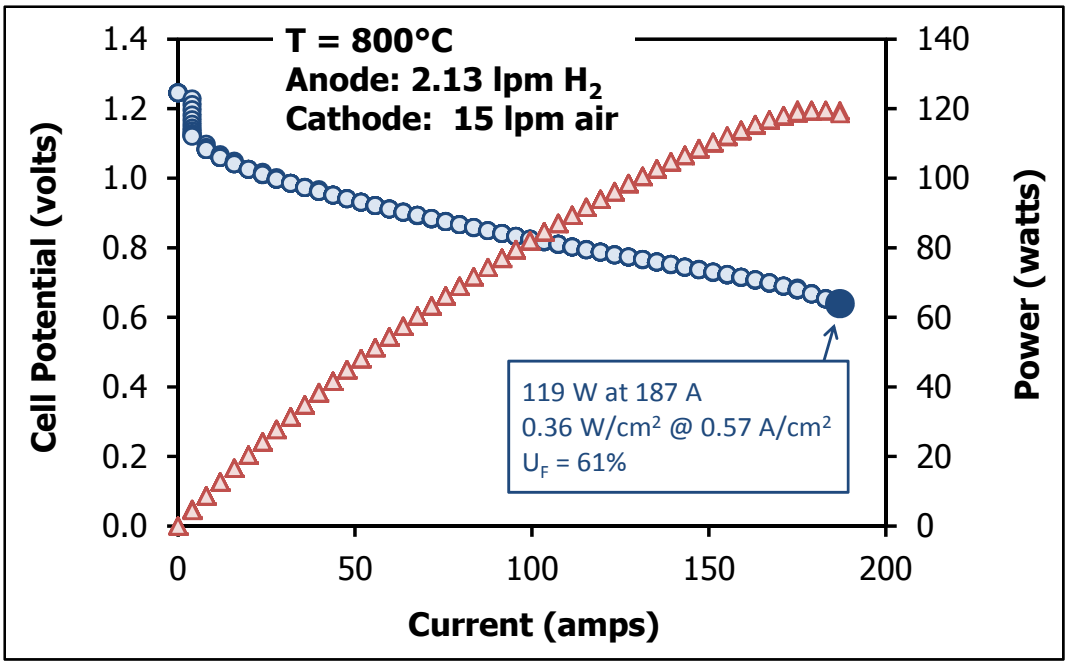

Figure 48. Large-area single cell test of large-area, YSZ-based *FlexCell* with hydrogen as fuel.

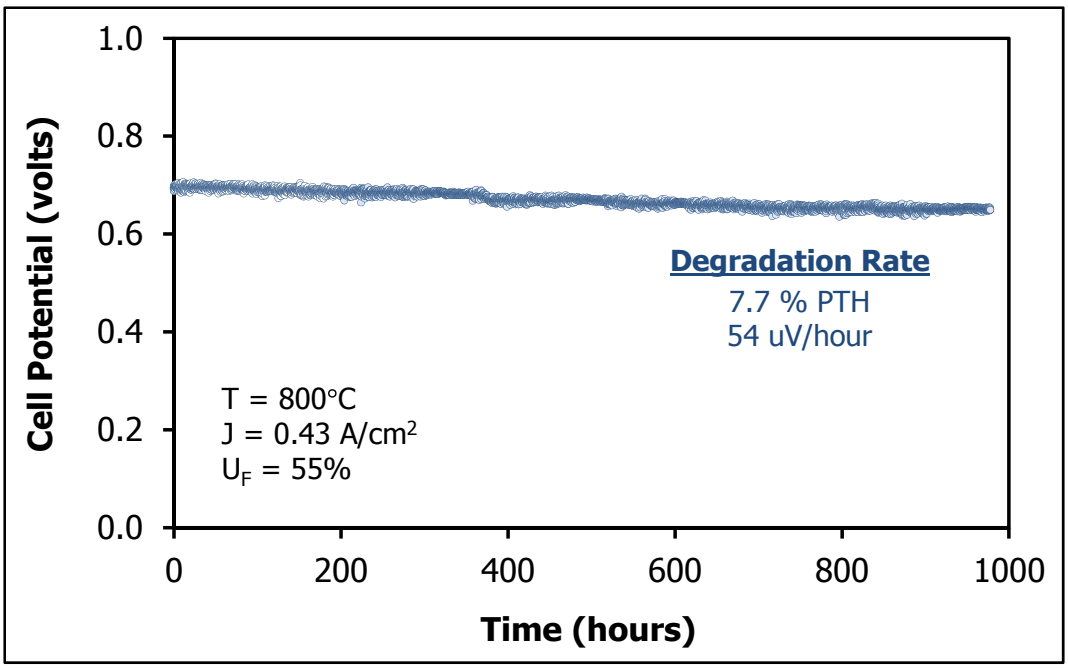

Figure 49. Long-term single-cell test of large-area, YSZ-based *FlexCell* with simulated coal gas as fuel.

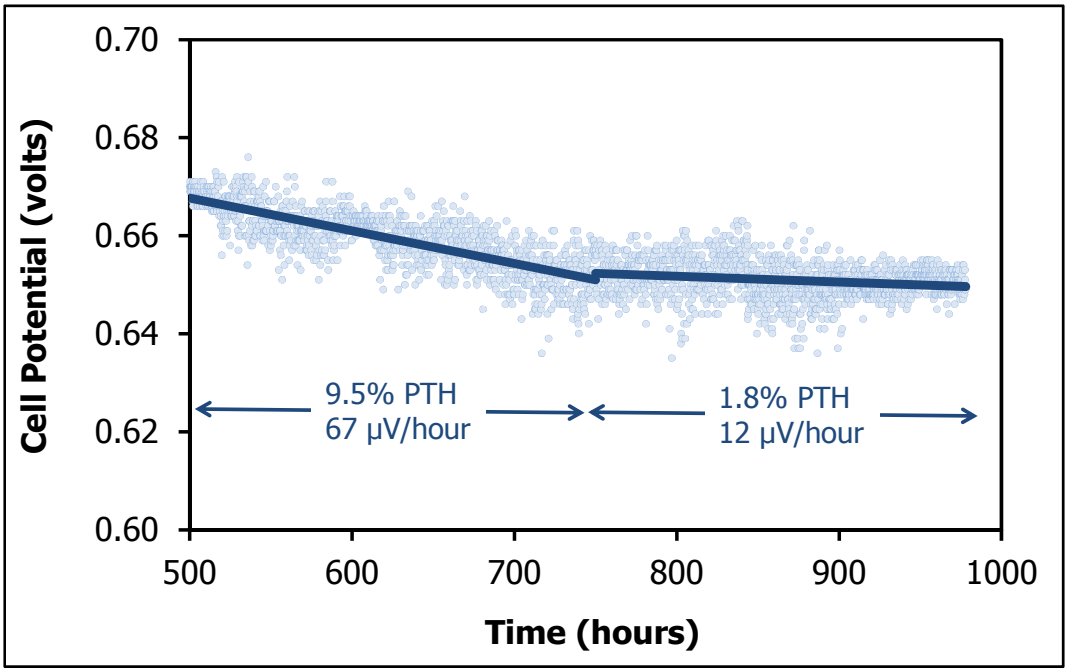

Figure 50. Expanded scale of long-term data presented in Figure 48, showing a reduction in degradation rate occurred after approximately 750 hours.

Tests also were conducted to assess the performance of three-cell stacks of YSZ-based *FlexCells*. These tests were conducted with NexTech's "G-13" stack design platform utilizing *FlexCells* with 320-cm^2 total and 160-cm^2 active areas (previously shown at the left in Figure 29). Pole curve data obtained on a three-cell stack is shown in Figure 51. This test was conducted with an average stack temperature of

approximately 800°C, and a simulated coal gas fuel composition of 29% H_2, 26% CH_4, 32% CO_2, and 13% H_2O (corresponding to an input steam-to-methane ratio of 0.5). The stack achieved 137 watts at a fuel utilization of 70.9 percent, corresponding to an LHV electrical efficiency of 41.7 percent. The current density was then lowered to 0.402 A/cm² to achieve a fuel utilization of 64 percent, lowering the LHV efficiency to 41.1 percent, and held at these conditions for almost 200 hours (see Figure 52).

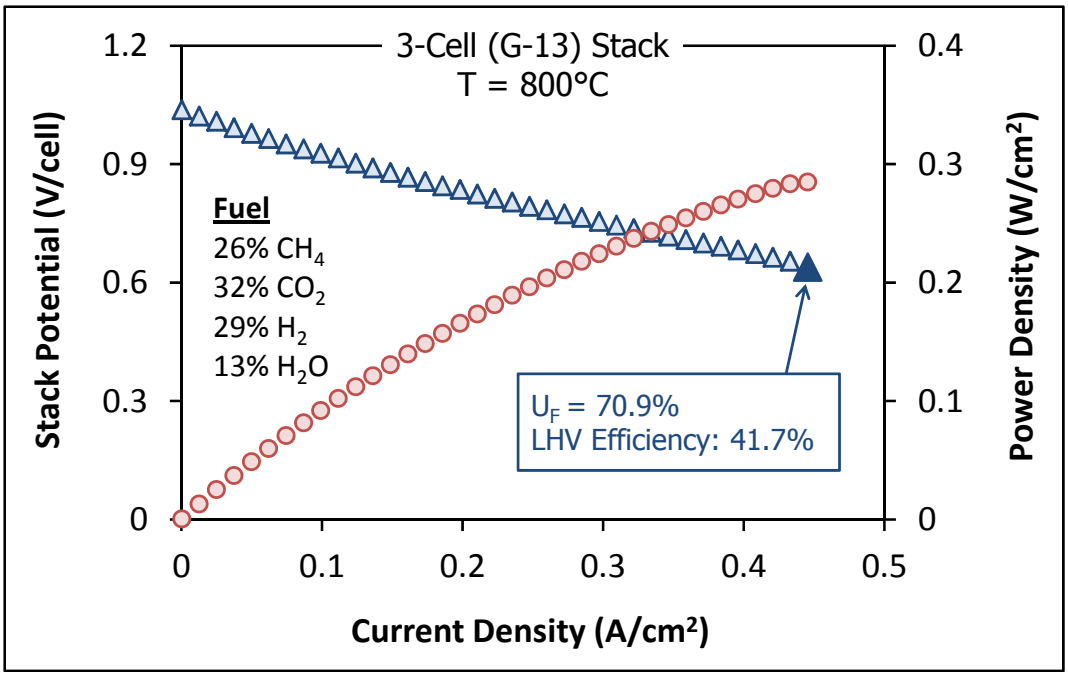

Figure 51. Performance of three-cell stack with simulated coal gas as fuel.

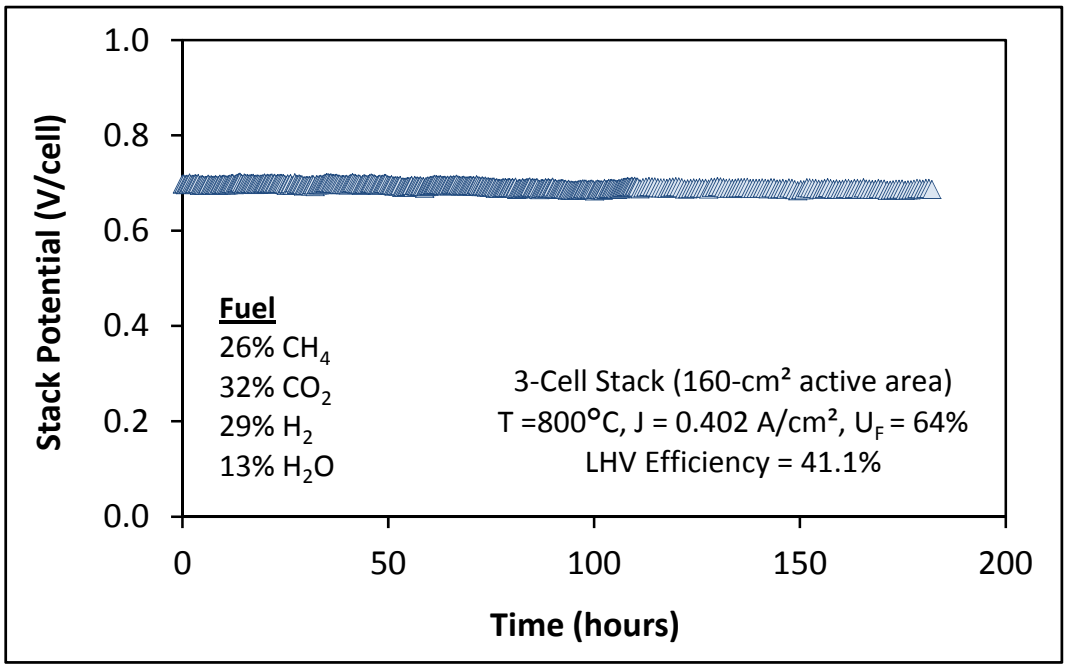

Figure 52. Long-term stability of three-cell stack with coal gas as fuel.

Design of Large-Area FlexCells

During the first two project years NexTech collaborated with The Ohio State University (OSU) to measure material properties and generate predictive models of the mechanical robustness of *FlexCells*. The work at OSU included material property measurements, finite element simulations at two different size scales, and experimental validation. Material properties were measured with the E1875-00 ASTM Standard which is based on measuring resonant frequencies and specimen dimensions. These measurements were taken temperatures ranging up to 800°C (see Figure 53).

Small-scale finite element simulations were conducted to analyze the localized mechanical effects of the repeating pattern of hexagonally thinned sections. A representative unit cell was selected from the repeating pattern and modeled using repeating boundary conditions, which imitate the effects of the surrounding cells. Figure 53 is a schematic of a *FlexCell's* active area with hexagonally thinned sections. Each of the 9 rectangles in Figure 54 are repeating cells. Figure 55 shows the stresses generated within a representative unit cell. Figure 55 also shows how the hexagonal shapes are thinned regions that reduce the equivalent resistance of the electrolyte. The frame around the hexagonal center portion provides the necessary mechanical strength. The geometry of the repeating unit has been varied to simulate different active areas. The active areas are converted to equivalent resistance for an eventual analysis of the trade-off between mechanical robustness and electro-chemical performance. Figure 56 shows the equivalent Young's modulus for the different hexagonally and circularly thinned regions. The equivalent materials properties are used as inputs for the large area simulations described next.

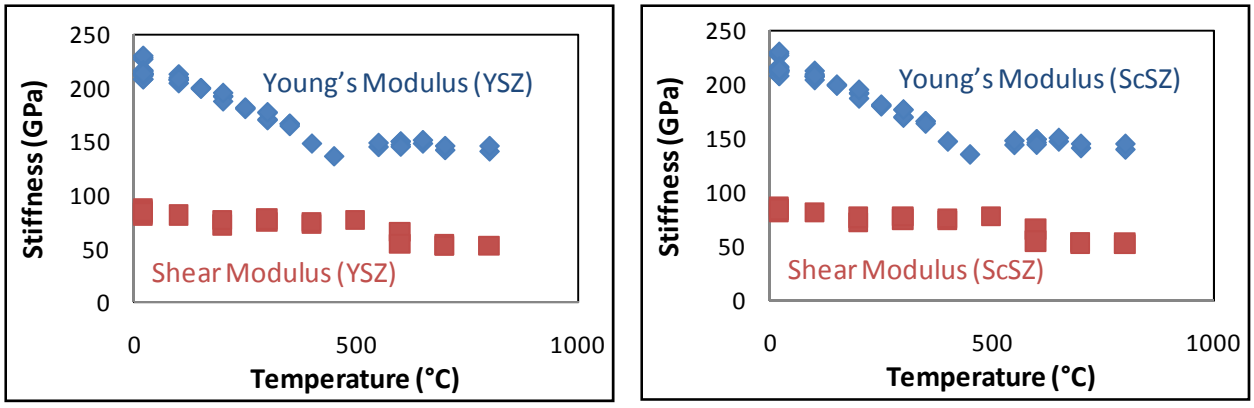

Figure 53: Elastic and Shear Modulus for YSZ (left) and ScSZ (right). Poisson's ratio for either material can be readily calculated from these moduli.

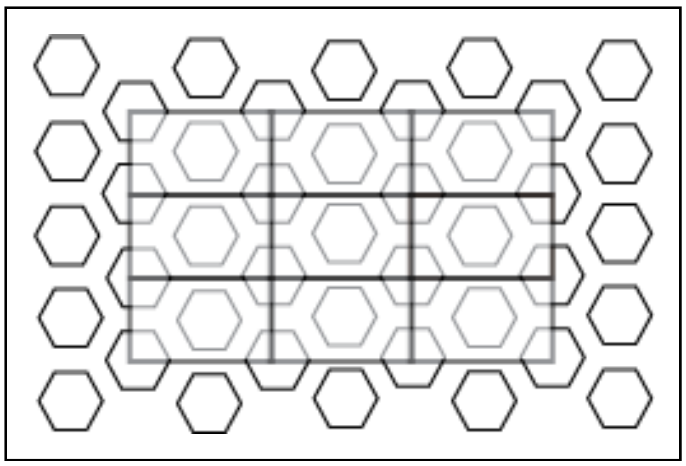

Figure 54. Illustration of the repeating unit cell used in conjunction with periodic boundary conditions to approximate large area simulations.

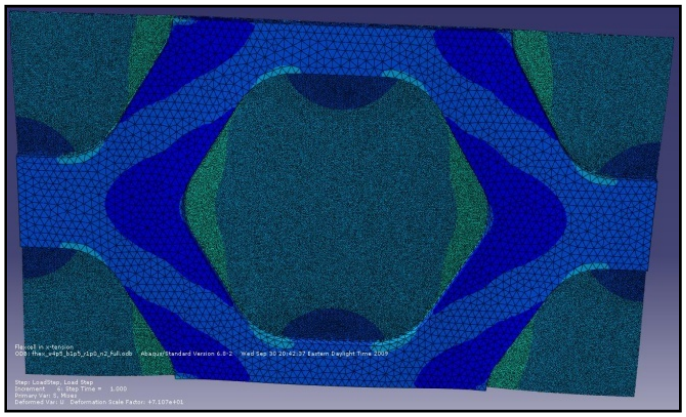

Figure 55. A contour map showing equivalent stresses associated with uniform stretching of the unit cell

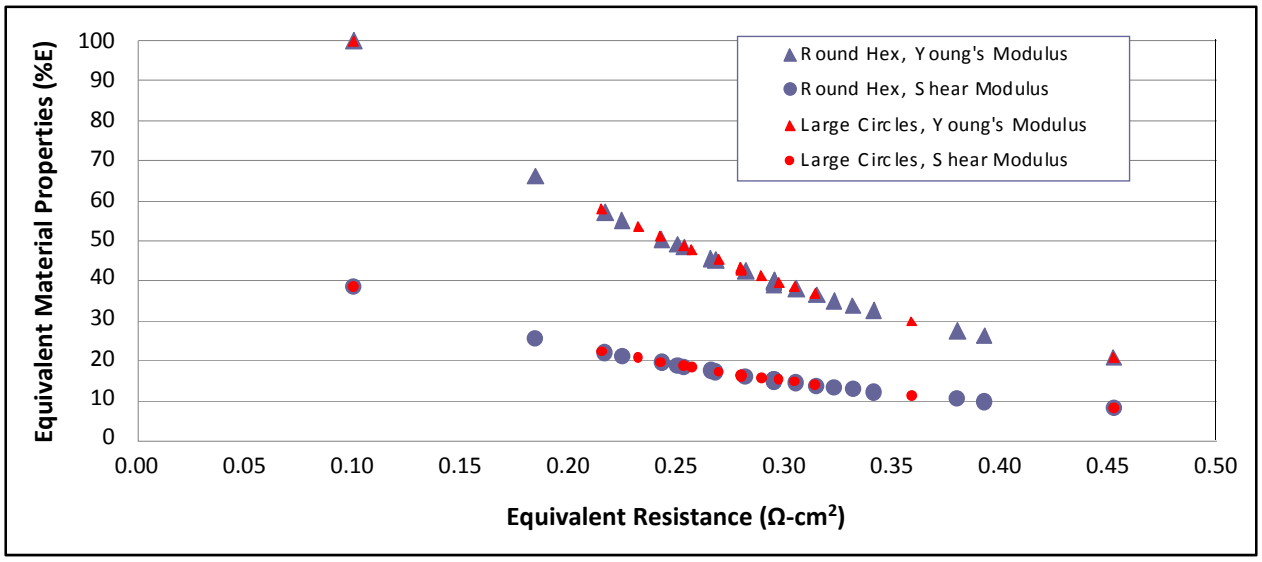

Figure 56. Equivalent Young's modulus and shear modulus determinations for unit cells with hexagonal and circular cutouts.

Large scale finite element simulations were performed on the *FlexCell* models to study the effect of geometry (small-scale patterns and support ribs) and loading during operation. Since the in-plane dimensions are much larger than the thickness, shell elements have been employed. Figure 57 shows the different areas (active and frame) having varying thickness and small-scale geometry.

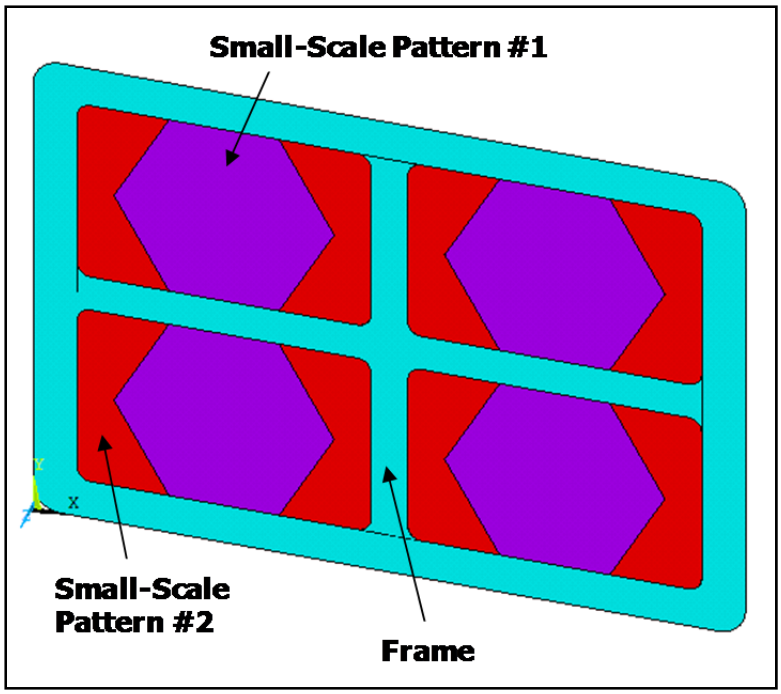

Figure 57. A representative model showing the differently designed areas on the electrolyte.

Using all of the material data collected, along with the generated small-scale and large-scale finite elemental analysis, simulations for the large-area cell design along with aspects of the design could be performed. Simulations were performed to analyze the role of cross ribs in providing support to the electrolyte. Loading is uniform pressure on the entire membrane with the outer frame area being fully constrained. Figure 58 shows the principal stress contour and areas of high stress concentration for the electrolyte membrane with both vertical and horizontal support ribs. As shown in Figure 59, different rib geometries are analyzed and compared to the deflection experienced by the model without support ribs at all. While the results indicate that 5-10 and 10-10 rib configurations have higher stresses than the 0-0 (no rib) configuration, the presence of cross ribs plays an important role in reducing the out-of-plane displacement. It is more important to have the vertical ribs to be wider than the horizontal ribs.

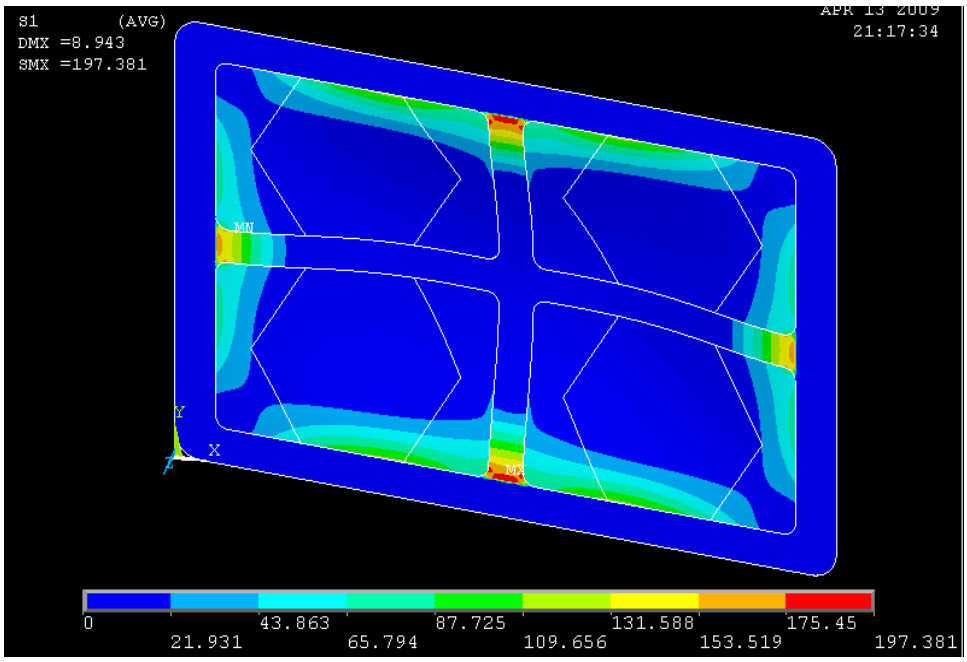

Figure 58. Principal stress contours for a large-area electrolyte membrane with the standard vertical and horizontal support rib.

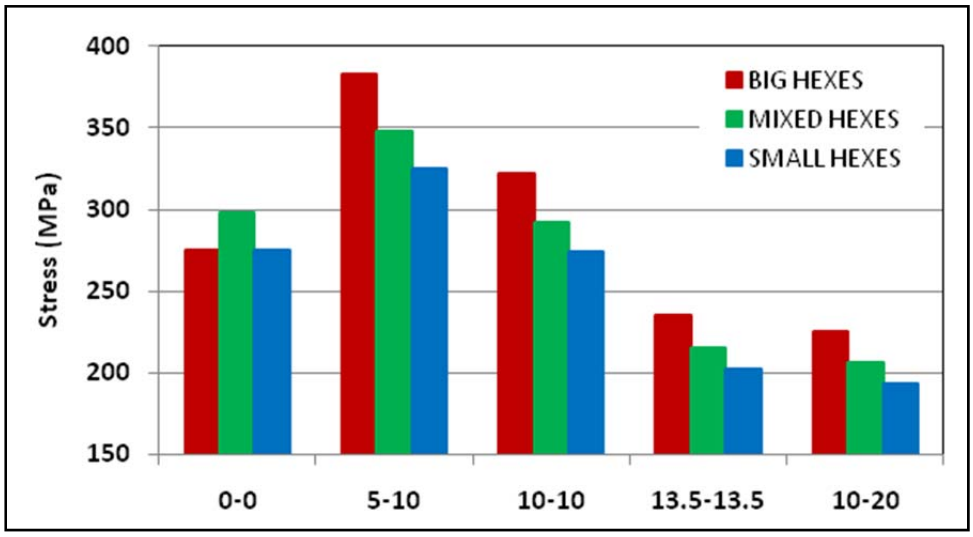

Figure 59. Variation of principal stresses for different rib configurations and active area geometry. Nomenclature: "5-10" represents a 5-mm wide horizontal rib and 10-mm wide vertical rib.

Having the results from the large-area cell model, scaling up the simulations to a 1000 cm^2 *FlexCell* models were easily incorporated. Figure 60 is a representation of the current design and the stress contours for a full-scale 1000 cm^2 model, respectively. Current models employ quarter symmetry to analyze the model more effectively.

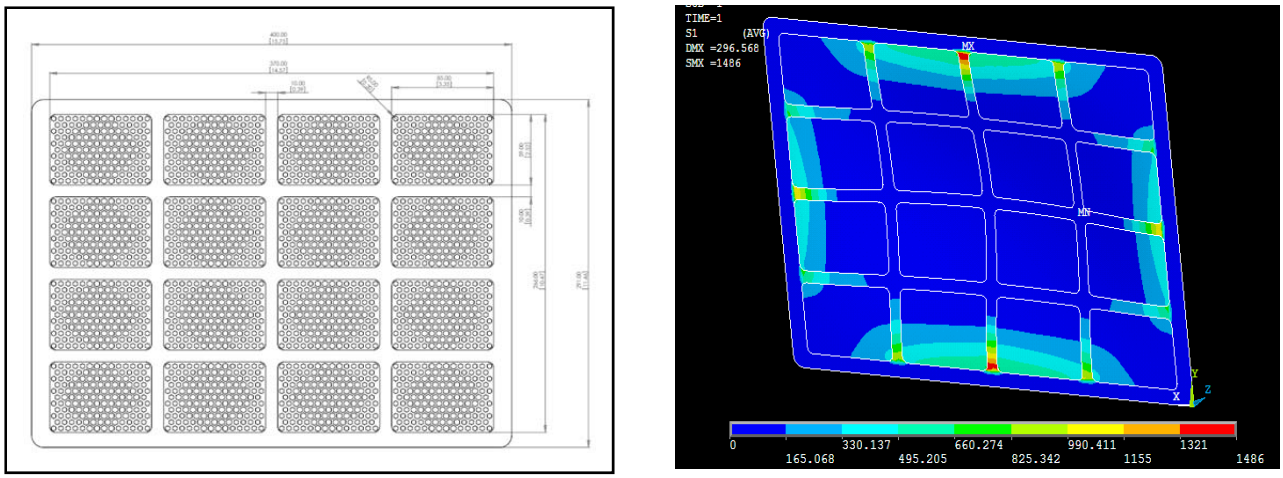

Figure 60. Mesh for a 1000 cm^2 cell design with mixed hexagonal cut-outs and equal rib widths (left); and corresponding principal stress contours (right).

To validate the simulations performed, experiments were designed and fixtures modeled. The two experiments were as follows:

- Four- point bend test on thin *FlexCell* strips to validate simulations.
- Compression test on the 28 cm^2 *FlexCell* assemblies (electrolyte sandwiched between metal foams) in order to validate the performance of electrolytes in the context of a stack.

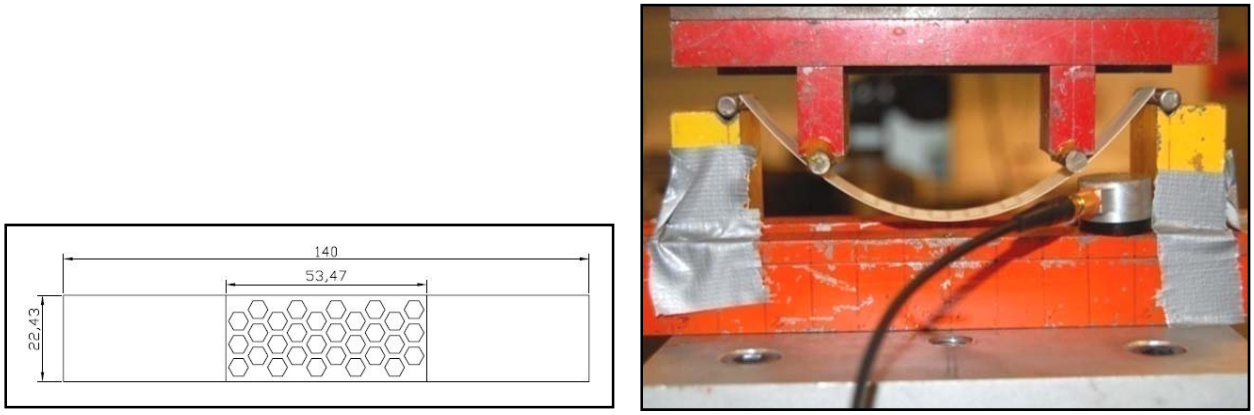

Figure 61. Experimental test specimen (left); and deformed thin strip (right).

Initial tests revealed that the thin strip is extremely elastic (see Figure 61). By carefully controlling the parameters like location of load and support in the experiment, good agreement was obtained between the experiment and simulation (see Figure 62).

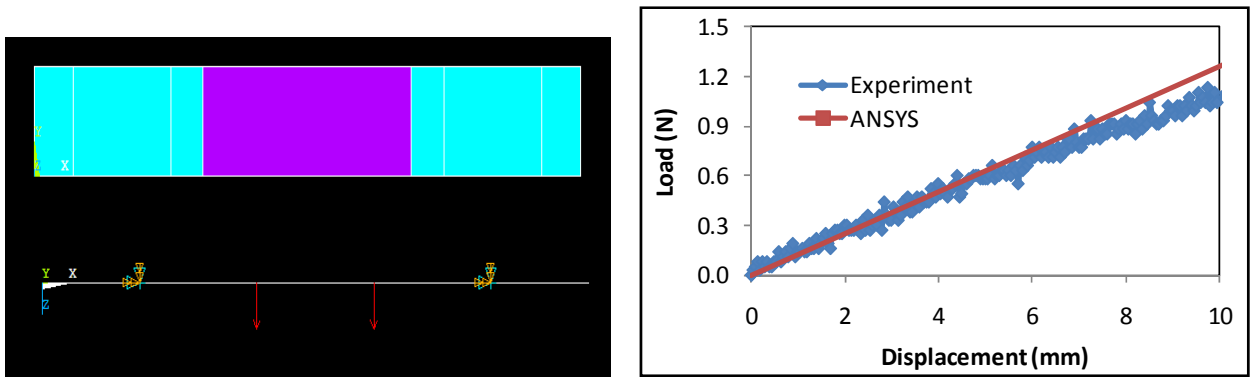

Figure 62. ANSYS simulation of 4-point bend test showing sample geometry and loads; and comparison of load-displacement data from the experiment and the simulation (right).

Simulations were performed at the Ohio Super Computer to obtain detailed small-scale stress analyses as described above. Efforts were made to develop an appropriate small-scale mesh, and then more detailed stresses near a single support hexagon were obtained. The complete 3-d mesh with approximately 1.5 million elements and a zoom-in near the support hexagon interface are shown in Figure 63.

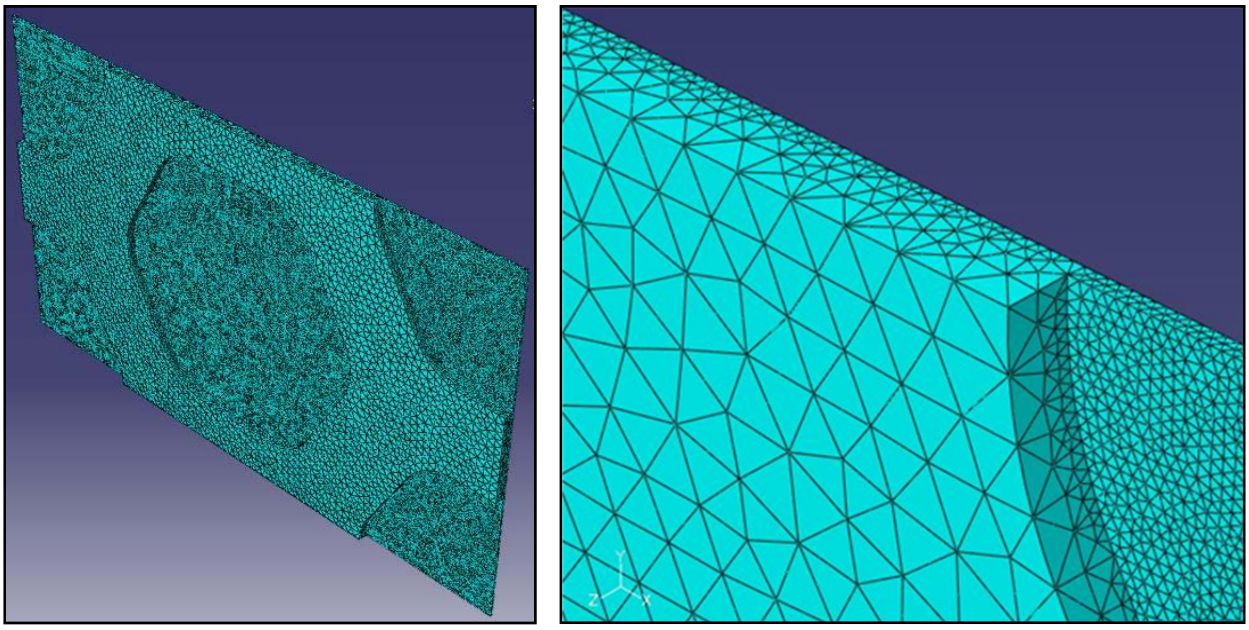

Figure 63. Complete small-scale mesh (left); and zoomed mesh showing element size transitions (right).

Von Mises stresses from the simulation ranged up to 600 MPa, however the sequence of images in Figure 64 shows where high stresses develop and also indicates that only a few outlying elements show stresses over 200 MPa. The 1.5 million element small-scale model has been used to explore a variety of hex-pattern geometries and under several biaxial loading geometries. A sample stress-contour is shown in Figure 65a. The stresses are analyzed through stress histograms. The Von Mises stress histogram corresponding to Figure 65a is shown in Figure 65b. To compare different geometries, the mean (or standard deviation) of a Gaussian curve fit to one self-similar feature of the histogram is tracked (see

Figure 65b). Since each geometry results in a different percent active area (percent of thin region of the electrolyte), the Gaussian characteristics are plotted as a function of active area. The resulting relationship between mean stress and active area is seen in Figure 65c and shows that stress decreases with increasing active area. The decrease in stress is a direct result of the displacement loading conditions in the model and the fact that increasing active area leads to a more compliant model. For a constant force loading, the geometries with increased active area would show higher stresses, thus validating the realization that increasing active area would make the electrolyte weaker. In order to quantify the increase in stresses with increasing active area a "magnification factor" has been developed. The magnification factor is determined from a ratio of the material modulus to equivalent modulus along with various constants. The magnification factor corresponding to Figure 65c is shown in Figure 65d. In going from approximately 35 to 90% active area, each stress in the finite model is multiplied by approximately two.

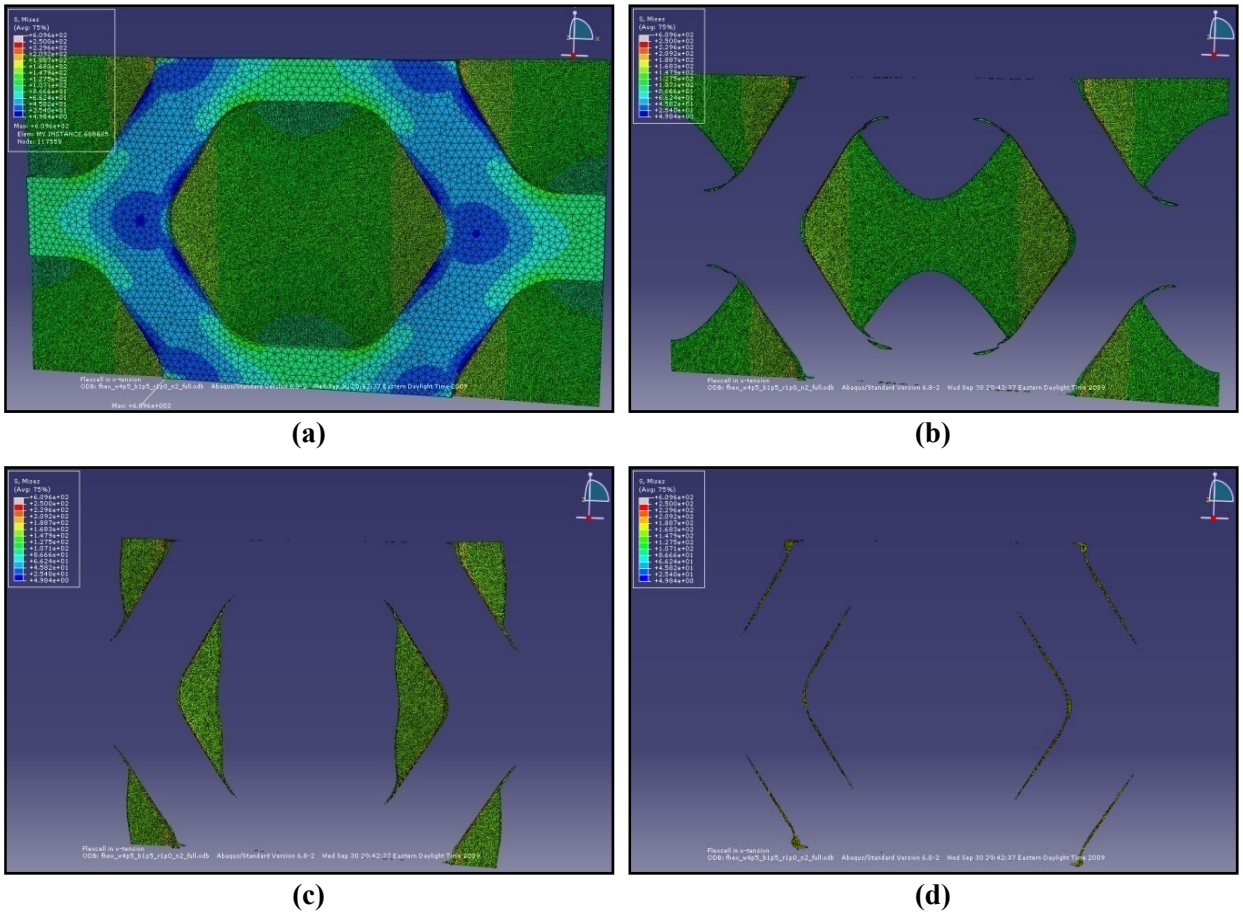

(a) **(b)**

(c) **(d)**

Figure 64. Stress contours: (a) all elements; (b) only elements with stresses over 125 MPa; (c) only elements with stresses over 150 MPa; and (d) only elements with stresses over 175 MPa.

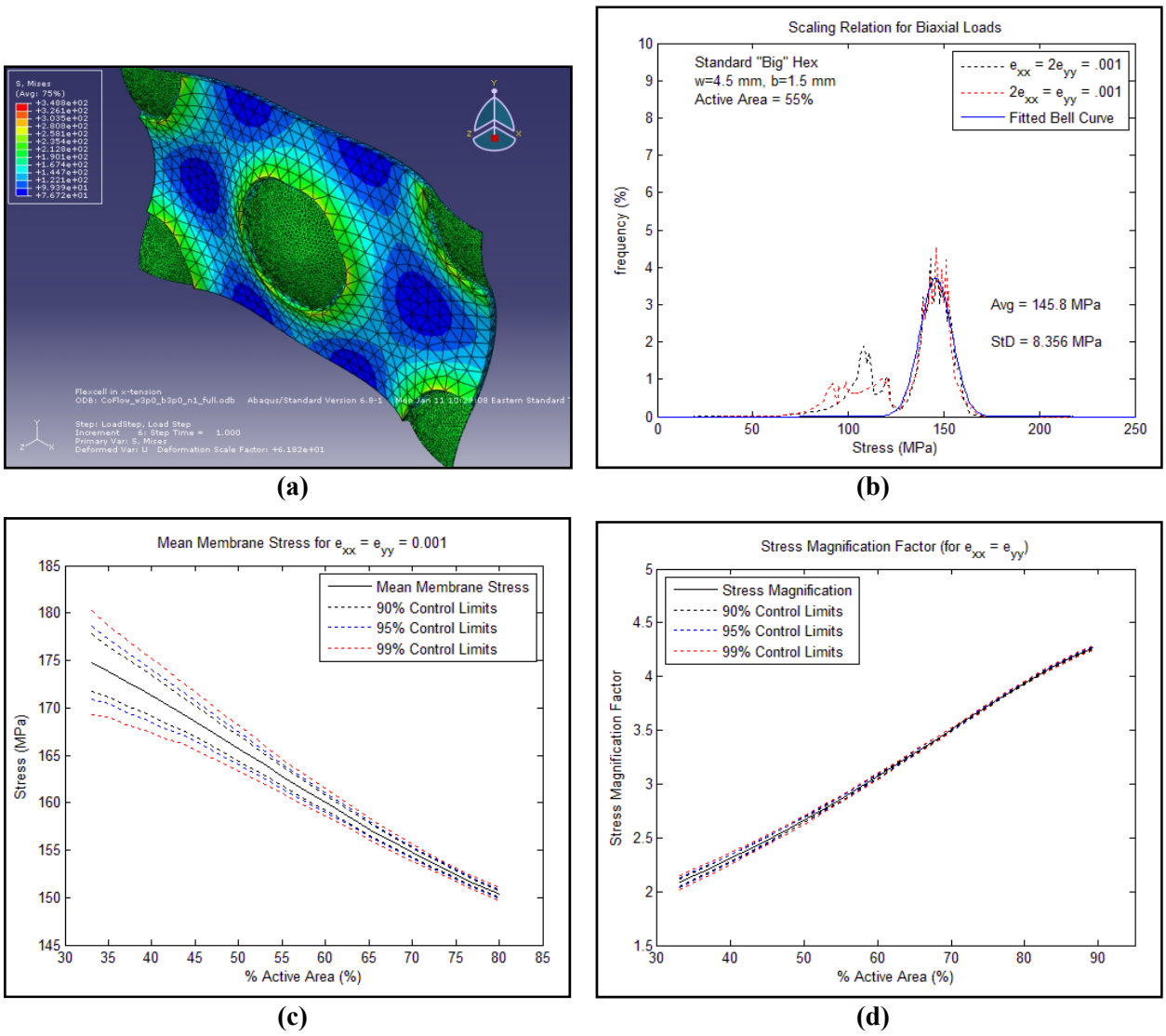

Figure 65. (a) Von Mises stress contour for bi-axial loading; (b) the corresponding stress histogram with a Gaussian fit to determine standard deviation of the distribution; (c) relationship between mean stress from the histograms for different active-area geometries versus active area; and (d) magnification factor that allows stresses to be scaled as a function of active area.

To determine what characteristics of the small-scale stress distribution result in macroscopic failure, bending experiments with *FlexCell* electrolyte membrane strips were performed using the apparatus shown at the left in Figure 66. Analysis of the experimental data provided the stress-strain data shown at the right in Figure 66, and it is seen that the stiffness scales with percent active area. Table 8 shows how scaling of the material modulus with the equivalent stiffness from the small-scale simulations shows good comparison with the measured modulus in the bend experiments.

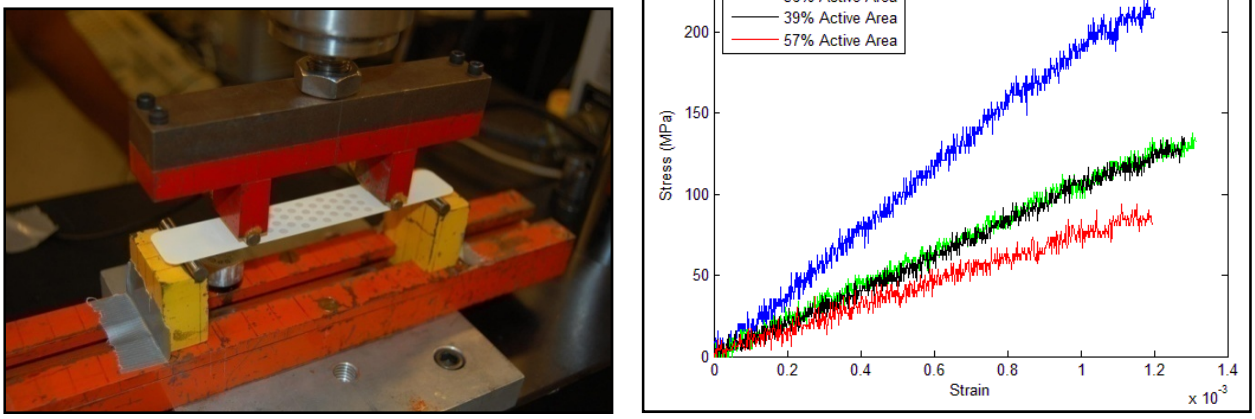

Figure 66. Experimental setup for four-point bend test (left); and experimental stress-strain curves from the bending experiments (right).

Table 8. Young's modulus from small-scale simulations and from bend experiments.

Type	% Active Area (%AA)	Equivalent Stiffness (%E)	Young's Modulus (Resonance)	Young's Modulus (bend test)	Percent Error
Unpatterned	0	100	204.6	202.23	1.15
Small circles	36	55	111.65	112.12	0.47
Small hexes	39	52	106.35	108.55	2.07
Large hexes	57	39	79.58	74.76	6.05

Ohio State characterized how the stresses vary for bi-axial loading of different small-scale geometries. These stresses were analyzed by fitting Gaussian curves to stress histograms. At the large scale, analysis of the bending of electrolyte strips has continued and the frame width and rib width was studied for large-area cells. In addition, stresses were determined for different temperature gradient patterns. Finally, the mechanical response of two metal foams used between electrodes and interconnects was determined.

New simulations of the 700 cm^2 electrolyte membranes were undertaken. The approach pursued was to keep the active area constant by narrowing the exterior frame width while widening internal ribs (while maintaining sufficient frame area for sealing). A CAD drawing of the cell is shown in Figure 67. For uniform pressure loading on the entire active area with a 5-mm overlap into the frame, Table 9 shows the effect of increasing the central horizontal and vertical rib widths (independently and also together), first by 2 mm and then by 4 mm. It is seen that increasing the vertical rib has the greatest improvement in stresses (S1) and displacements (U1). The effect of going from a 2-mm to a 4-mm increase is minimal.

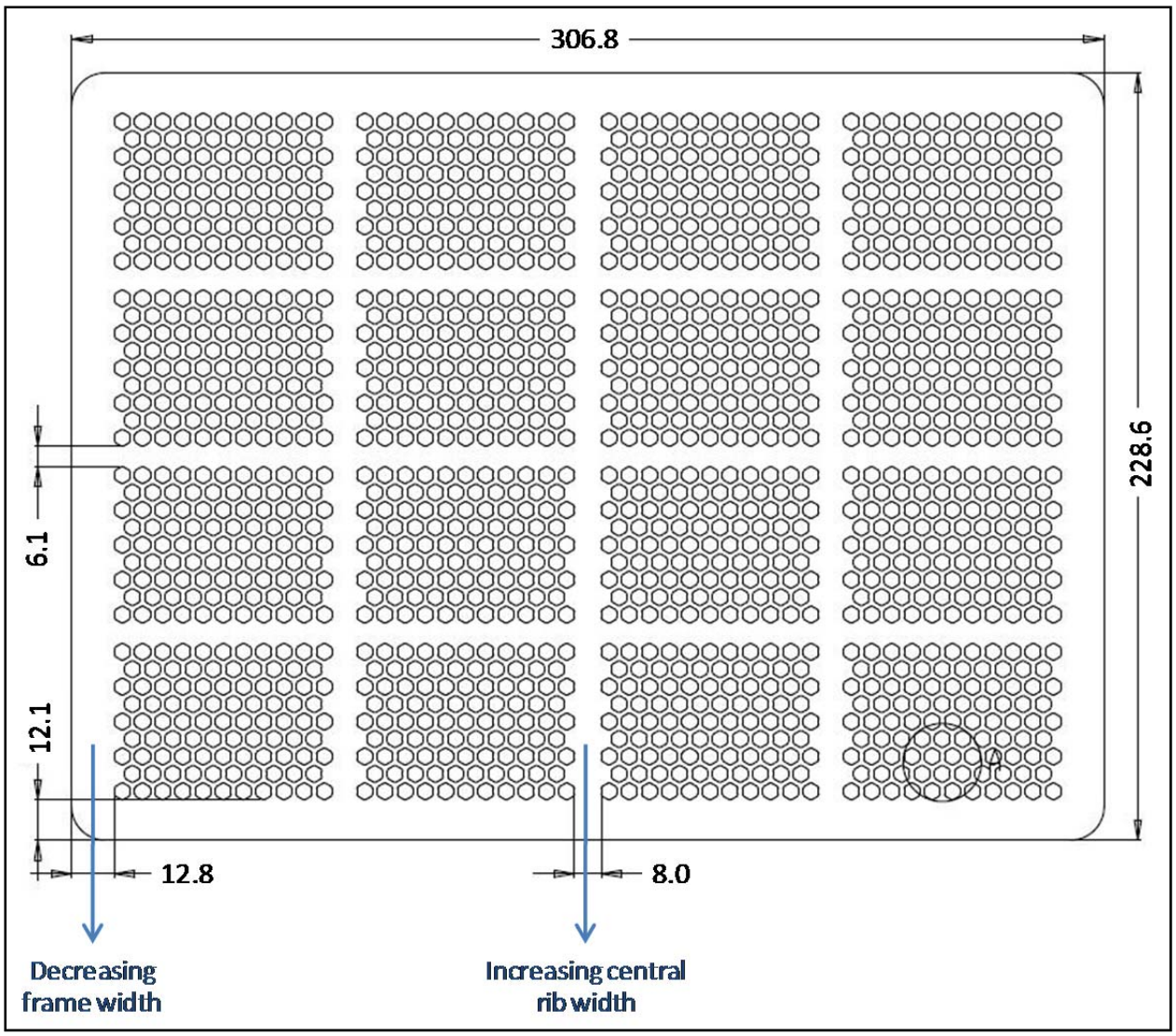

Figure 67. CAD drawing of a 700 cm^2 area *FlexCell* membrane with the two main modeling variables indicated (dimensions in mm).

Table 9. Effects of changing the central rib widths for uniform pressure loading of the entire active area plus a 5-mm overlap into the frame.

Central Rib Width	Stresses and Displacements	Standard	Vertical Rib	Horizontal Rib	Vertical and Horizontal Ribs
2 mm	S1	409.6	386.7	415.37	397.95
	U1	23.034	22.765	23.08	22.813
4 mm	S1	409.6	384.74	432.39	422.04
	U1	23.034	22.509	23.13	22.61

At the large scale, simulations were also performed to determined stresses associated with temperature gradients. Temperature boundary conditions which closely replicate temperature distributions in a stack with co-flow reactant manifolding were used (based on CFD analyses performed by NexTech). The temperature distribution is shown at the left in Figure 68, with stresses corresponding to this distribution shown at the right in Figure 68.

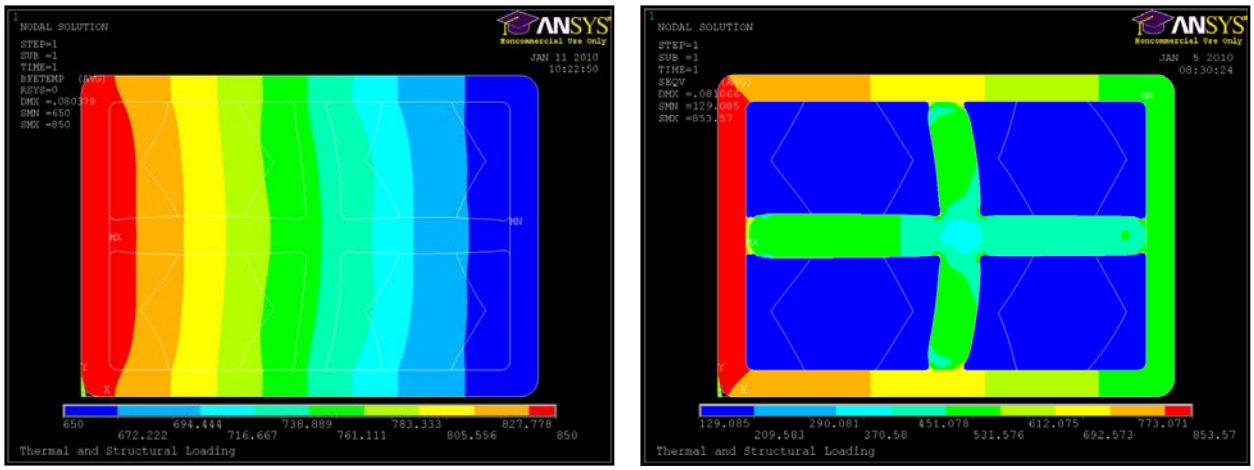

Figure 68. Temperature distribution for co-flow manifolding (left); and corresponding stresses (right).

The final design of the large-area cell for the next phase of work took all of OSU's modeling work into consideration based on the small-scale mesh modeling for the optimum thin membrane within the active area and then the rib thickness and spacing form the incorporated lager area cell modeling to produce a final design for the YSZ-based large-area *FlexCell* for fabrication and testing work at NexTech. The design of this cell was shown earlier in Figure 39. The total cell area is 475 cm² and the active cell area (exclusive of internal ribs) is 330 cm².

Manufacturing Cost Analysis

Large-area *FlexCell* manufacturing costs were evaluated at both pilot scale (10 MW/year) and full-scale (250 MW/year) production levels. As shown schematically in Figure 69, NexTech's manufacturing process for *FlexCells* involves the following steps:

(1) Tape casting of the electrolyte tape (30 to 50 microns thick).

(2) Multiple layers of tape are cut to size and isostatically laminated to form a green mechanical support (100 to 200 microns thick).

(3) The resultant blank is cut using a laser cutter to produce a support mesh (with external frame).

(4) The electrolyte layer is cut from a single tape to the same size as the support tape.

(5) Support and electrolyte layers are isostatically laminated to form a green *FlexCell* membrane element.

(6) The green *FlexCell* membrane is subjected to thermal treatments for binder removal and sintering.

(7) Interfacial, active and current collecting anode layers are deposited by spraying and then annealed.

(8) Interfacial, active and current collecting cathode layers are deposited by spraying and then annealed.

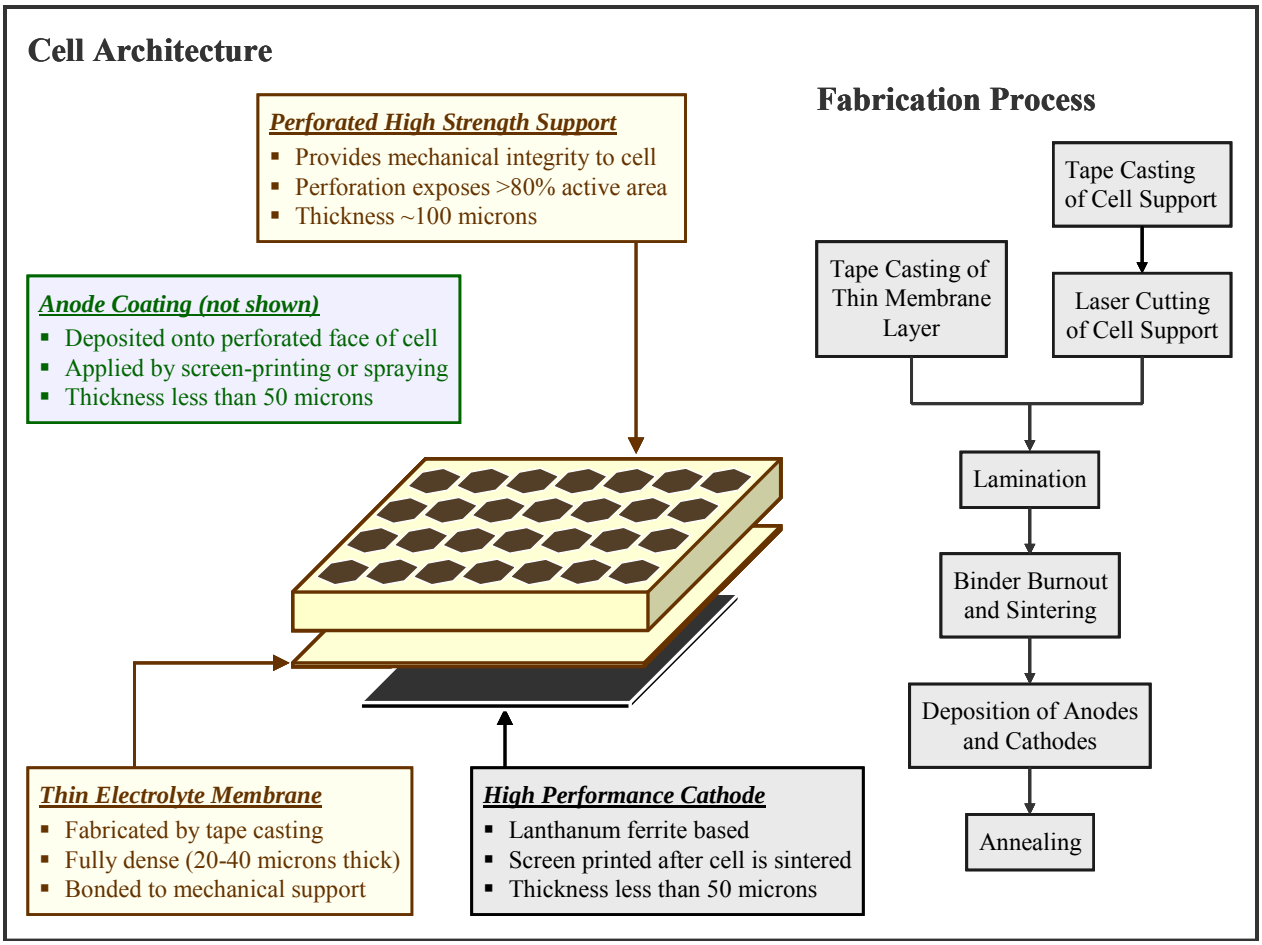

Figure 69. Schematics of the *FlexCell* architecture (left) and manufacturing process (right).

Manufacturing Cost Analysis Assumptions

For both pilot and full-scale manufacturing cost analyses, the area of YSZ-based *FlexCell* was assumed to be 500 cm^2, and such cells were assumed to produce 125 watts (corresponding to an active-area specific power density of 313 mW/cm^2. For comparative purposes, NexTech also analyzed the manufacturing cost of anode supported cells (ASC) at the 500 MW scale, assuming a slightly higher power output of 160 watts for the same cell size. The impact of larger-area cells and higher power densities on *FlexCell* cost were also considered and are presented later in the cost sensitivity analysis section. A production yield of 90 percent was used in both cases in the initial topical report, requiring daily production volumes of 352 and 6,197 cells at the 10 MW and 250 MW per year volumes, respectively, and sensitivity analysis was conducted at 98 percent yield in the full scale production case. In this updated analysis, we are assuming a manufacturing yield of 98 percent at 250 MW per year, for both the *FlexCell* and ASC technologies, consistent with similar high volume ceramic based products such as multilayer capacitors and planar oxygen sensors. A five-day single-shift operation was assumed for the pilot scale, with furnaces running continuously seven days per week. A seven-day three-shift operation was assumed at full scale. From these assumptions, annual and daily *FlexCell* production demands were calculated for the two production scales, as shown in Tables 1 and 2.

Table 9. Pilot-scale cost analysis assumptions.

Assumption	Value	Units
Annual plant capacity	10	MW
Operation time (per week)	5	days
Operation time (per day)	8	hours
Total cell area	500	cm^2
Active cell area	400	cm^2
Area-specific power density	0.313	W/cm^2
Power output per cell	125	Watts
Cells per year (required)	80,000	cells
Cells per year (90% yield)	88,000	cells
Cells per day (90% yield)	352	cells

Table 10. Full-scale cost analysis assumptions.

Assumption	Value	Units
Annual Plant Capacity	250	MW
Operation time (per week)	7	days
Operation time (per day)	24	hours
Total cell area	500	cm^2
Active cell area	400	cm^2
Area-specific power density	0.313	W/cm^2
Power output per cell	125	Watts
Cells per year (required)	2,000,000	cells
Cells per year (98% yield)	2,040,000	cells
Cells per day (98% yield)	5746	cells

FlexCell Manufacturing Costs at Pilot-Scale Production Volume

NexTech considered a 10 MW per year production volume for its pilot scale cost analysis. To achieve this production volume, 352 cells must be fabricated every day of a 5-day workweek, assuming a 90% production yield. From this daily demand, equipment capacity requirements were determined for each unit operation of the *FlexCell* manufacturing process. The production process was separated into two general steps: (1) fabrication of the YSZ electrolyte membrane; and (2) deposition of electrodes onto the YSZ membranes. Value stream maps for each of these *FlexCell* production steps are shown in Figures 70 and 71. Capital investment equipment and labor requirements for each unit operation, identified in the value stream maps, are detailed in Table 11.

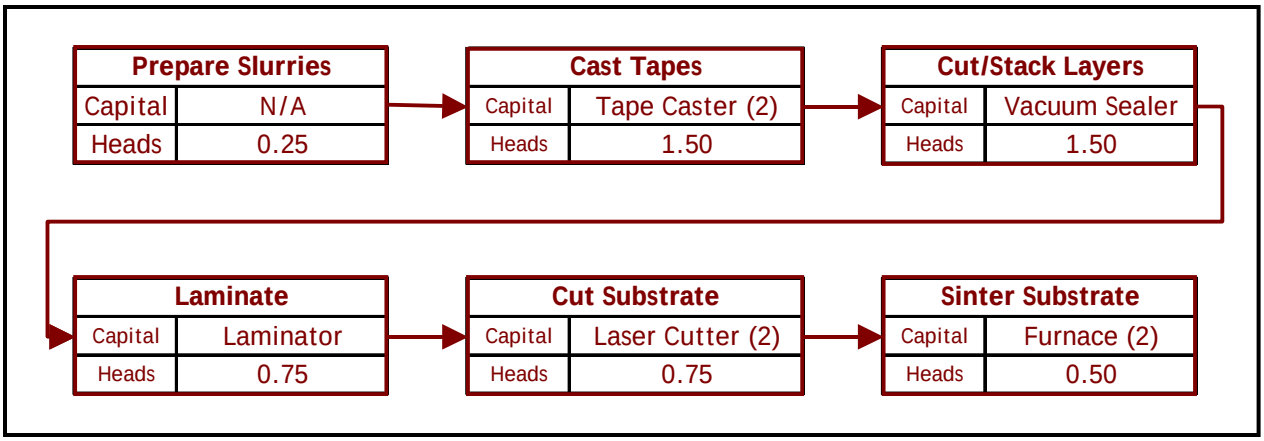

Figure 70. Electrolyte fabrication value stream map.

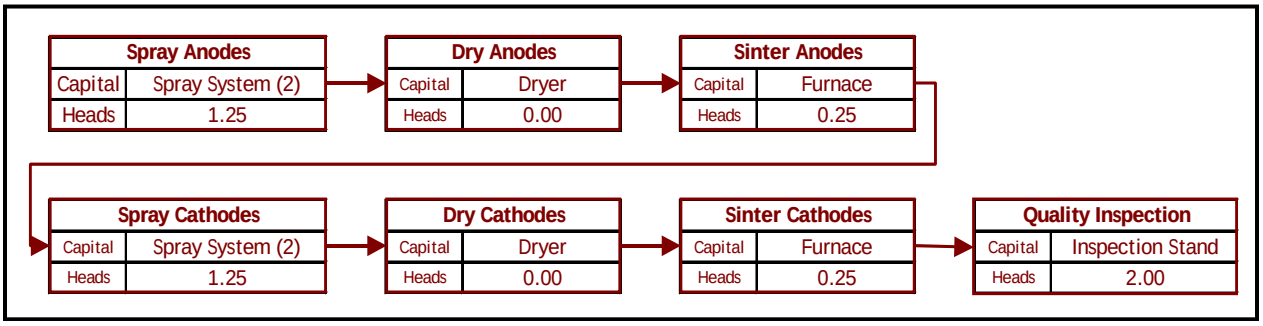

Figure 71. Electrode deposition value stream map.

In the pilot line cost analysis, a time frame of five years was used to calculate the depreciation of assets. A direct labor rate of $17.50 per hour for pilot-line operators was used in the labor calculations. At this 10 MW/year scale, the fabrication of large-area *FlexCells* is labor intensive. Many unit operations, such as cutting and stacking of electrolyte tapes, are highly manual at this scale. Labor cost, therefore, is a major contributor of the total cell manufacturing cost. The raw material cost estimates were based on the current fabrication and labor involved in acquiring these materials at the pilot scale. Raw material costs at the 10 MW/year scale are given in Table 13.

From these cost estimates, an updated total cell manufacturing cost of $41.50 per cell ($365 per kW) was estimated, as shown in Table 14. The main contributors to this cost are the raw materials for the cell, depreciation of capital equipment, and operating labor. At the full-scale production level, these factors will be greatly reduced due to the increased level of automation that will be implemented.

Table 12. Capital equipment and labor requirements at 10 MW/year scale.			
Manufacturing Operation	**Capital Equipment**	**Labor (FTE's)**	**Labor Cost**
Electrolyte Fabrication			
Clean Room	$600,000	-	-
Prepare Tape Slurries	$20,000	0.25	$26,000
Cast Tape	$258,000	0.60	$62,400
Cut and Stack Layers	$290,000	2.60	$270,400
Sinter electrolyte	$1,000,000	0.20	$20,800
Electrode Deposition			
Anode Deposition	$166,000	1.25	$130,000
Dry Anode	$20,000	0.50	$52,000
Sinter Anode	$700,000	0.10	$10,400
Cathode Deposition	$203,000	1.25	$130,000
Dry Cathode	$20,000	0.50	$52,000
Sinter Cathode	$500,000	0.10	$10,400
Total	***$3,777,000***	***7.35***	***$764,400***

Table 13. Raw material costs at pilot-line production volume (10 MW/year).	
Material	**$/cell**
Cathode materials (LSCF-based)	$1.22
Cathode interlayer materials (ceria-based)	$0.72
Anode materials (Ni-Co/ceria-based)	$4.16
Electrolyte materials (YSZ-based)	$5.11
Direct Supplies (Mylar, etc.)	$3.90
Total	**$15.11**

Table 14. Breakdown of *FlexCell* production costs at 10 MW/year scale.			
Contribution to Cost	**Yearly Cost**	**Cost Per Cell**	**Cost Per kW**
Raw Materials	$1,329,874	$15.11	$132.99
Depreciation	$943,041	$10.72	$94.30
Operating Labor	$772,873	$8.69	$76.44
Utilities	$355,688	$4.24	$37.29
Operating Supplies	$132,987	$1.51	$13.30
Local Taxes	$58,940	$0.67	$5.89
Maintenance & Repairs	$26,597	$0.30	$2.66
Insurance	$23,576	$0.27	$2.36
Total	**$3,652,290**	**$41.50**	**$365.23**

***FlexCell* Manufacturing Costs at Full-Scale Production Volume**

At the 250 MW/year volume level, the work week will be increased to a seven-day, three-shift operation to maximize capacity of the highly automated manufacturing equipment. Continuous tunnel kilns will be used for all firing operations in order to achieve the demanding cycle times and capacity requirements at such volumes. A gas-fired tunnel kiln will be used for sintering electrolyte substrates, while electrically heated kilns will be used for firing electrodes. Capital equipment cost needed for the full-scale (250 MW) *FlexCell* production facility is provided in Table 15, based on values obtained from vender surveys and quotations. Where necessary, equipment costs were estimated by scaling up the cost and throughput quotes for pilot-plant production equipment. Such equipment will likely require customization in order to meet the process, quality control, and capacity requirements at this volume level, and was also considered in the cost estimates. At this volume, the direct labor rate was reduced to $15/hour based on the difference in skill sets required in this highly automated production process. The overhead rate was reduced to 75%, typical of a high volume production facility.

Raw material costs for full-scale production were based on high volume estimates and raw material costs provided by SECA (see Table 16). The fixed capital investment, based on the direct and indirect costs for building the full-scale production plant, comprehends the land, building, equipment, and labor necessary for the plant to be operational. A breakdown of the fixed capital investment is given in Table 17.

Table 15. Capital equipment and labor requirements at 250 MW/year scale.

Manufacturing Operation	Capital Equipment	Labor (FTE's)	Labor Cost
Electrolyte Fabrication			
Clean Room	$3,000,000	-	-
Prepare Tape Slurries	$20,000	0.25	$73,357
Cast Tape	$160,000	0.25	$73,357
Cut and Stack Layers	$500,000	1.00	$293,429
Laminate	$500,000	0.25	$73,357
Final cut	$1,250,000	0.25	$73,357
Sinter electrolyte	$6,400,000	0.05	$14,671
Deposit Electrodes			
Anode Deposition/Dry	$1,780,000	2.00	$586,858
Sinter Anode	$2,000,000	0.10	$29,343
Cathode Deposition/Dry	$890,000	2.00	$586,858
Sinter Cathode	$1,750,000	0.10	$29,343
Totals	**$18,250,000**	**6.25**	**$1,833,930**

Table 16. Raw material costs at full-scale production volume (250 MW/year).	
Material	**$/cell**
Cathode materials (LSCF-based)	$0.13
Cathode inner layer materials (ceria-based)	$0.17
Anode materials (Ni/Co/ceria-based)	$0.61
Electrolyte materials (YSZ-based)	$0.44
Total	**$1.34**

Table 17. Fixed capital investment at 250 MW/year scale.	
Cost Category	**Estimated Cost**
Direct Costs	
Purchased Equipment	$18,250,000
Installation	$4,562,500
Instrumentation and Controls	$2,737,500
Piping	$1,825,000
Electrical	$3,650,000
Buildings	$4,562,500
Service Facilities	$7,300,000
Land	$730,000
Total Direct Costs	*$43,617,500*
Indirect Costs	
Engineering and Supervision	$4,361,750
Construction Expenses	$4,361,750
Total Indirect Costs	*$8,723,500*
Working Capital	***$1,825,000***
Total Fixed Capital Investment	**$54,166,000**

Using the above-described costs, along with an asset depreciation range of 15 years and bulk raw material costs provided by SECA, an updated cost estimate of $35.47 per kW is estimated (Table 18). Increased automation within the production line greatly reduced the labor cost for the fabrication of these YSZ-based *FlexCells* over the pilot scale cost model. Although raw material costs increased due to the increased cathode material usage, the impact of the clean room cost reduction more than offset this. Moving from a batch process to continuous firing and continuous spray deposition of electrodes also substantially reduced operating costs.

Table 18. Breakdown of *FlexCell* production costs at 250 MW/year scale.			
Cost Category	**Yearly Cost**	**Cost Per Cell**	**Cost Per kW**
Raw Materials	2,735,977.27	1.34	10.94
Depreciation	2,031,225.00	1.00	8.12
Operating Labor	1,833,930.00	0.90	7.34
Utilities	904,973.81	0.44	3.62
Operating Supplies	547,195.45	0.27	2.19
Local Taxes	541,660.00	0.27	2.17
Maintenance & Repairs	54,719.55	0.03	0.22
Insurance	216,664.00	0.11	0.87
Total	**$8,866,345**	**$4.35**	**$35.47**

Anode Supported Cell Cost Analysis (250 MW Scale)

For benchmarking against its electrolyte supported *FlexCell* technology, NexTech also analyzed the manufacturing cost of anode supported cells. In a recent DOE funded SBIR project (Contract Number DE-SC0004845), NexTech analyzed the manufacturing cost of anode supported cells at the 500 MW production scale. In this project, we modified that model to estimate manufacturing cost at the 250 MW scale to enable direct comparison to the estimated *FlexCell* cost at that volume.

Similar assumptions were used for cell size (500 cm^2 total area, 400 cm^2 active area), work schedule (7-day, 3-shift operation), labor rate ($15 per hour), overhead rate (75%), and production yield (98%). A slightly higher power output of 160 watts was assumed, reducing the cell production requirement to 4,491 per day. The unit operations and process flow assumed in the ASC manufacturing cost analysis is shown in Figure 72. From this, equipment and labor requirements were determined. Using SECA-provided raw materials costs, where available, and the same depreciation schedule used in the *FlexCell* cost model, a manufacturing cost estimate of $33.94 per kW was determined for anode supported cells (see Table 19).

Table 19. Breakdown of *ASC* production costs at 250 MW/year scale.			
Cost Category	**Yearly Cost**	**Cost Per Cell**	**Cost Per kW**
Raw Materials	2,454,865.28	1.57	9.82
Depreciation	2,031,225.00	1.30	8.12
Operating Labor	1,833,930.00	1.17	7.34
Utilities	866,867.52	0.55	3.47
Operating Supplies	490,973.06	0.31	1.96
Local Taxes	541,660.00	0.35	2.17
Maintenance & Repairs	49,097.31	0.03	0.20
Insurance	216,664.00	0.14	0.87
Total	**$8,485,282**	**$5.43**	**$33.94**

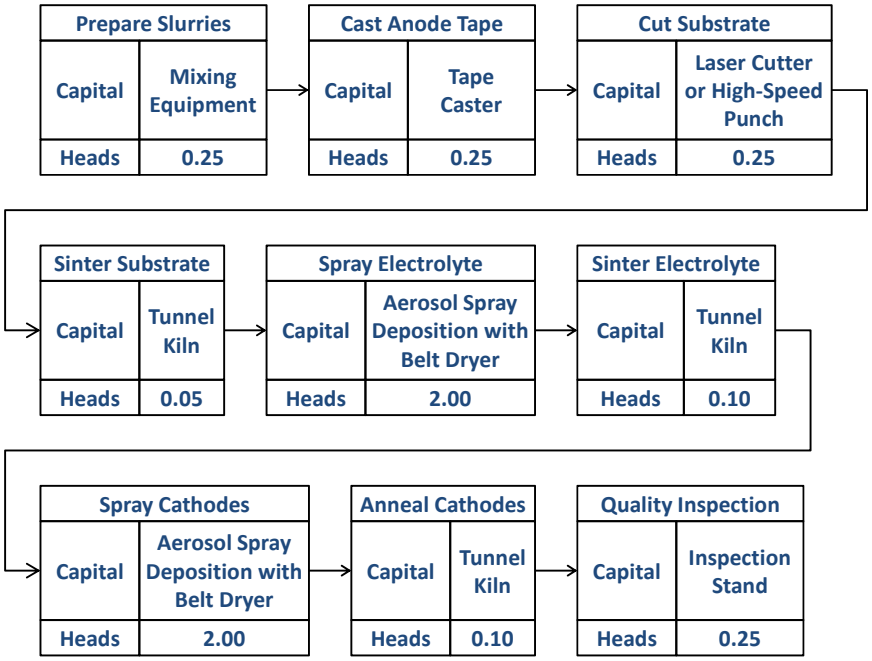

Figure 3. Anode Supported Cell manufacturing process at 250 MW scale production

Opportunities for Cost Reduction and Sensitivity Analysis

The impacts of various assumptions (cell size, thickness, active area, power density, and manufacturing yield) were considered to identify cost reduction opportunities (see Tables 20, 21 and 22). For reference, the baseline cost analysis, detailed above, is provided in the first row of Table 20, for 90% and 98% yield scenarios. Membrane thickness has the greatest impact on cell cost due primarily to the expected improvement in area-specific power density. Comparing rows one and three in Table 20, a $4/kW cost reduction is anticipated by reducing the membrane from 32 to 24 microns and the support from 160 to 80 microns. A decrease in support thickness alone, from 160 to 120 microns only marginally affects cell cost. NexTech has fabricated and tested *FlexCells* of such thin dimensions successfully. However, mechanical integrity of such thin cells will need to be confirmed for such a change to be practical.

In Table 20, we also consider the impact of the support architecture (i.e., the relative percentage of thin membrane area to the total active area of the cell). By changing this ratio from 62 percent to 70 percent, a modest reduction in cell cost can be realized ($1/kW). As shown in the last row of Table 20, cell costs of $31/kW can be achieved at the 500 cm^2 cell size if these improvements can be implemented.

Scalability of the *FlexCell* technology allows consideration of cells that are substantially larger than the 500 cm^2 assumed in the baseline cost analysis. NexTech has successfully fabricated *FlexCells* as large as 1200 cm^2. In Tables 21 and 22, we consider the effect of cell size on manufacturing cost at 650 and 800 cm^2, respectively. If a fixed sealing width around the cell perimeter is assumed, the active area of the cell increases as a percentage of total cell size. Using the same power densities and yields as those considered at the 500 cm^2 size, this greater active area results in further cell cost reductions. At the 650 cm^2 cell size, an ultimate cell cost of $28/kW can be achieved, while this is further reduced to $27/kW at 800 cm^2 cell area.

Table 20. Cost reduction opportunities for *FlexCells* with 500-cm^2 area.

Support/Membrane Thicknesses (microns)	Percent Thin Membrane in Active Area	Ratio of Active Cell Area to Total Area	Expected Power Density	Cells /day (90% yield)	Cell cost (90% yield)	Cells/day (98% yield)	Cell cost (98% yield)
160 / 32	62%	80%	313 mW/cm^2	6,198	$36.63/kW	5,746	$35.47/kW
120 / 32	62%	80%	325 mW/cm^2	5,959	$35.19/kW	5,526	$34.14/kW
80 / 24	62%	80%	375 mW/cm^2	5,165	$32.17/kW	4,789	$31.33/kW
160 / 32	70%	80%	325 mW/cm^2	5,959	$35.32/kW	5,526	$34.26/kW
120 / 32	70%	80%	337 mW/cm^2	5,739	$34.18/kW	5,321	$33.19/kW
80 / 24	70%	80%	387 mW/cm^2	5,004	$31.54/kW	4,640	$30.73/kW

Table 21. Cost reduction opportunities for *FlexCells* with 650-cm^2 area.

Support/Membrane Thicknesses (microns)	Percent Thin Membrane in Active Area	Ratio of Active Cell Area to Total Area	Expected Power Density	Cells /day (90% yield)	Cell cost (90% yield)	Cells/day (98% yield)	Cell cost (98% yield)
160 / 32	65%	85%	312 mW/cm^2	4,487	$33.34/kW	4,160	$32.42/kW
120 / 32	65%	85%	325 mW/cm^2	4,314	$32.08/kW	4,000	$31.25/kW
80 / 24	65%	85%	375 mW/cm^2	3,739	$29.54/kW	3,467	$28.89/kW
160 / 32	70%	85%	325 mW/cm^2	4,314	$32.20/kW	4,000	$31.36/kW
120 / 32	70%	85%	337 mW/cm^2	4,160	$31.21/kW	3,858	$30.44/kW
80 / 24	70%	85%	387 mW/cm^2	3,623	$28.99/kW	3,359	$28.38/kW

Table 22. Cost reduction opportunities for *FlexCells* with 800-cm^2 area.

Support/Membrane Thicknesses (microns)	Percent Thin Membrane in Active Area	Ratio of Active Cell Area to Total Area	Expected Power Density	Cells /day (90% yield)	Cell cost (90% yield)	Cells/day (98% yield)	Cell cost (98% yield)
160 / 32	62%	90%	312 mW/cm^2	3,443	$31.25/kW	3,192	$30.48/kW
120 / 32	62%	90%	325 mW/cm^2	3,310	$30.11/kW	3,070	$29.43/kW
80 / 24	62%	90%	375 mW/cm^2	2,869	$27.89/kW	2,660	$27.36/kW
160 / 32	70%	90%	325 mW/cm^2	3,310	$30.23/kW	3,070	$29.53/kW
120 / 32	70%	90%	350 mW/cm^2	3,193	$29.33/kW	2,960	$28.70/kW
80 / 24	70%	90%	400 mW/cm^2	2,780	$27.41/kW	2,578	$26.91/kW

At the 250 MW production scale, raw material costs are the largest contribution to total manufacturing cost as shown previously in Table 18 for *FlexCells* and Table 19 for anode supported cells. In NexTech's analysis, SECA raw material costs were used where available; elsewhere, current manufacturing costs were used with reductions assumed for high volume scaling (summarized in Table 23). Current costs of several of these raw materials are significantly higher than the values in Table 23. Specifically, GDC, LSZF, NiO, and YSZ represent the greatest risk to the estimated costs if these high volume costs are not realized. In Table 24, the impact on *FlexCell* manufacturing cost was analyzed under scenarios in which costs of each of these materials was higher than that assumed in the baseline analysis. Costs were based on vendor quotes at 250 MW scale volumes for YSZ and NiO, and scaling assumptions using current NexTech manufacturing costs. In all cases, the baseline cell configuration (32 micron thick membrane, 160 micron thick support) was used, yielding an estimated cost of $35.47/kW.

Table 23. Raw Material Costs Used in Analysis

Raw Material	Cost ($/kg)
GDC	$60
LSF	$10
LSM	$12
LSZF	$25
NiO	$8
YSZ (8 mol% Y_2O_3)	$10
YSZ (3 mol% Y_2O_3)	$10
YSZ-NiO Ink	$34
GDC-NiO	$55
LSF	$10
LSM - GDC	$45
LSZF-GDC	$45

Table 24. Impact of Raw Material Costs on *FlexCell* Manufacturing Cost Estimate

Material	Higher Cost Assumption ($/kg)	Raw Material Costs ($/cell)	Cell Cost (98% yield) ($/kW)
--	--	$1.34	$35.47
GDC	$218	$2.00	$42.80
LSZF	$99	$2.11	$43.92
NiO	$53	$1.44	$36.57
YSZ-3 YSZ-8	$67 $71	$3.98	$64.63
All of above	**listed above**	**$5.68**	**$83.46**

As Table 24 shows, YSZ cost has the greatest impact on total cell manufacturing cost, due to the amount of YSZ used in the electrolyte support and membrane. An increase in YSZ cost from the $10/kg value provided by SECA to those shown in Table 14 results in an 82% increase in cell cost. Higher LSZF and GDC costs also significantly impact cell cost, yielding a 24% and 21% increase in cell manufacturing cost, respectively. Combining all of these higher cost values, yields an estimated cell manufacturing cost of $83.64, a factor of 2.3 higher than that estimated with the raw material costs presented in Table 9. Efforts must, therefore, focus on reducing raw material costs (and/or usage) in order to achieve cell cost targets.

Similarly, NexTech analyzed the impact of these higher raw material costs on anode supported cell manufacturing cost (see Table 16). While the estimated cell cost is slightly lower than the *FlexCell* using SECA-provided raw material costs, this materials sensitivity analysis shows that the ASC is at risk of substantially higher manufacturing cost if these raw material cost targets are not achieved. As Table 25 shows, an increase in NiO to $53 per kg would result in a cell cost of $83 per kilowatt. Combining all higher raw material cost values presented in Table 14 would result in an ASC cost of $93 per kilowatt.

Table 25. Impact of Raw Material Costs on Anode Supported Cell Manufacturing Cost Estimate

Material	Higher Cost Assumption ($/kg)	Raw Material Costs ($/cell)	Cell Cost (98% yield) ($/kW)
--	--	$1.54	$33.94
GDC	$218	$2.05	$38.34
LSZF	$99	$2.34	$40.85
NiO	$53	$7.29	$83.63
YSZ-3	$67	$1.88	$36.89
All of above	**listed above**	**$8.43**	**$93.48**

Summary and Conclusions

Significant work was accomplished over this three-year project to validate YSZ-based, electrolyte-supported *FlexCells* for coal-based, megawatt-scale power generation systems. This project was focused on the fabrication and testing of electrolyte-supported *FlexCells* with yttria-stabilized zirconia (YSZ) as the electrolyte material. YSZ based *FlexCells* were made with sizes ranging from 100 to 500 cm^2. Single-cell testing was performed to confirm high electrochemical performance, both with diluted hydrogen and simulated coal gas as fuels. Finite element analysis modeling was performed at The Ohio State University was performed to establish *FlexCell* architectures with optimum mechanical robustness. A manufacturing cost analysis was completed, which confirmed that manufacturing costs of less than $50/kW are achievable at high volumes (500 MW/year). The following summarizes achievements over the three-year project duration:

- YSZ-based *FlexCell* membranes were made from mixtures of YSZ-3 and YSZ-8 powders, with the aim of increasing ionic conductivity without sacrificing mechanical robustness. This goal was met, and better than expected electrochemical performance of these *FlexCells* was observed.
- High power densities were achieved with YSZ-based *FlexCells* that surpassed the milestone of 300 mW/cm^2 at 0.7 volts on diluted hydrogen with 70% fuel utilization.
- YSZ-based *FlexCell*s were fabricated with reduced membrane and support thickness (as low as 24 and 80 microns, respectively) to enhance power density. Power density of 475 mW/cm^2 was achieved on these thin cells at 800°C at 0.7 volts and 70% fuel utilization.
- Large-area YSZ-based *FlexCells* were fabricated with total areas ranging from 320 to 540 cm^2. Testing of cells with 475-cm^2 area (330 cm^2 active area) produced 135 and 148 watts per cell with diluted hydrogen as fuel and under high fuel utilization conditions (70 and 60 percent, respectively).
- Simulated coal gas testing was performed at temperatures ranging from 750°C to 850°C with complete methane reforming occurring throughout this test temperature range.
- Long term testing of the YSZ-based *FlexCell* was performed for over 1300 hours under diluted hydrogen conditions.
- Long term testing was performed under simulated coal gas conditions over a range of *FlexCell* membrane thicknesses and test configurations. Testing showed a significant improvement in methane reforming activity when nickel foam anode current collectors were infiltrated with reforming catalyst material.
- Long term testing was performed at 800°C under H_2O/CH_4 ratios varying from 2.2 down to 0.5. Both initial power density and degradation rates were observed to improve with lower steam content.
- Improvements were implemented to improve long term cell degradation, including: improved steam delivery methods, optimized catalyst loading in the anode current collector foam, replacement of silver cathode current collector meshes with manganese cobalt oxide coated alloy current collector meshes, and optimization of cell anode and cathode electrode layer thicknesses. In a 1000 hour test, degradation rates of 12 μV/hour were measured over the final 230 hours of testing.

- Process and quality control improvements were implemented throughout the entire *FlexCell* fabrication process including: raw material receiving and qualification, electrolyte tape casting, substrate fabrication, electrode deposition, and final QC. Yields of fully qualified 475-cm^2 area *FlexCells* exceeded 85 percent with these improved process controls.
- Ohio State University completed a computational model of the *FlexCell* design, based on finite element analysis, which was used to optimize the mechanical robustness of *FlexCell* membranes. The accuracy of the model was validated through experimental testing. The model currently is being employed for the design of current and future generation *FlexCells*.
- Comprehensive cost analysis was completed for pilot and full-scale production for large area YSZ-based *FlexCells* and updated throughout the project. From this cost model, a cost of 35.47 dollars per kilowatt was projected for full-scale production of large area YSZ-based *FlexCells.*
- For comparative purposes, a manufacturing cost analysis was performed for anode supported cells, projecting a full scale production cost of 33.94 dollars per kilowatt.
- A sensitivity analysis was performed to identify opportunities to further reduce full-scale production costs of *FlexCells* including thinner membranes, higher yields, and larger cell area. With these improvements, costs as low as 27 dollars per kilowatt were projected.
- Further sensitivity analyses were performed on both the *FlexCell* and anode supported cell cost model to evaluate the impact of potentially higher raw material costs on full-scale manufacturing costs. Using current raw material quotations, costs of 83 and 93 dollars per kilowatt were projected, respectively driven primarily by the cost of YSZ (in the case of the *FlexCell*) and NiO (in the case of ASC).
- YSZ-based *FlexCells* were validated in three-cell stack tests under simulated coal gas fuel conditions. The stack achieved 136.6 watts at a fuel utilization of 70.9 percent, corresponding to an LHV electrical efficiency of 41.7 percent. Long term testing was conducted at 800°C under 0.402 A/cm^2 and 64 percent fuel utilization conditions for 200 hours.

Advancements in YSZ-based *FlexCell* fabrication, testing, modeling and cost analysis has provided a realistic path forward for use of large-area YSZ-based *FlexCells* in coal-based, megawatt-scale power generation systems.